## AD NUMBER

**AD838297**

## NEW LIMITATION CHANGE

TO

**Approved for public release, distribution unlimited**

FROM

**Distribution authorized to U.S. Gov't. agencies and their contractors; Administrative/Operational use; Aug 1968. Other requests shall be referred to EdgeWood Arsenal, Aberdeen Proving Ground, MD.**

## AUTHORITY

**EA d/a ltr, 15 Jun 1978**

AD

Report Number 6

# SORPTION PROPERTIES OF ACTIVATED CARBON

Comprehensive Progress Report
June 1966 - April 1968

by

E. D. Tolles

August 1968

DEPARTMENT OF THE ARMY
EDGEWOOD ARSENAL
Research Laboratories
Physical Research Laboratory
Edgewood Arsenal, Maryland 21010

Contract DA 18-035-AMC-1053(A)

Charleston Research Laboratory
WEST VIRGINIA PULP AND PAPER COMPANY
P. O. Box 5207
North Charleston, South Carolina

## Distribution Statement

This document is subject to special export controls and each transmittal to foreign governments or foreign nationals may be made only with prior approval of the CO, Edgewood Arsenal, ATTN: SMUEA-TSTI-T, Edgewood Arsenal, Maryland 21010.

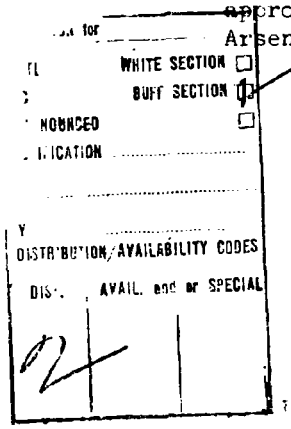


## Disclaimer

The findings in this report are not to be construed as an official Department of the Army position unless so designated by other authorized documents.

## Disposition

Destroy this document when no longer needed. Do not return it to the originator.

Report Number 6

# SORPTION PROPERTIES OF ACTIVATED CARBON

Comprehensive Progress Report
June 1966 through April 1968

by

E. D. Tolles



August 1968

DEPARTMENT OF THE ARMY
EDGEWOOD ARSENAL
Research Laboratories
Physical Research Laboratory
Edgewood Arsenal, Maryland 21010

Contract DA-18-035-AMC-1053(A)

Charleston Research Laboratory
West Virginia Pulp and Paper Company
P. O. Box 5207
North Charleston, South Carolina

## FOREWORD

This work was authorized under Project 1C622401A095, Chemical and Biological Physical Protection Investigations (U), under the direction of Mr. L. A. Jonas and Miss Virginia Bauer, Contract Project Officers, Edgewood Arsenal Research Laboratories. The work was started in June 1966 and completed in April 1968. The experimental data are contained in notebooks 2122, 2240, 2230, and 2345.



## ACKNOWLEDGMENTS

We wish to thank Mrs. Mary Ellen Fink and Mrs. Janet Evans who performed the experimental measurements and made the many calculations and drawings required to present these data.

## SUMMARY

Equilibrium adsorption isotherms were determined experimentally at several temperatures using the agents GB, GA, and GF, the simulent DMMP and also carbon tetrachloride and benzene. The adsorbents used were Pittsburgh Activated Carbon Co. Type BPL and a "super activated" Barnebey-Cheney coconut shell carbon. Efforts to predict adsorption isotherms for the agents based upon the adsorptive behavior of the simulents and using the relationship $\ln W = \ln W_o - B/\beta^2 (T \log Po/P)^2$ after Dubinin et al., were not successful. This was because plots of the experimental data as $\ln W$ vs. $(T/\beta \log Po/P)^2$ were not linear as implied by the equation. Despite this reasonably good isotherm predictions were obtained by assuming that the resultant curves were characteristic of the particular adsorbent and by working directly from such plots. Values of the term $\beta$ which represents the strength of the adsorptive interaction of a particular adsorbate relative to that of a reference adsorbate were determined experimentally. This was done by adjusting the value until the best fits were obtained between the predicted isotherms and the experimental data for the Pittsburg carbon. The same values were found to produce reasonably good fits for the "super activated" carbon. Values of $\beta$ calculated from the ratios of molar parachors did not lead to acceptable isotherm predictions in the cases studied.

The present work indicates that the adsorption properties of a carbon can be characterized by a plot of $\ln W$ vs. $(T \log Po/P)^2$ using adsorption data for a reference adsorbate. The adsorptivity of another adsorbate relative to that of the reference material should be determined experimentally. Such relative adsorptivities are expected to be independent of the adsorbate for most carbons.

The physical and adsorptive properties of an activated carbon impregnated with siloxane resins were investigated. Such impregnation caused a large loss in surface area and adsorptive capacity but did not selectively increase the hydrophobic properties of the carbon. Deposition of the resin appeared to have taken place principally in the larger pores and resulted in the blockage of a portion of the micropores.

Flow adsorption experiments were performed using the Pittsburgh Type BPL carbon and the simulent DMMP. Predictions of the breakthrough properties of this system were attempted for a range of adsorbate/air concentrations around 100 µg/l and at linear velocities of flow of about 90 cm/sec. These predictions were based upon the theoretical methods of Wheeler and of Allen and Joyce and neither was found to yield accurate description of the experimental breakthrough curves. It is thought that the results may have been adversely influenced by the very high experimental flow rates.

TABLE OF CONTENTS


| Technical Discussion | | Page |
|---|---|---|
| I. | INTRODUCTION | 7 |
| II. | EQUILIBRIUM ADSORPTION | |
| | A. Background | 7 |
| | B. Experimental | 8 |
| | C. Results of Experimental Measurements with Agents and Simulents | 13 |
| | D. Equilibrium Adsorption Measurements with Other Adsorbents | 24 |
| | E. Summary of Results of Equilibrium Experiments | 56 |
| III. | PHYSICAL AND ADSORPTIVE PROPERTIES OF IMPREGNATED CARBONS | |
| | A. Effect on Activity | 72 |
| | B. Porosity Measurements | 72 |
| | C. Water Adsorption | 74 |
| IV. | DYNAMIC ADSORPTION STUDIES | |
| | A. Apparatus | 75 |
| | B. Experimental Procedure | 80 |
| | C. Systems Studied | 82 |
| | D. Results of Flow Adsorption Experiments | 82 |
| | E. Methods of Analysis of Breakthrough Data | 85 |
| | F. Discussion of Flow Adsorption Results | 95 |
| V. | GENERAL SUMMARY | 98 |
| Nomenclature | | 101 |
| Literature Cited | | 103 |
| Distribution List | | 105 |
| Document Control Data - R&D, DD Form 1473 With Abstract and Keyword List | | 107 |


FIGURES


| | | |
|---|---|---|
| 1 - | Adsorption Apparatus | 9 |
| 2 - | Thermistor Manometer Calibration for GB | 11 |
| 3 - | Test of $(\delta\Delta F/\delta T)_V = 0$ for PCC | 14 |
| 4 - | Test of $(\delta\Delta F/\delta T)_V = 0$ for BC | 15 |

| | | | |
|---|---|---|---|
| 5 | - | Characteristic Curve for DMMP on PCC | 16 |
| 6 | - | Characteristic Curve for GB on PCC | 17 |
| 7 | - | Characteristic Curve for DMMP on BC | 18 |
| 8 | - | Characteristic Curve for GB on BC | 19 |
| 9 | - | Characteristic Plots for Adsorbates on PCC Affinity Coefficients Calculated from Parachors | 21 |
| 10 | - | Characteristic Plots for Adsorbates on BC Affinity Coefficients Calculated from Parachors | 22 |
| 11 | - | Characteristic Plots for Adsorbates on PCC Empirical Affinity Coefficients | 23 |
| 12 | - | GB on PCC - Adsorption Isotherms | 25-27 |
| 13 | - | GA on PCC - Adsorption Isotherms | 28-30 |
| 14 | - | GF on PCC - Adsorption Isotherms | 31-33 |
| 15 | - | Characteristic Plots for Adsorbates on BC Empirical Affinity Coefficients | 34 |
| 16 | - | GB on BC - Adsorption Isotherms | 35-37 |
| 17 | - | GA on BC - Adsorption Isotherms | 38-40 |
| 18 | - | Characteristic Curve for $CCl_4$ on PCC | 42 |
| 19 | - | DMMP on PCC - Adsorption Isotherms | 43-45 |
| 20 | - | GB on PCC - Adsorption Isotherms | 46-48 |
| 21 | - | GA on PCC - Adsorption Isotherms | 49-51 |
| 22 | - | GF on PCC - Adsorption Isotherms | 52-54 |
| 23 | - | Characteristic Curve for $CCl_4$ on BC | 55 |
| 24 | - | DMMP on BC - Adsorption Isotherms | 57-59 |
| 25 | - | GB on BC - Adsorption Isotherms | 60-62 |
| 26 | - | GA on BC - Adsorption Isotherms | 63-65 |
| 27 | - | Benzene on PCC - Adsorption Isotherms | 66-68 |
| 28 | - | Benzene on BC - Adsorption Isotherms | 69-71 |
| 29 | - | $H_2O$ on Resin Impregnated Sample No. 9 at 20°C | 76 |
| 30 | - | $H_2O$ on Resin Impregnated Sample No. 11 at 20°C | 77 |
| 31 | - | $H_2O$ on Control Sample at 20°C | 78 |
| 32 | - | Elements of Flow Adsorption Apparatus | 79 |
| 33 | - | Bed Flow Characteristics | 81 |
| 34 | - | Typical Detector Response Curves | 83 |
| 35 | - | Characteristic Curves for Adsorption of DMMP on PCC | 87 |
| 36 | - | Breakthrough Curves for DMMP on PCC - Run 1 | 89 |
| 37 | - | Breakthrough Curves for DMMP on PCC - Run 2 | 90 |
| 38 | - | Breakthrough Curves for DMMP on PCC - Run 3 | 91 |
| 39 | - | Breakthrough Curves for DMMP on PCC - Run 4 | 92 |
| 40 | - | Breakthrough Curves for DMMP on PCC - Run 5 | 93 |
| 41 | - | Breakthrough Curves for DMMP on PCC - Run 6 | 94 |
| 42 | - | Correlation of Breakthrough Results with Wheeler's Equation | 96 |

SORPTION PROPERTIES OF ACTIVATED CARBON

Technical Discussion

## I. INTRODUCTION

This report covers research efforts made in three areas of study:

1. Equilibrium adsorption studies were made to investigate methods of predicting the adsorptive capacity of activated carbon for CW agents. By such methods the relationship between the capacity of a given carbon, the temperature of adsorption and the concentration of a given agent might be calculated from physical properties of the agent and adsorptive properties of the carbon determined previously with nontoxic simulents.

2. Dynamic adsorption studies were performed to test methods of determining adsorption kinetics parameters and predicting the adsorptive performance of packed carbon beds. Such methods would find use in estimating the service life of protective devices under a variety of service conditions and provide insight into the design of such devices.

3. The physical and adsorptive properties of siloxane impregnated activated carbons were investigated to determine the effects of this special treatment. By impregnation it was intended to alter the water adsorption properties of carbon to maintain capacity for CW agents under wet conditions.

Each of the above areas are discussed separately in the following sections.

## II. EQUILIBRIUM ADSORPTION

### A. Background

The most successful theory leading to an analytical description of equilibrium vapor phase adsorption on activated carbons is that of Polanyi and Dubinin, which in its present stage of development has been called by Bering, Dubinin, and Serpinsky the "Theory of Volume Filling Micropores." (1) According to this method, the volume, W, of condensed adsorbate in the micropores of an adsorbent at a pressure P is given by

$$\ln W = \ln W_o - \frac{B}{\beta^2} (T \log \frac{P_o}{P})^2, \qquad [1]$$

where $W_o$ and B are constants related to the pore structure of the adsorbent and are independent of the adsorbate. Po is the normal liquid vapor pressure of the adsorbate at the temperature, T, of adsorption. $\beta$ is a constant which compares the strength of the adsorptive interaction of the adsorbate to that of some reference substance. It is apparent that if one measures the adsorption isotherm of one vapor on a particular carbon, the characteristic constants of this adsorbent, $W_o$ and B, may be determined by assuming $\beta = 1$. The equation then contains the necessary information to calculate the adsorption isotherm of other vapors on this carbon if one knows the strength of adsorption relative to that of the adsorbate for which $\beta$ was taken as unity. Since it is a premise of the theory that the adsorptive interaction arises due to dispersion forces (nonspecific van der Waals' forces) the relative strength of the interaction should be given by the relative polarizabilities of the adsorbates. Lacking specific information on polarizabilities, their ratios may be approximated by the ratio of molar volumes, or better, by the ratio of molar volumes corrected for compression due to intramolecular forces. The latter is defined by the ratio of parachors. With parachor data which are determined from easily measured physical properties, one can, if the theory holds true, calculate adsorption isotherms for any adsorbate on any carbon on which isotherm data has been obtained for a reference vapor. Furthermore, since temperature is explicit in the equation, the temperature for which these calculations are made need not be the same as that used for the reference isotherm.

In the past, good results have been obtained using this theory to correlate the adsorption performance of many common vapors. The predictive value of this theory has now been tested for agents GB, GA, GF, and a simulent, DMMP.

B. Experimental

Adsorption isotherms were measured on a Pittsburgh Activated Carbon Company carbon (PCC) at 20°, 30° and 40°C for GA, GB, GF, and DMMP. Isotherms were also determined on a Barnebey-Cheney carbon (BC, additionally activated by Mine Safety Appliances Research) at 20°, 30° and 40°C for GB and DMMP, and at 20° and 30°C for GA. These isotherms were measured over a pressure range extending from a little less than the liquid vapor pressure to about $10^{-5}$ torr.

1. Apparatus

The vacuum apparatus which was used for these measurements is shown schematically in Figure 1. It is made up of two basic sections, of which one is used for vapor handling operations such as trap to trap distillation for degassing adsorbates, and the other is used for adsorption measurements.

FIGURE 1

Adsorption Apparatus

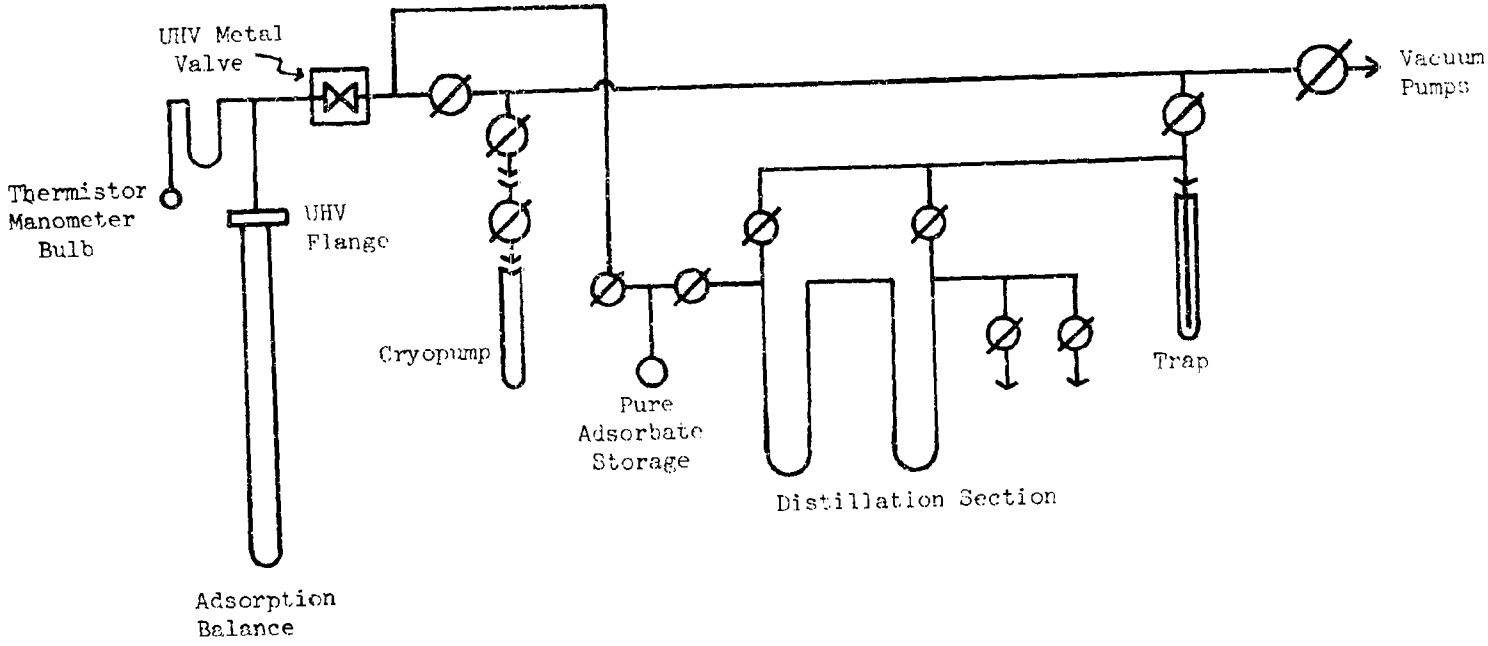

This second section includes a McBain type adsorption balance and a thermistor manometer sensor. The balance employs a fused silica spring from which the carbon sample is suspended and measurement of the mass of vapor adsorbed is made by determining the extension of this spring with a cathetometer. Repeatable accuracy of this balance is judged to be 0.10 mg. The removable lower section of the balance case is attached to the apparatus by a Granville-Phillips metal flange sealed with a copper gasket.

The thermistor manometer which has been described previously (2) was designed in this laboratory and is useful in a pressure range of about 2 torr to $1 \times 10^{-5}$ torr.

The adsorption balance system is connected to the distillation and pumping section through an all metal ultra-high vacuum valve (Granville-Phillips). It is an important feature of this apparatus that no vacuum grease is present in the measurement section. The slow outgassing or organic adsorbates from grease would make very low pressure adsorption measurements impossible.

It was determined in previous work in this laboratory (2) that desorption measurements gave the most reliable results at low pressures since the balance system was automatically cleared of significant traces of air or low boiling impurities each time a dose was desorbed. As a matter of safety when using toxic agents, desorption was carried out by condensing most of the adsorbate vapor into a "cryopump." This is simply a removable glass tube which was connected to the main vacuum manifold through a pair of large bore stopcocks. By immersing the tube in liquid nitrogen the agents could be pumped off without contaminating the main vacuum line trap.

## 2. Procedures

The experimental procedures involved in measurements with each vapor and adsorbent were practically identical. For each adsorbate the first step was to distill the vapor from trap to trap under vacuum in order to remove volatile gases. Then, with no carbon sample in the balance case a small amount of the liquid adsorbate was distilled into a U-trap between the manometer sensor bulb and the balance case. In order to calibrate the measurements for the particular vapor, the adsorbate sample was then brought to a series of temperatures between about -75°C and 20°C and the manometer indications were recorded at each temperature. Working from the best available data on vapor pressure *vs.* temperature a calibration curve was then constructed showing vapor pressure *vs.* manometer reading. An example of such a calibration curve for the agent GB is shown in Figure 2. Here the manometer indication in microamperes is plotted against GB vapor pressure.

FIGURE 2 Thermistor Manometer Calibration for GB

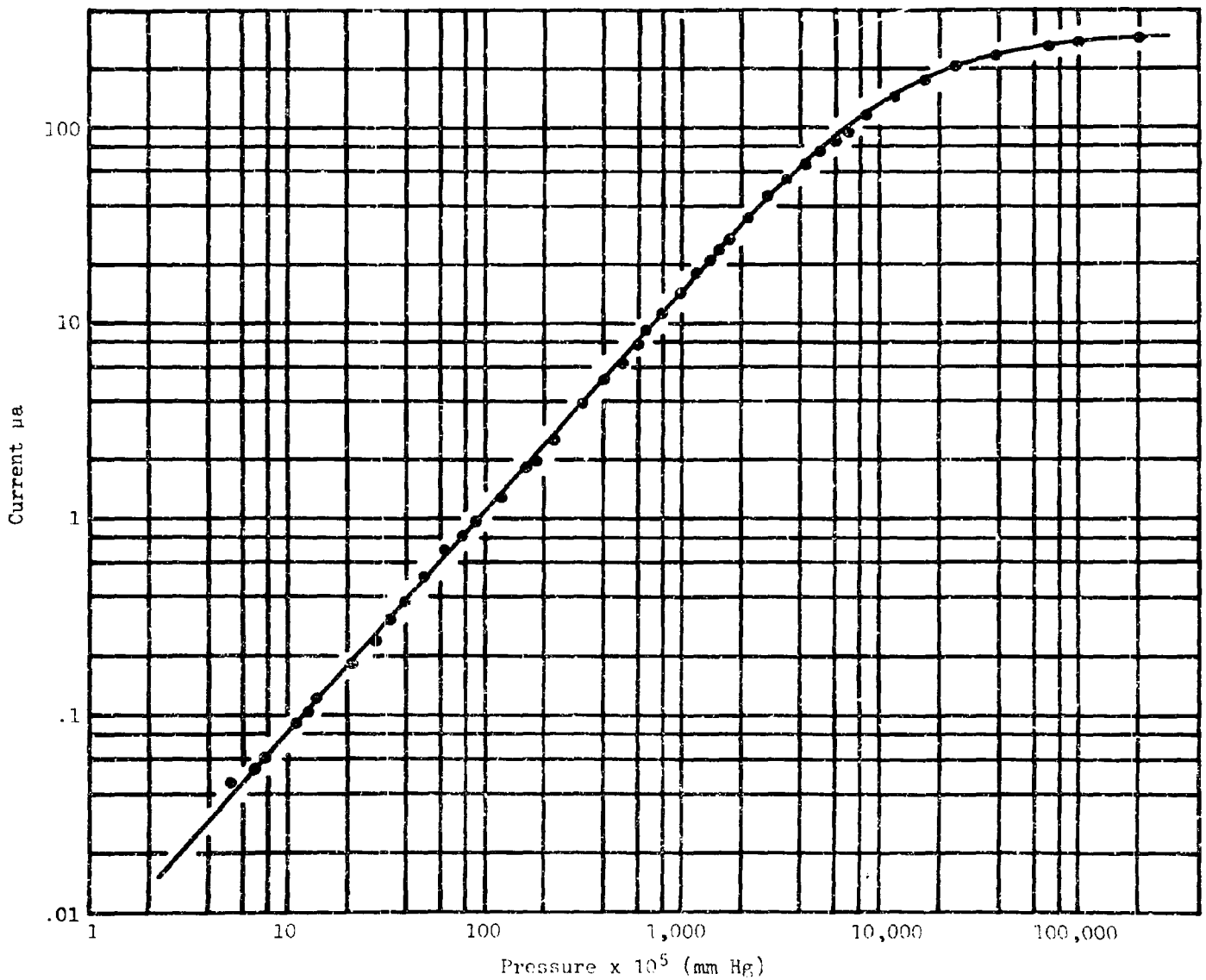

Following this calibration procedure the U-tube was pumped out and a carbon sample was introduced into the balance case where it was degassed by heating at 350°C for about 15 hours under high vacuum.

The sample was then brought to a thermostat temperature for which adsorption data were to be obtained and the degassed adsorbate vapor was admitted until the carbon was completely saturated. The metal vacuum valve was then closed and after equilibrium, the pressure and amount adsorbed were noted. Doses of vapor were then desorbed in a stepwise fashion and the amount adsorbed and equilibrium pressure were recorded at each step. At lower pressures where there was difficulty in removing the adsorbate by simple pumping, the temperature of the sample was raised as high as 100°C.

3. Experimental Samples

The adsorbents used in this work included the following:

(1) Pittsburgh Activated Carbon Company Type BPL in 12x30 mesh. This sample was supplied by Edgewood Arsenal from Lot 6098.
(2) Barnebey-Cheney coconut based carbon which had been additionally activated to 149% carbon tetrachloride value by Mine Safety Appliances Research.

Chemical agents GB, GA, and GF were supplied by Edgewood Arsenal in sealed glass ampoules. The purity given for these materials was 96.6%, 99.6%, and 92%, respectively. Since distillation in the vacuum apparatus involved taking a middle fraction of distillate, the final purity as used should have been somewhat higher but the exact purity is not known. The simulent dimethyl methylphophonate (DMMP) was obtained from Virginia Carolina Chemical Company and carefully redistilled using a Podbielniak column. The purity was judged to be above 99.5%.

One of the reasons for using a thermistor manometer in this work was that the sensor is a low temperature resistance device and would therefore not cause decomposition of the agents. However in the case of GA, decomposition appears to have occurred for other reasons. We found that it was impossible to obtain steady equilibrium pressures at each point on the desorption isotherms and that instead the pressure increased constantly over periods as long as 72 hours. Experiments showed that this effect was not due to air leakage and blank runs with no carbon present indicated that the decomposition was not catalyzed by the carbon surface. However, the rate of decomposition was quite low and since the volatile product was removed at each desorption point we judged that there was a fair chance of obtaining valid isotherms.

C. Results of Experimental Measurements With Chemical Agents and Simulents

In order that the characteristic equation $\ln W = \ln W_o - B/\beta^2 (T \log P_o/P)^2$ succeed as a means of predicting adsorption isotherms there are several conditions that must be met:

(a) The equation must correctly describe the way in which the isotherm is affected by temperature.
(b) The terms B and $W_o$ must be constant and true characteristics of the adsorbent and be independent of the adsorbate.
(c) The term $\beta$ must be a characteristic of the adsorbate independent of the adsorbent.
(d) The porosity of carbons to which the equation is applied must be such that most of the adsorption space is in micropores, i.e., pores less than about 35 Å in diameter.

1. Prediction of Temperature Effects

The earlier theory of Polanyi upon which the above characteristic equation is based stated that the free energy of adsorption (going from bulk liquid to the adsorbed phase at a constant temperature) should be a temperature invarient function of the volume adsorbed. Therefore a plot of W vs. $\Delta F = RT \ln P_o/P$ should yield a single line for data obtained at any temperature. To test this, DMMP data on the PCC and BC carbons were plotted for temperatures of 20°, 30° and 40°C. Figures 3 and 4 show that in these cases the temperature predicting capabilities of the theory are quite good. We have also found this to be generally true with the other systems studied.

2. Characteristic Curves

Equation [1] is written in such a form that if the terms B, $\beta$, and $W_o$ are constant, plots of $\ln W$ vs. $(T \log P_o/P)^2$ should be linear. Figures 5 - 8 show the results of plotting these functions for some experimental data and it is easily seen that linearity is not obtained. One generally expects to find nonlinearity for small values of $(T \log P_o/P)^2$ since these correspond to high relative pressures and to adsorption principally on the part of the outside of the micropore range. However, in the cases shown, curvature exists throughout the measured pressure range. Although adsorption outside of the micropore range does affect all of the data it has generally been found that corrections for surface adsorption do not alter the linearity of characteristic curves at higher values of $(T \log P_o/P)^2$. For the carbons used in this work it can further be stated that the adsorption space outside the micropore range is relatively small.

FIGURE 3

Test of $(\partial U/\partial V)_T = 0$ for PEC

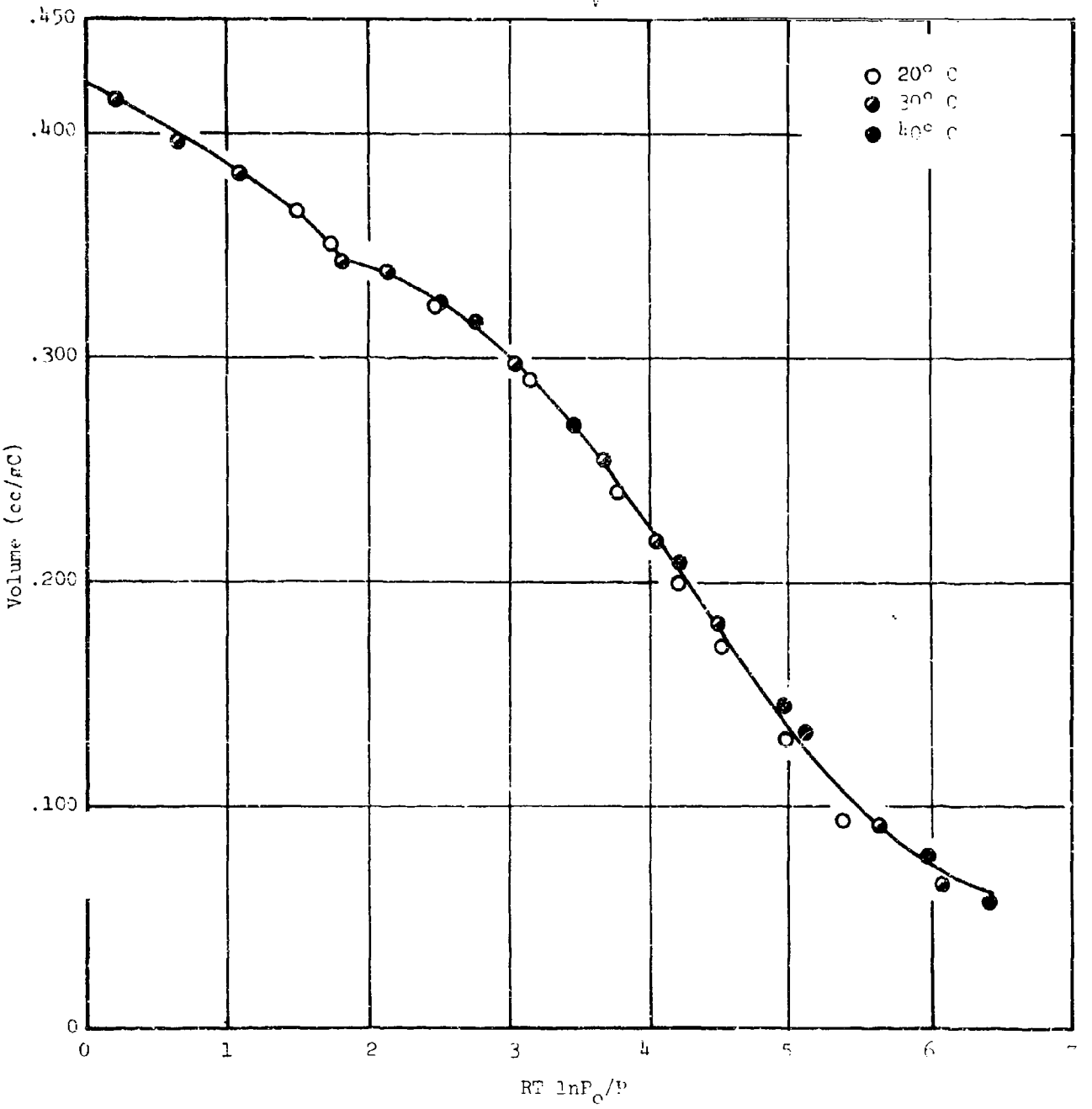

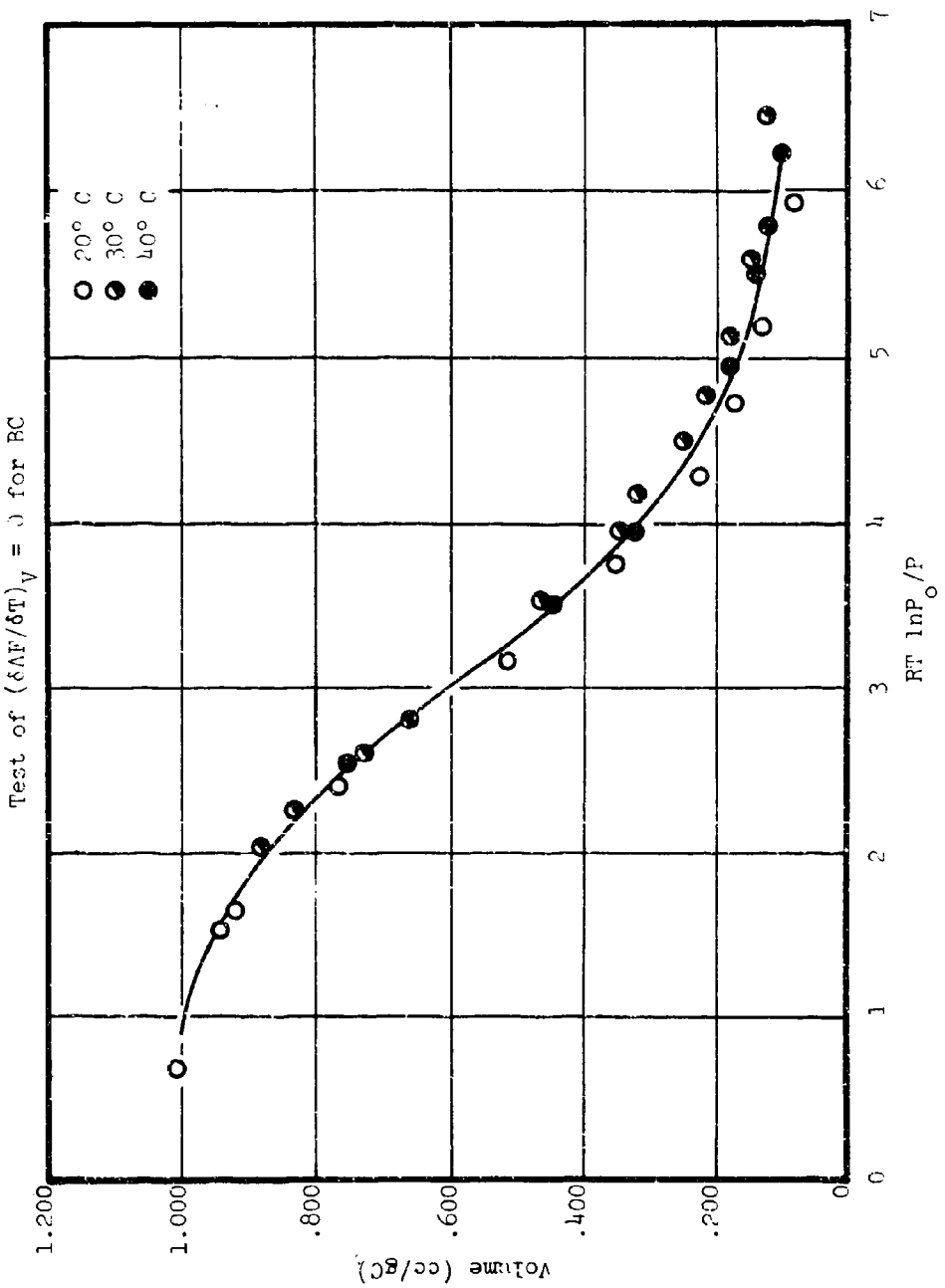


FIGURE 4
Test of $(\delta A F/\delta T)_V$ = 0 for BC

Figure 5

Characteristic Curve for DMMP on PCC

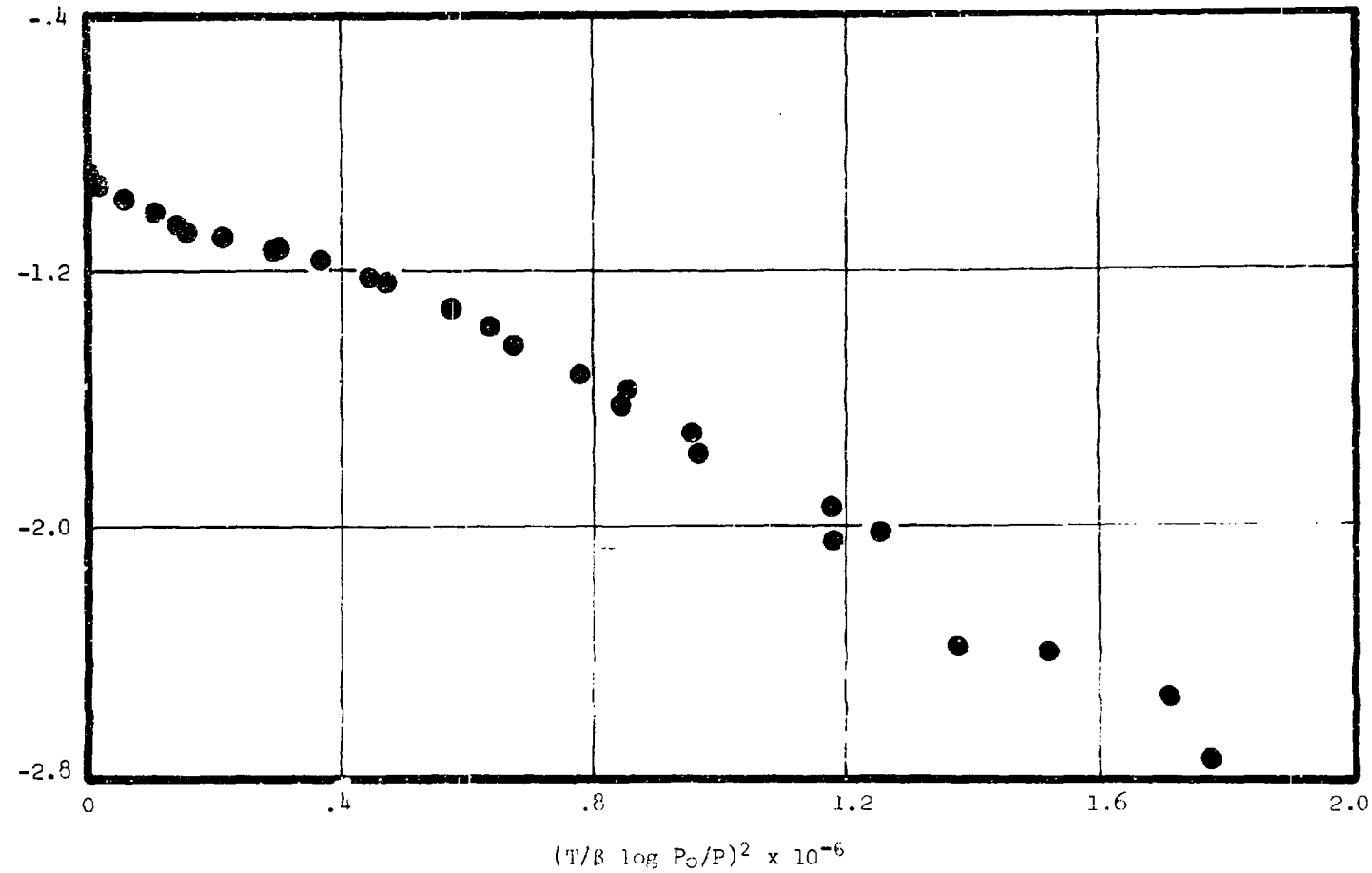

Figure 6

Characteristic Curve for GB on PCC

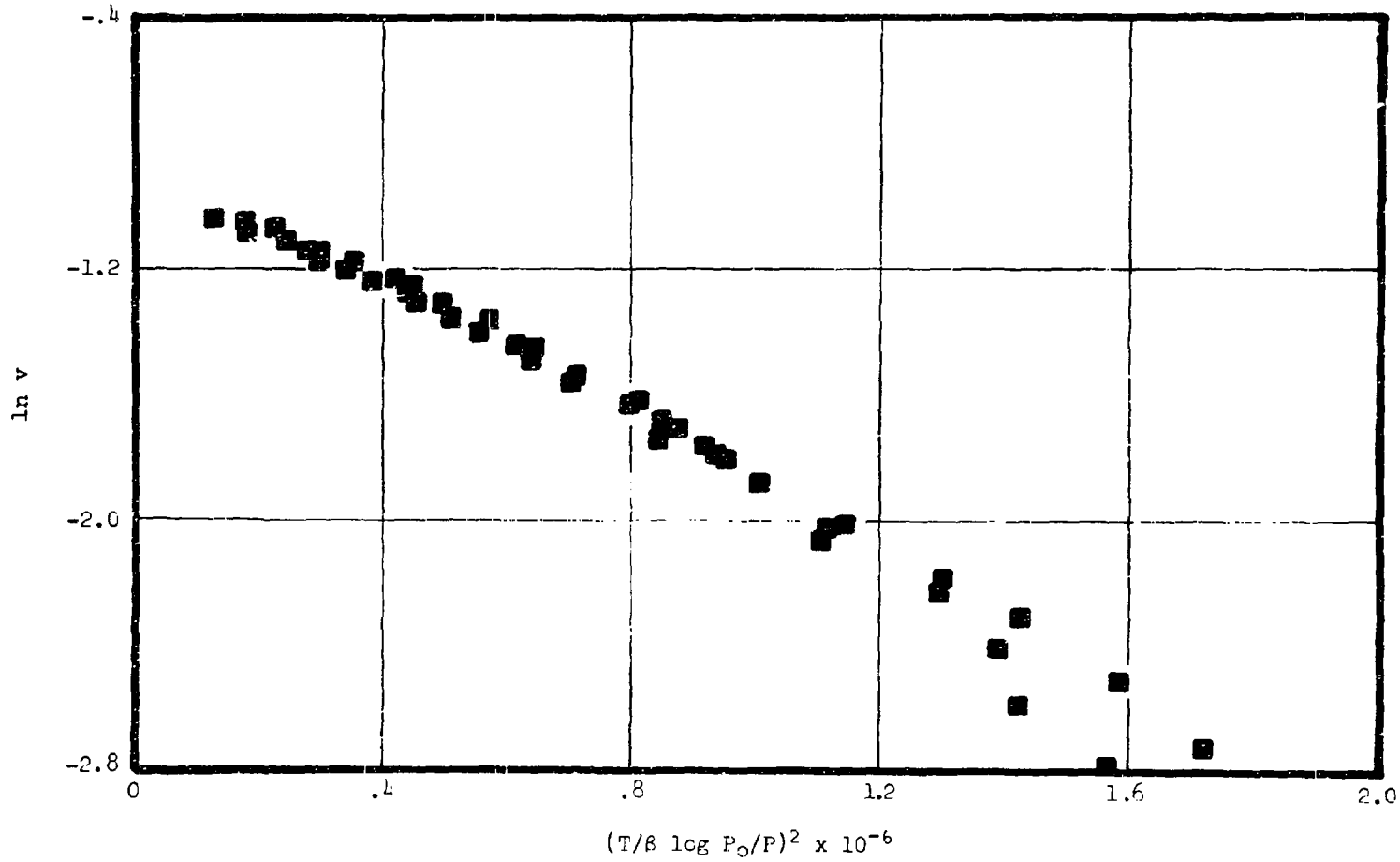

Figure 7
Characteristic Curve for DMMP on BC

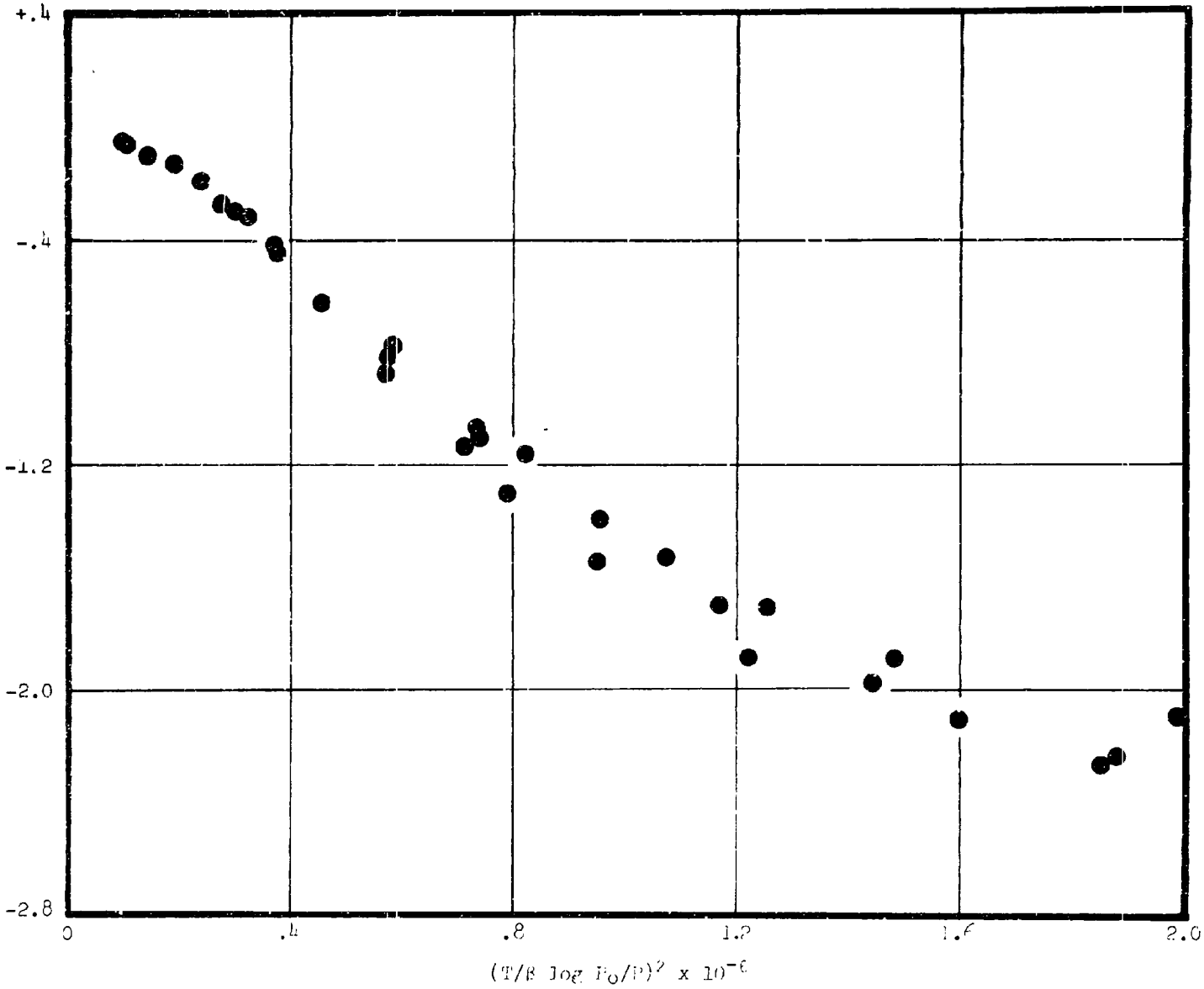

Figure 8

Characteristic Curve for GB on BC

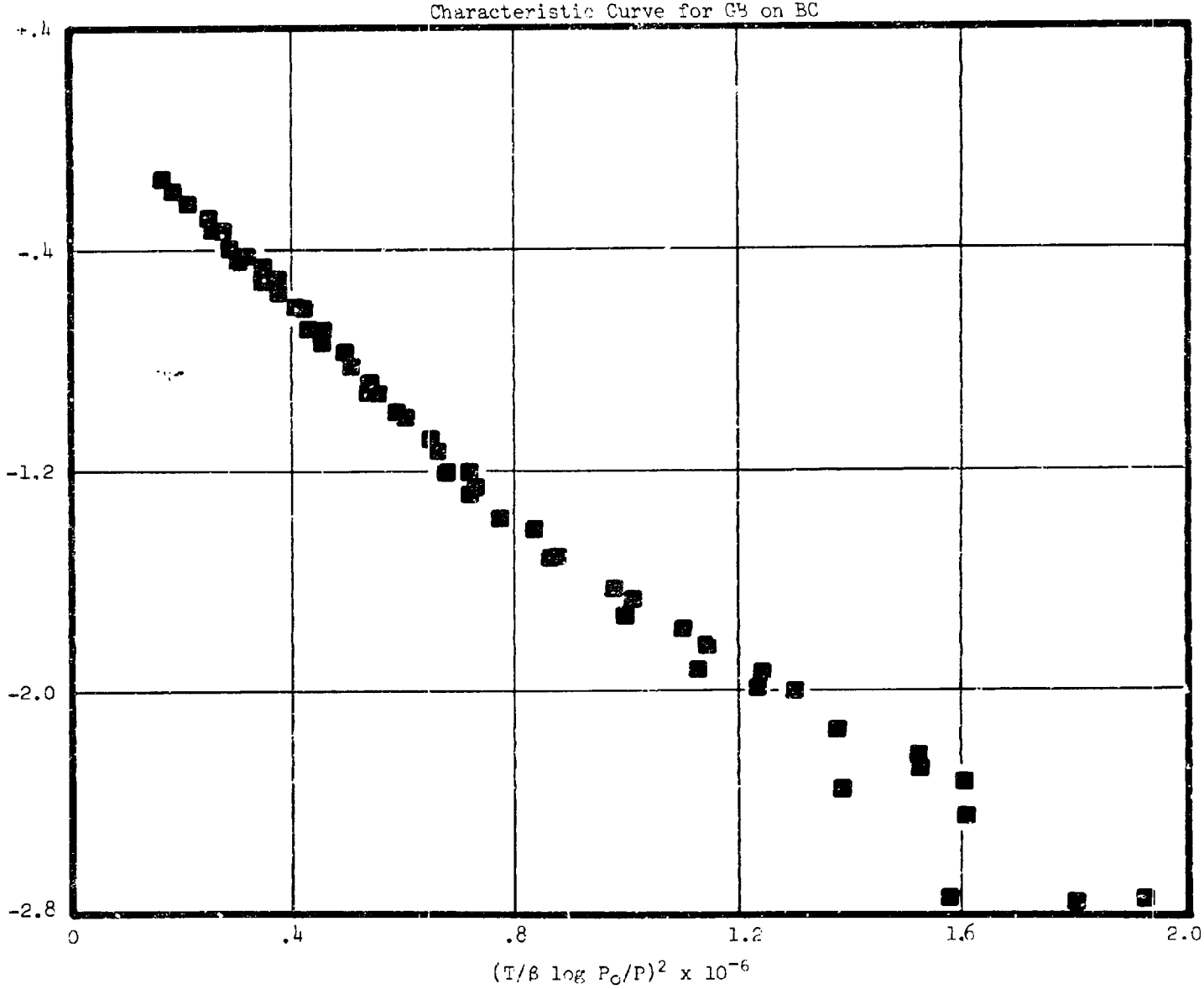

The validity of the method as a predictive device does not, however, rest theoretically on the linearity of these plots. In fact it can be shown that the linearity requires a particular type of adsorption energy distribution and there is no reason that this distribution would necessarily be a natural consequence of the manufacture of activated carbon. Therefore the method might still be useful if the assumption is made that while there may be no unique value of β for a particular carbon, the adsorbent structure is accurately characterized by the whole curve given by plotting ln W vs. $(T/\beta \log Po/P)^2$. Thus, these curves for different vapor on the same carbon should coincide with one another provided that the "affinity coefficient" β is properly selected.

Using values of β calculated by the ratio of the parachors of GA, GB and GF to DMMP, the combined adsorption data for all of these vapors are shown in Figure 9 for the PCC carbon and Figure 10 for BC carbon. It is seen that the bulk of these data does not coincide with those for DMMP.

It must be remembered, however, that the use of parachors to calculate the relative strengths of the adsorptive interactions is only an approximation. We therefore attempted to determine if there was another number which would produce the desired coincidence. The result of this is shown in Figure 11 for PCC carbon where it is seen that adjustments in the values of β could produce a reasonably close match between characteristic curves. The empirical values of β required to produce coincidence are listed in Table I along with the values calculated from the parachor ratios. It should be noted that the empirical β for GB was listed in earlier reports as 1.10 but that the characteristic curve upon which this was based was somewhat in error so that the value given below is more accurate.

TABLE I

AFFINITY COEFFICIENTS CALCULATED FROM PARACHORS AND BY CURVE MATCHING WITH PCC DATA

| | β from Parachors | Empirical β |
|---|---|---|
| DMMP | 1.00 | 1.00 |
| GB | 1.10 | 1.04 |
| GA | 1.36 | 1.70 |
| GF | 1.44 | 1.77 |

In order to give a more meaningful picture of the coincidence obtained, isotherms were predicted for the agents using the DMMP characteristic curve and the empirical values of β. The

Figure 9

Characteristic Plots for Adsorbates on PCC
Affinity Coefficients Calculated from Parachors

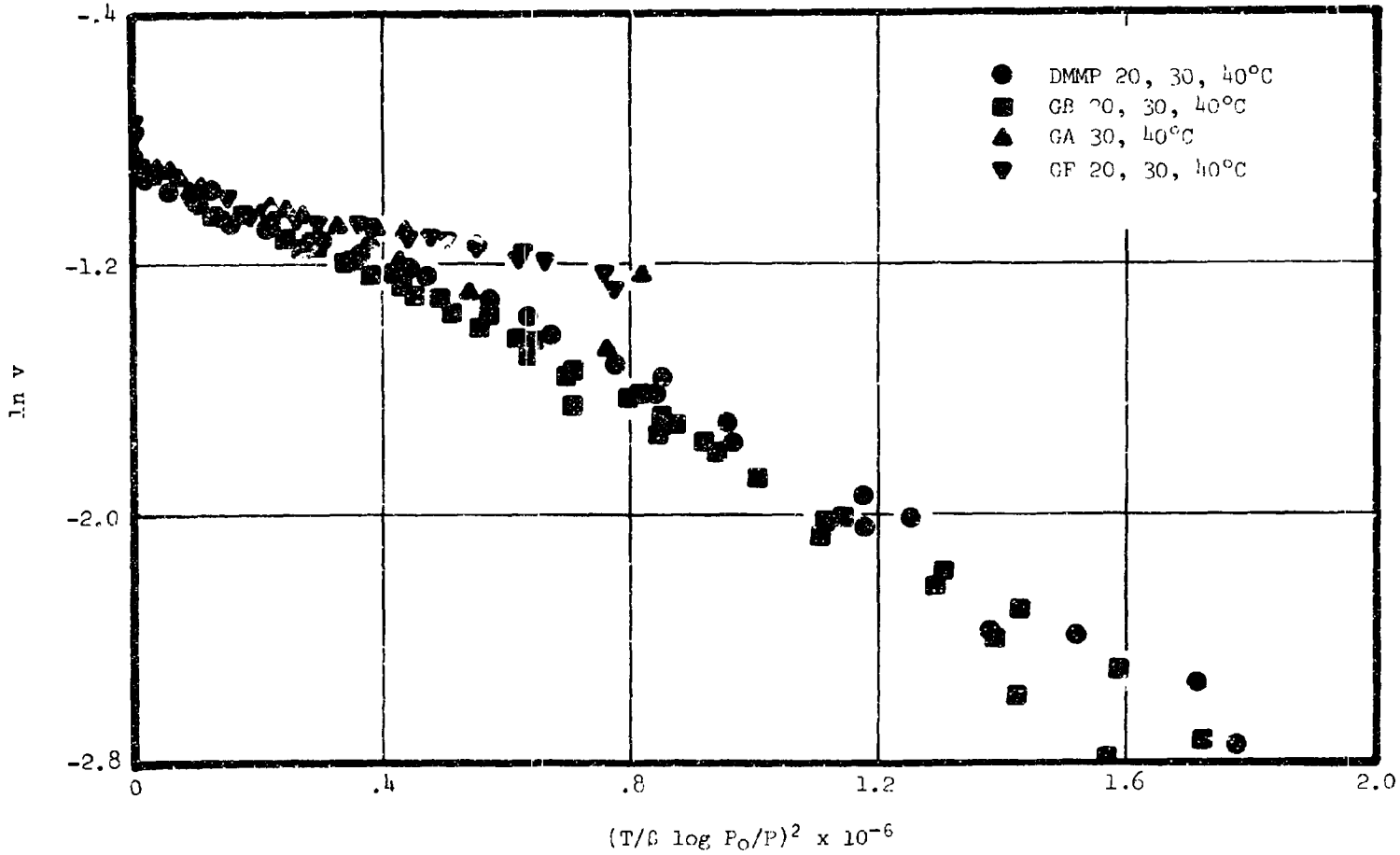

Figure 10

Characteristic Plots for Adsorbates on BC
Affinity Coefficients Calculated from Parachors

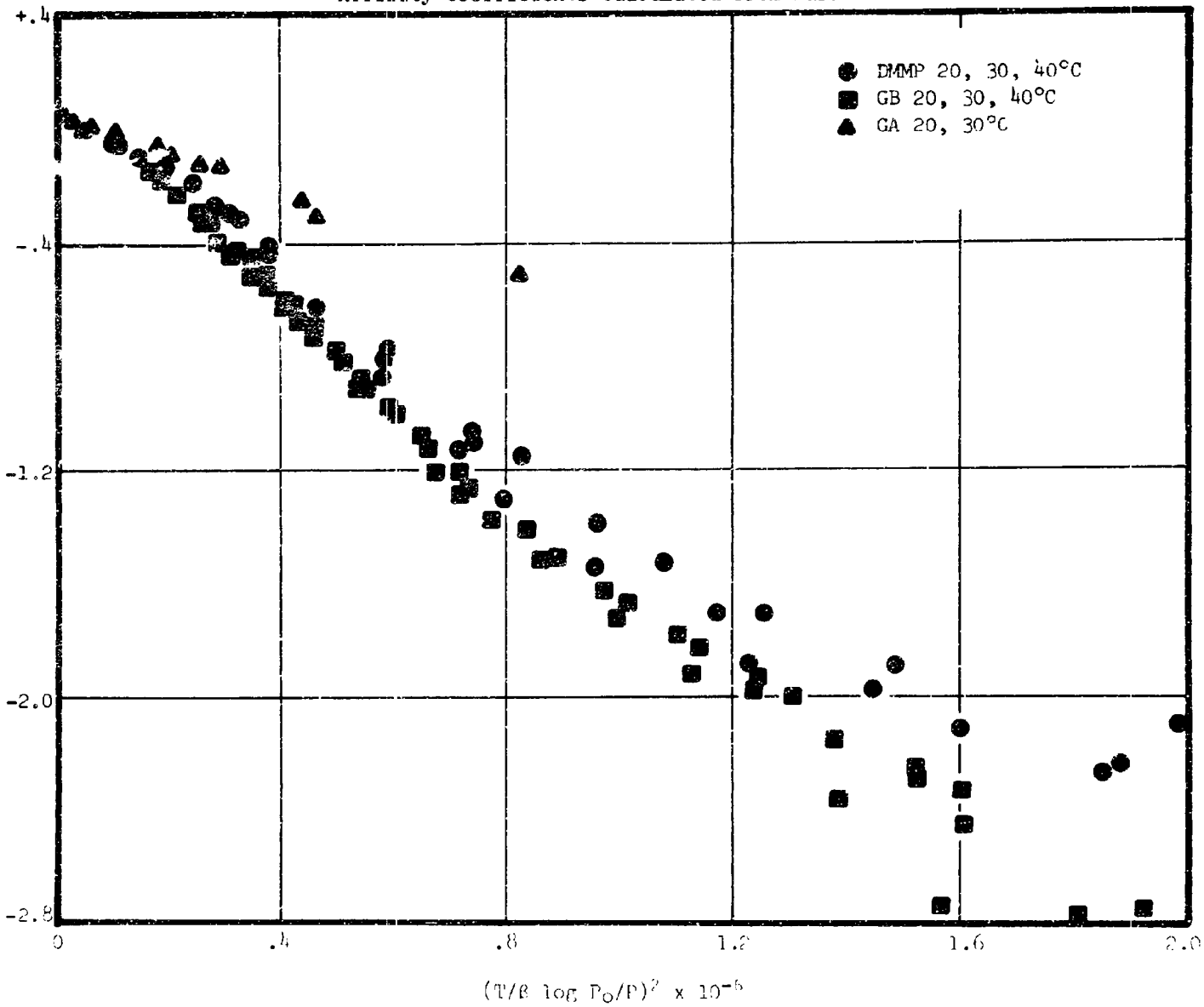

Figure 11

Characteristic Plots for Adsorbates on PCC
Empirical Affinity Coefficients

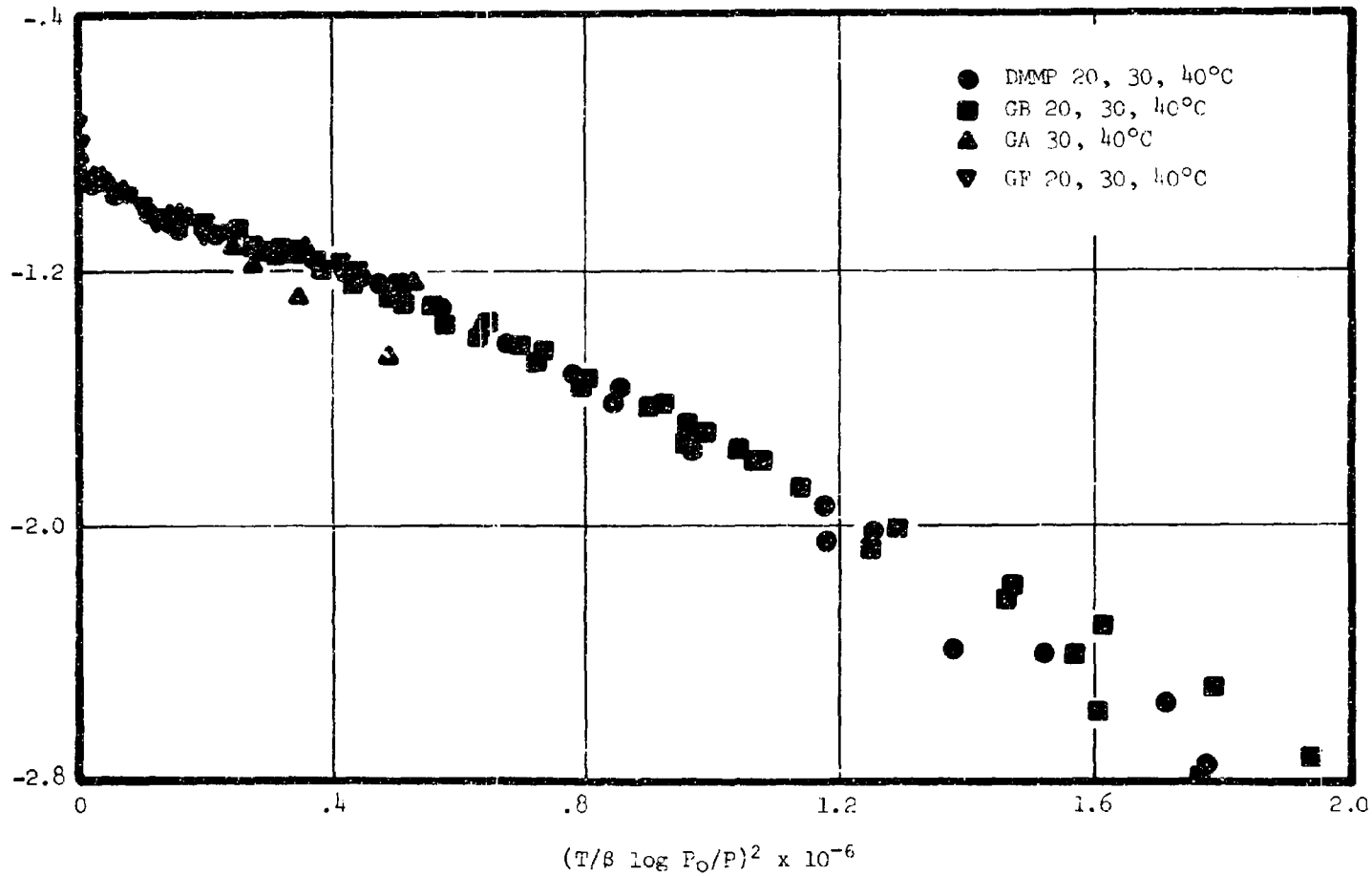

results for GB, GF and GA are shown in Figures 12, 13 and 14, respectively, where the lines represent the predicted isotherms and the points show experimental data. These predictions are seen to be reasonably good with the exception of GA at 40°C. Problems with GA may be related to the decomposition effects noted above.

If the empirical values of β are true characteristics of the adsorbates, then it should be possible to use these values to obtain coincidence between the characteristic curves of other carbons and to predict other isotherms. The characteristic curves for DMMP, GA and GB on the BC carbon are shown in Figure 15. The values of β used are the empirical values shown in Table I. The resulting adsorption isotherms predicted from the DMMP characteristic curve are shown in Figure 16 for GB and in Figure 17 for GA. It appears from this that the affinity coefficients determined for the agents from the results of work with the PCC carbon were reasonably successful in describing the relative adsorptivity of GB and GA on the BC carbon. This result is especially encouraging because of the very large differences in pore structure between the two carbons.

D. Equilibrium Adsorption Measurements With Other Adsorbates

Another phase of the experimental program was intended to investigate the effects of adsorbate properties such as chemical type upon the shape of characteristic curves and trends in the affinity coefficients.

The adsorbates which were to be used were common organic vapors having relatively well defined physical properties and good stabilities. They were also quite volatile relative to the previously investigated agents and auxiliary pressure measuring instruments were installed in order to determine isotherms at pressures above the range of the thermistor manometer. The manometer used for this was a Granville-Phillips capacitance manometer which had a differential pressure range of 100 torr. Originally this instrument was calibrated against an accurate mercury U-tube manometer and a wide range McLeod gauge so that direct readings might be made but it was discovered after a considerable amount of work had been expended that the instrument would not hold its calibration and that readings had to be made by a null balance technique. Because of this and other experimental difficulties the only data in which much confidence can be placed are those for carbon tetrachloride and benzene on the PCC and BC carbons.

Because the original objectives could not be realized with these data, it was decided to find out how well isotherms for GB, GA and GF and the simulent DMMP could be predicted using characteristic curves for carbon tetrachloride on the PCC and BC carbons. Because of the great differences in properties

Figure 12a

GB on PCC - High Pressure Range

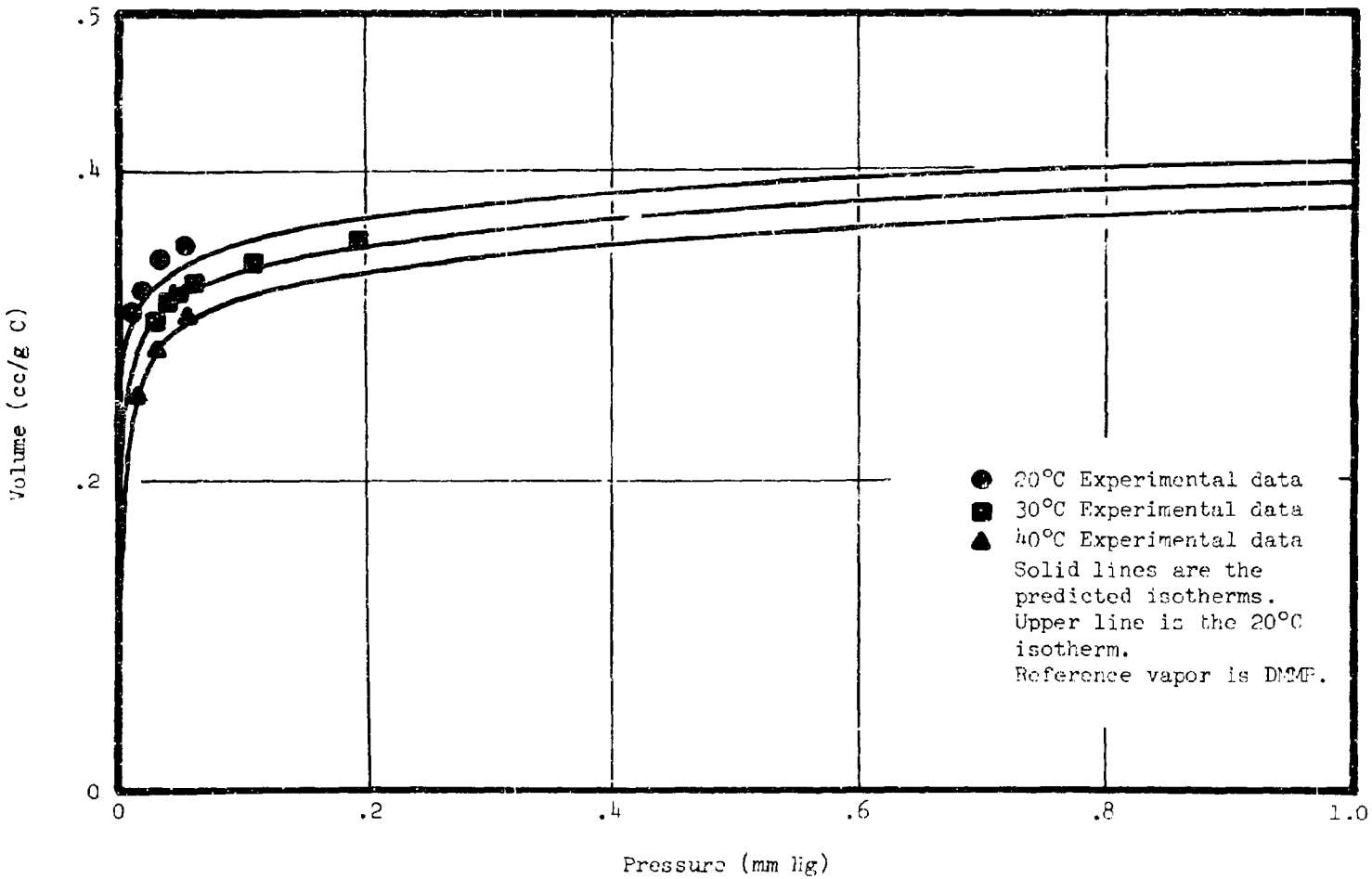

Figure 12b

GB on PCC - Medium Pressure Range

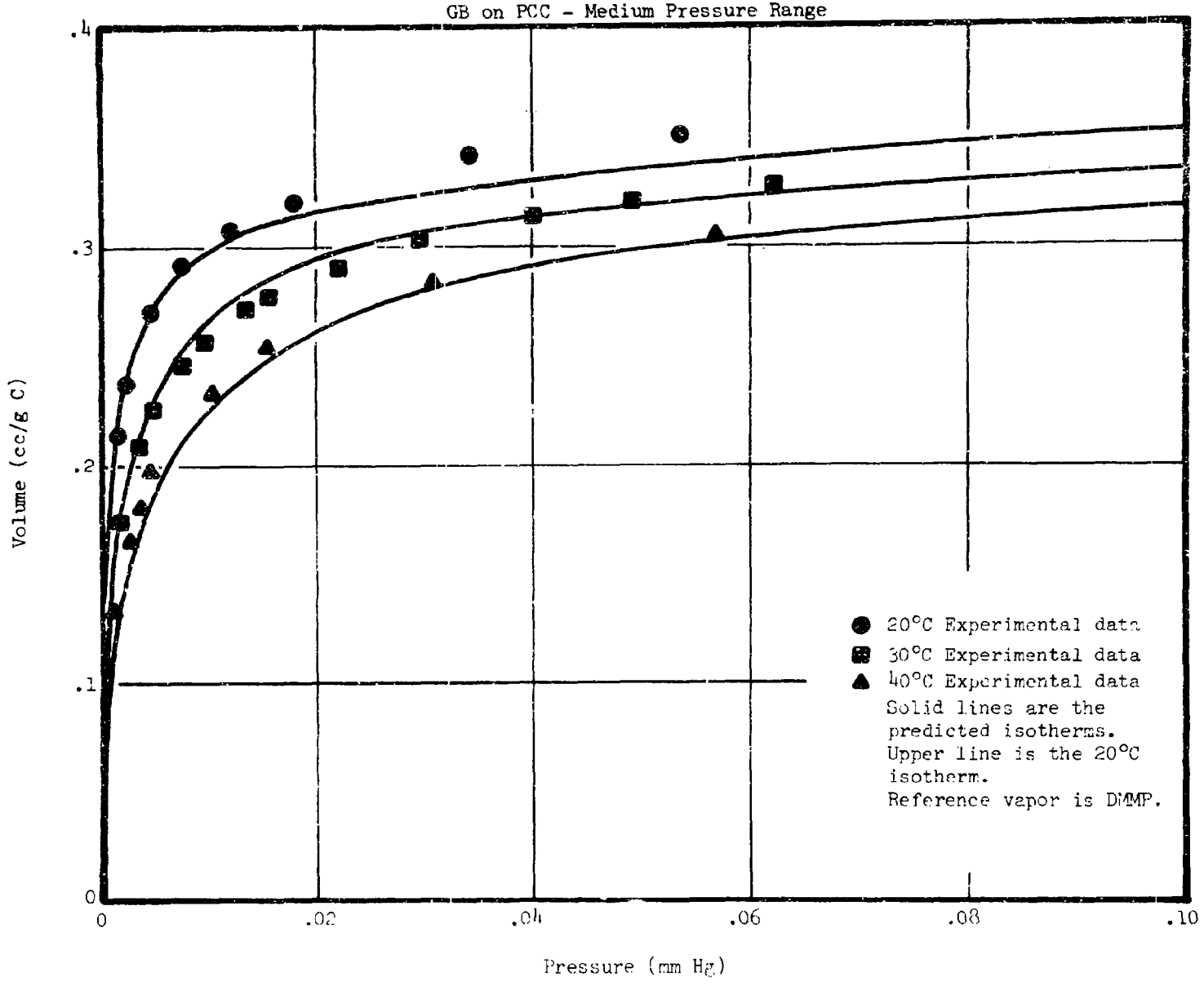

Figure 12c

GB on PCC - Low Pressure Range

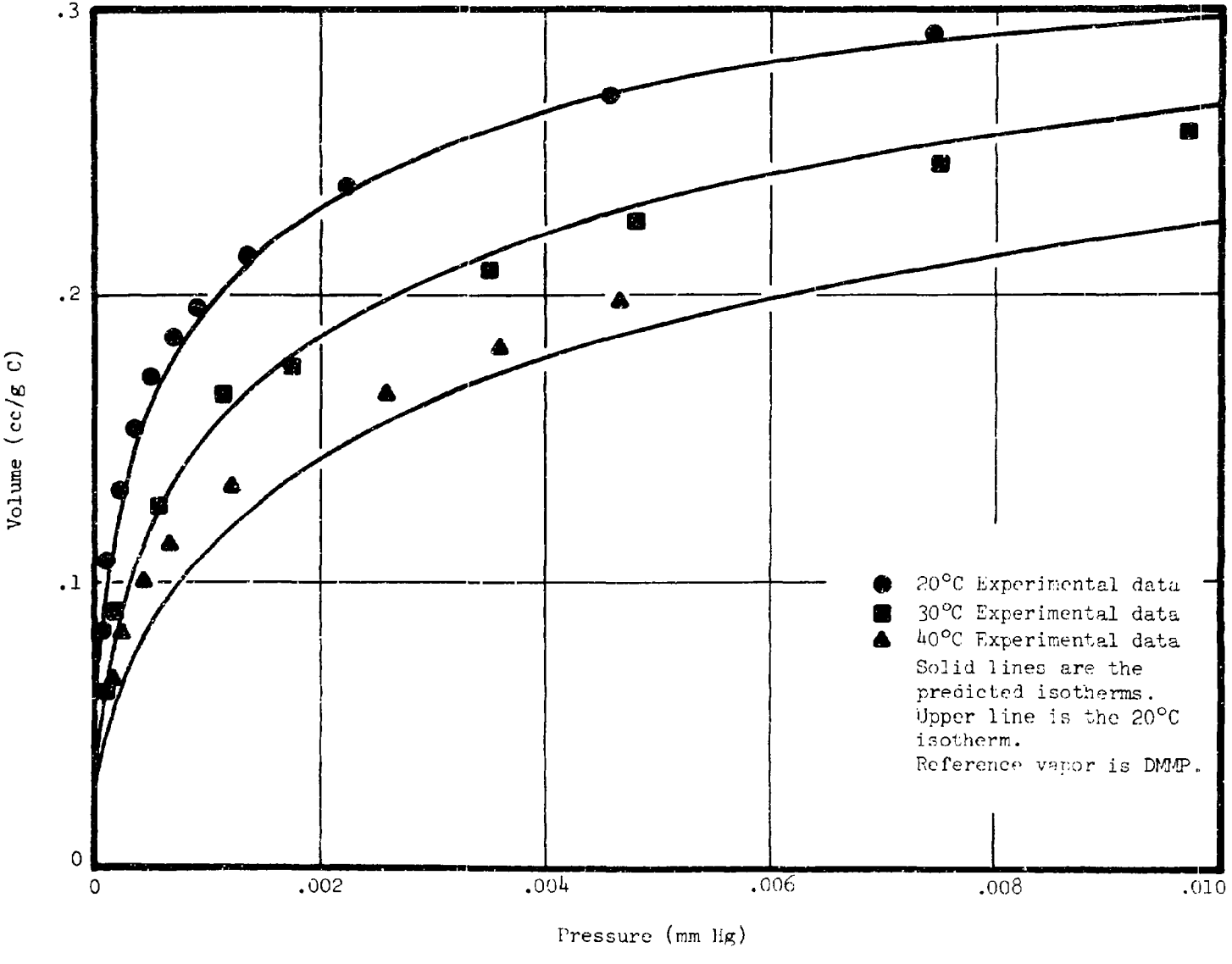

Figure 13a

GA on PCC - High Pressure Range

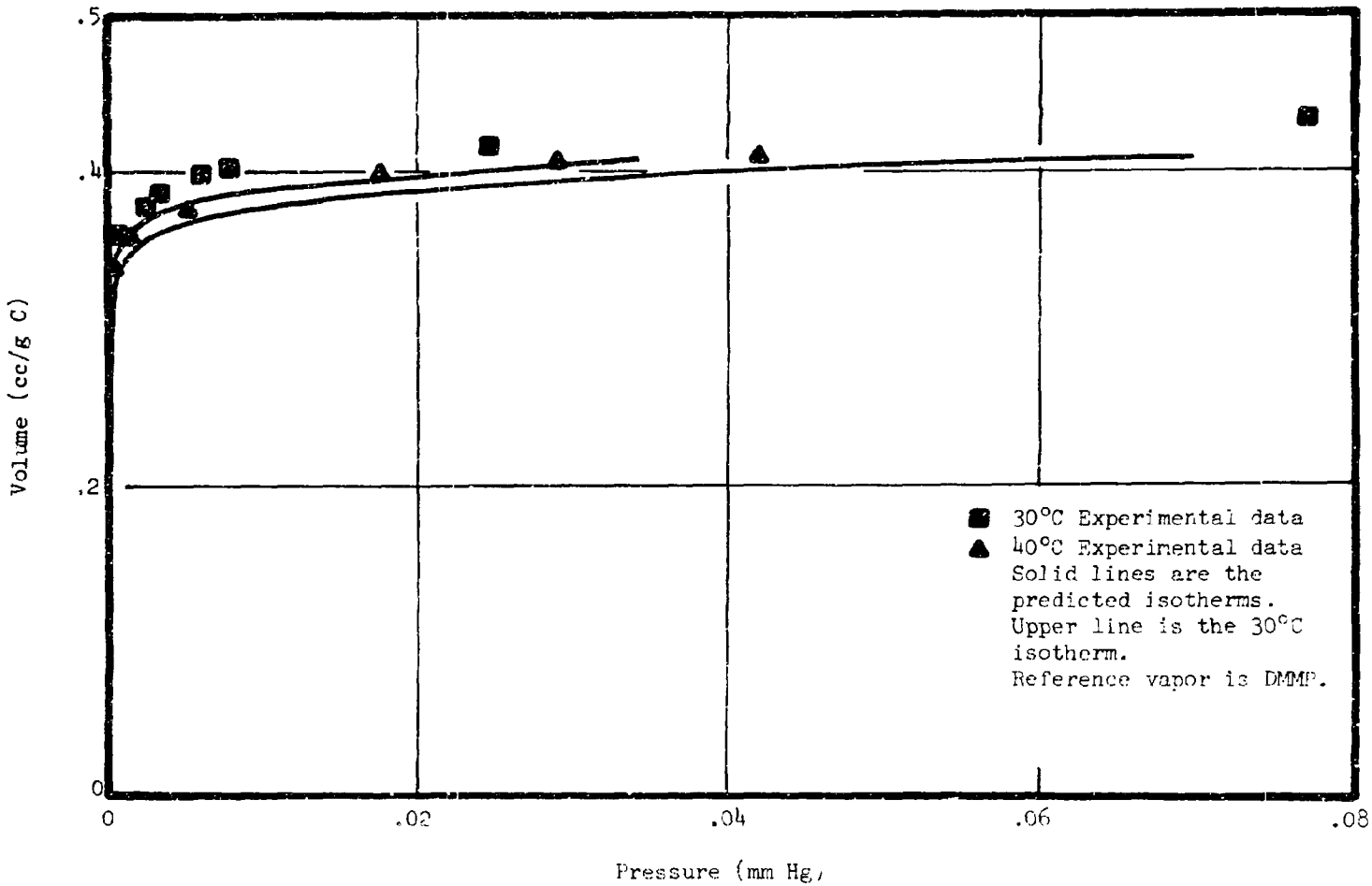

Figure 13b

GA on PCC - Medium Pressure Range

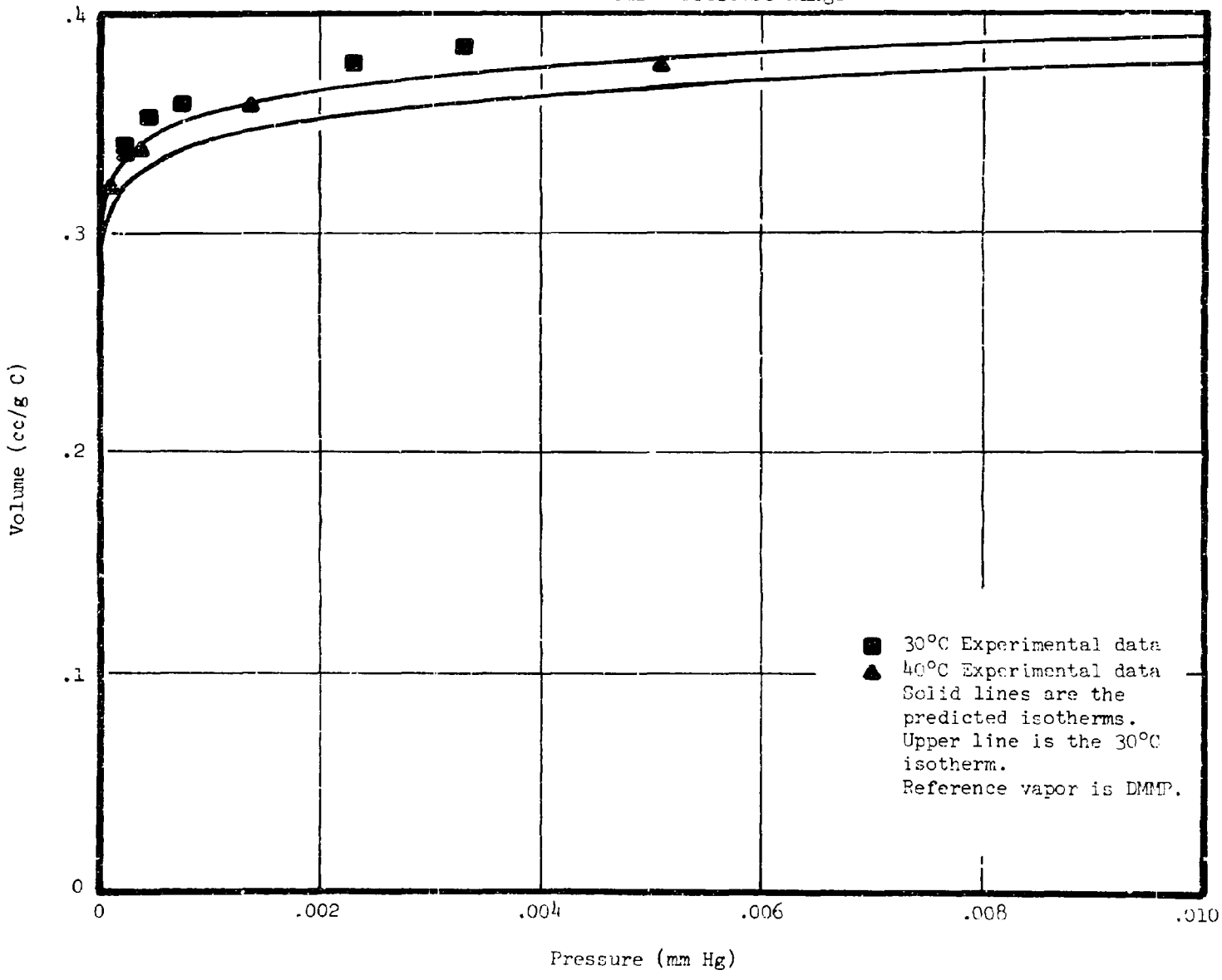

Figure 13c

GA on PCC - Low Pressure Range

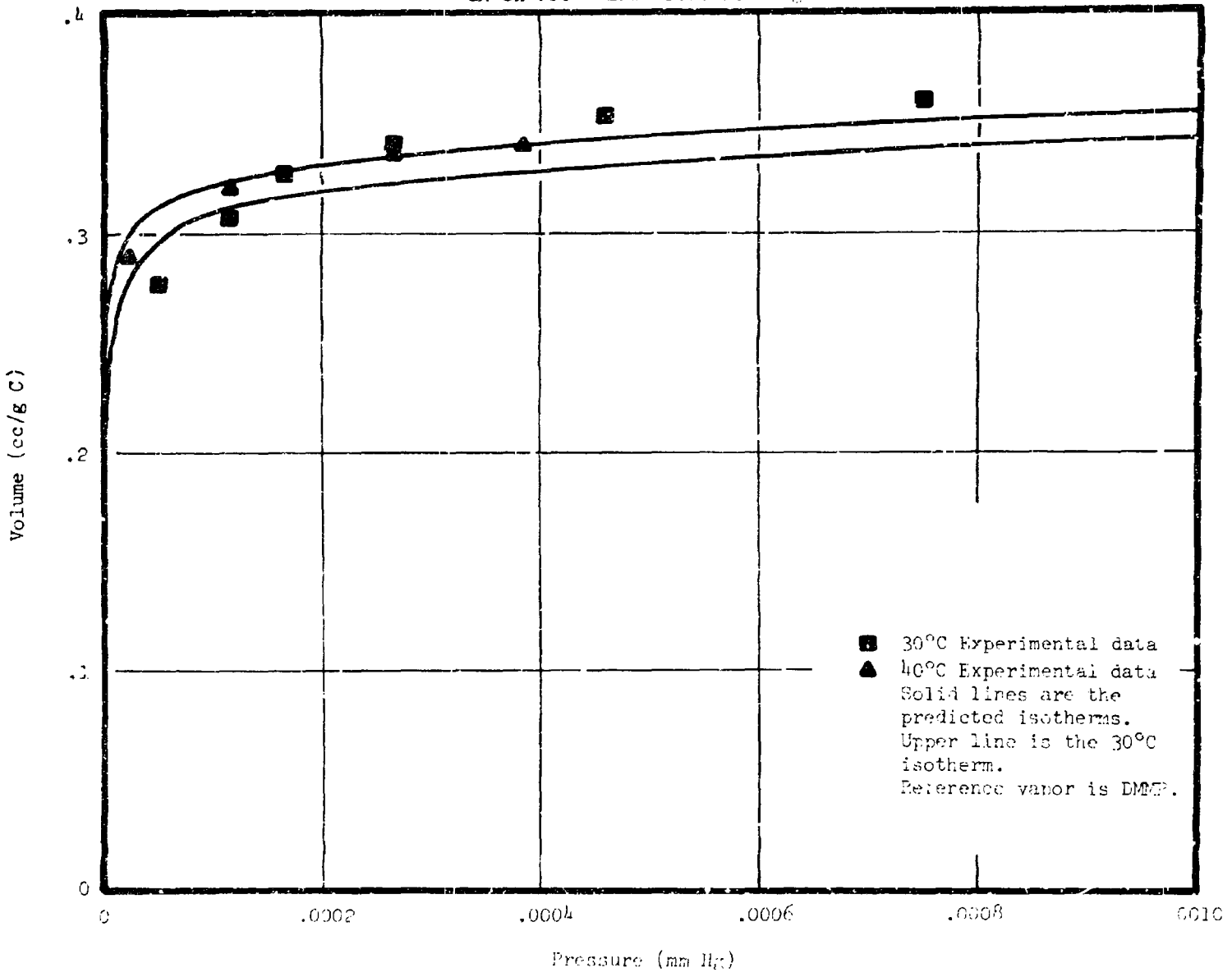

Figure 14a

CF on FCC - High Pressure Range

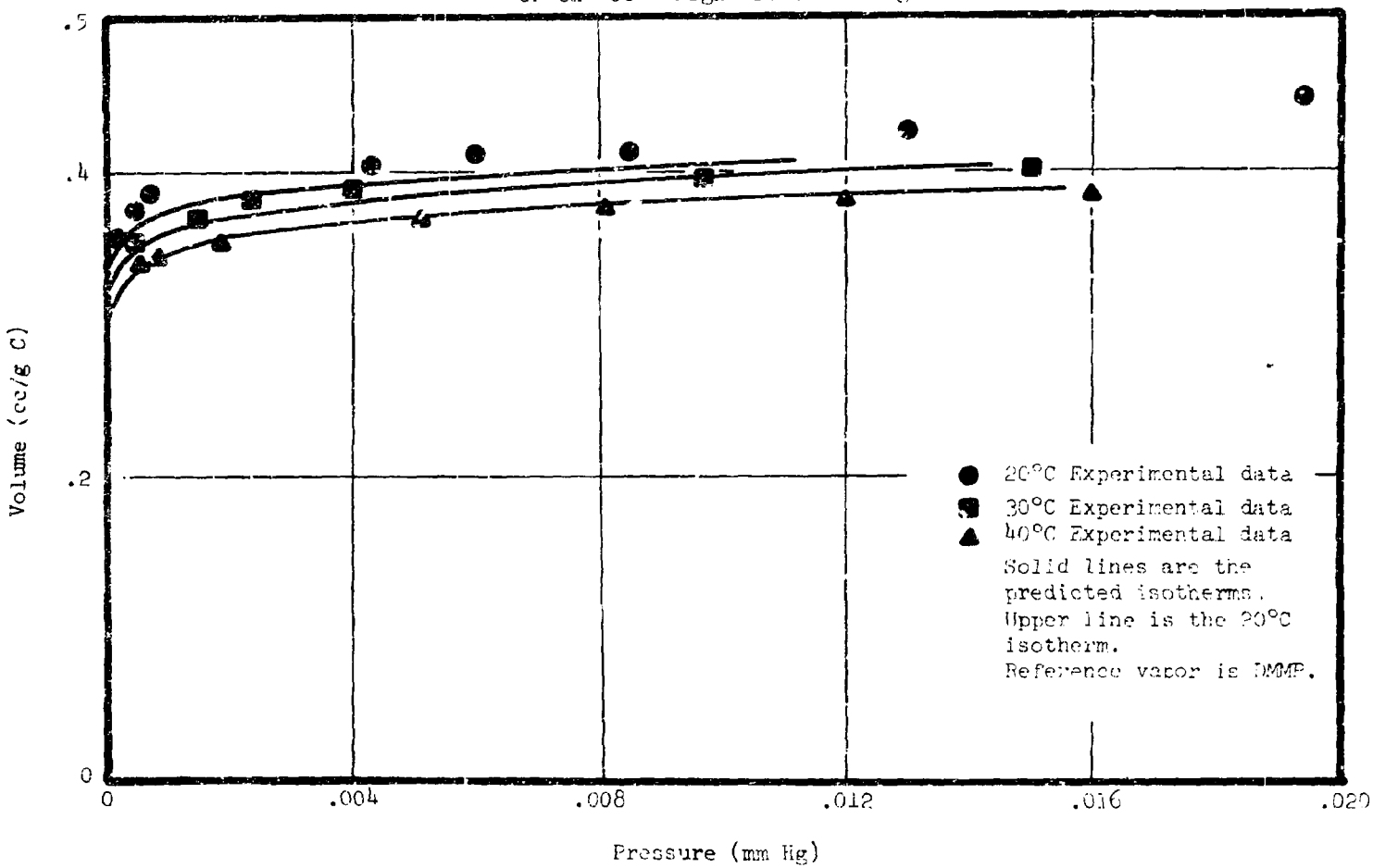

Figure 14b

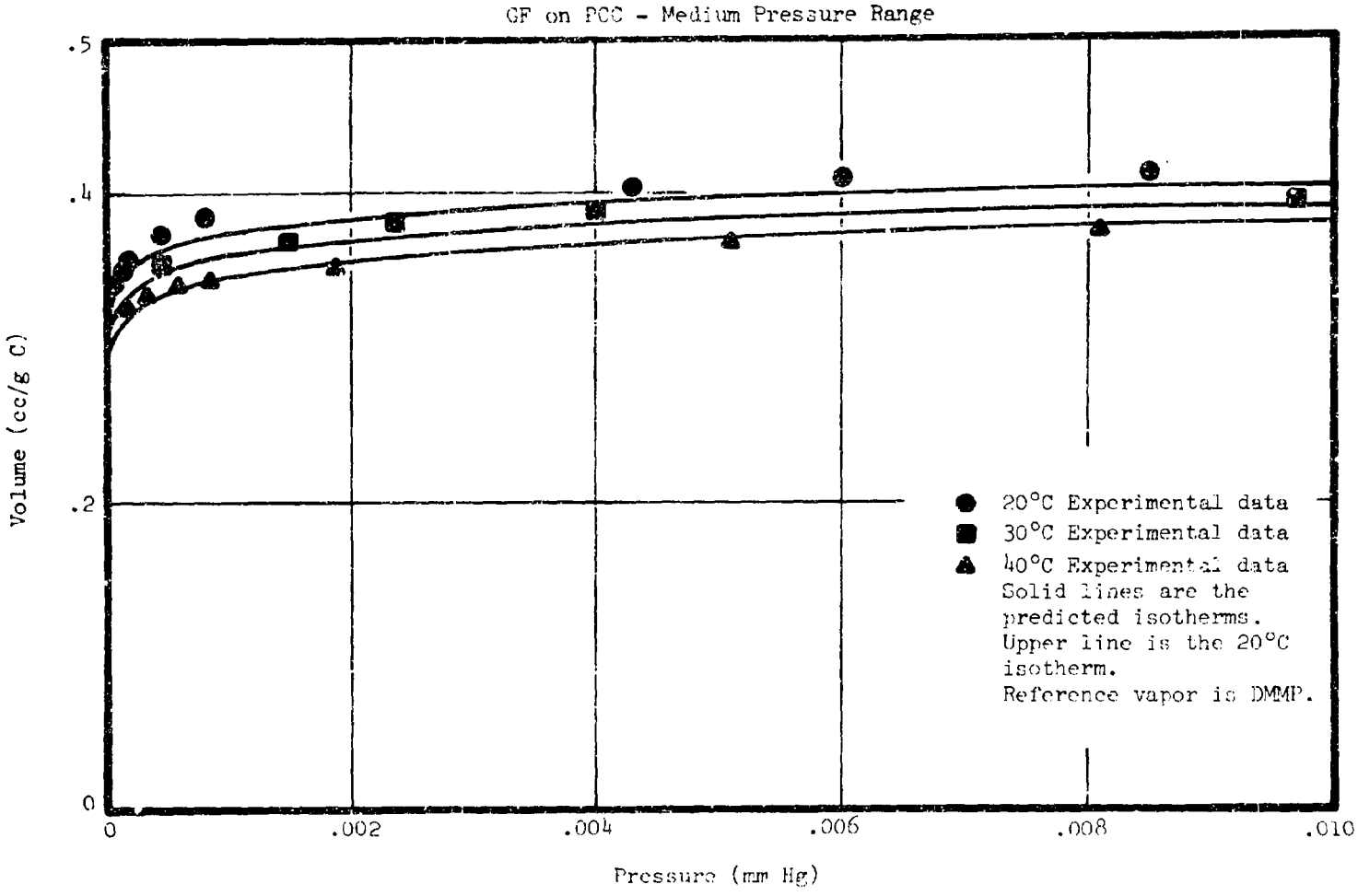
GF on PCC - Medium Pressure Range
Volume (cc/g C)
.5
.4
.2
0
0
.002
.004
.006
.008
.010
Pressure (mm Hg)
20°C Experimental data
30°C Experimental data
40°C Experimental data
Solid lines are the predicted isotherms.
Upper line is the 20°C isotherm.
Reference vapor is DMMP.

Figure 14c

GF on PCC - Low Pressure Range

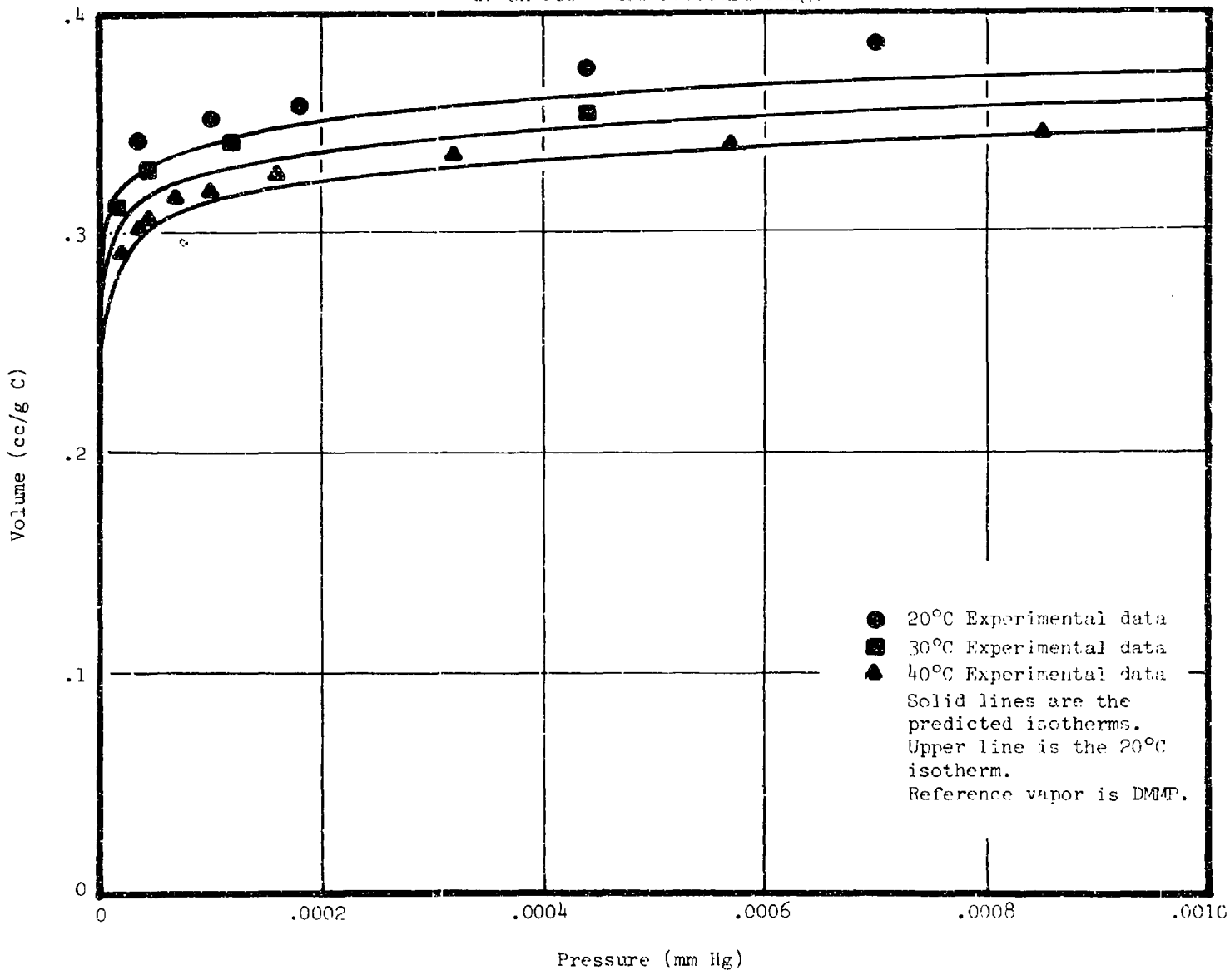

Figure 15

Characteristic Plots for Adsorbates on BC
Empirical Affinity Coefficients

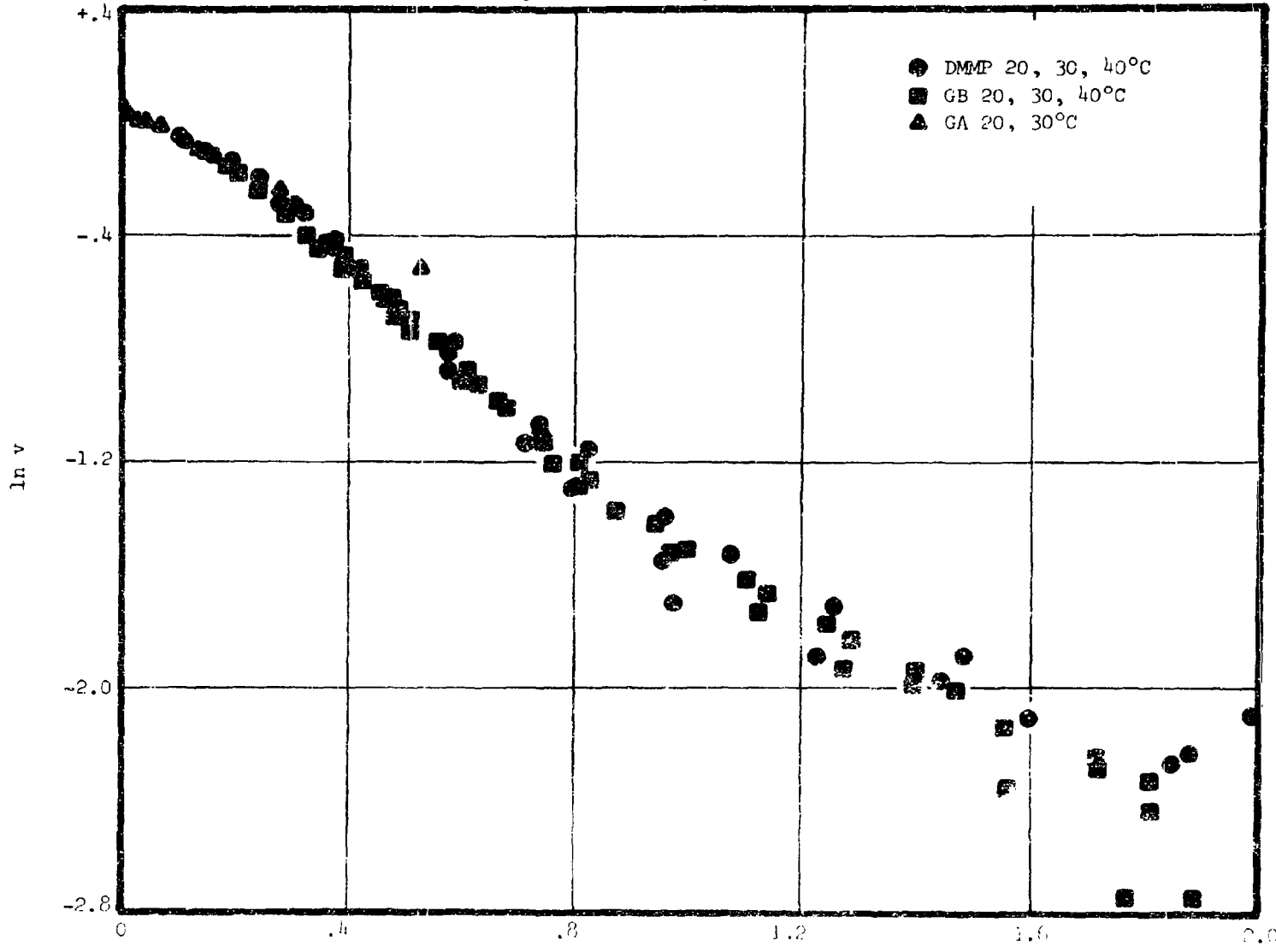

Figure 16a

GB on BC - High Pressure Range

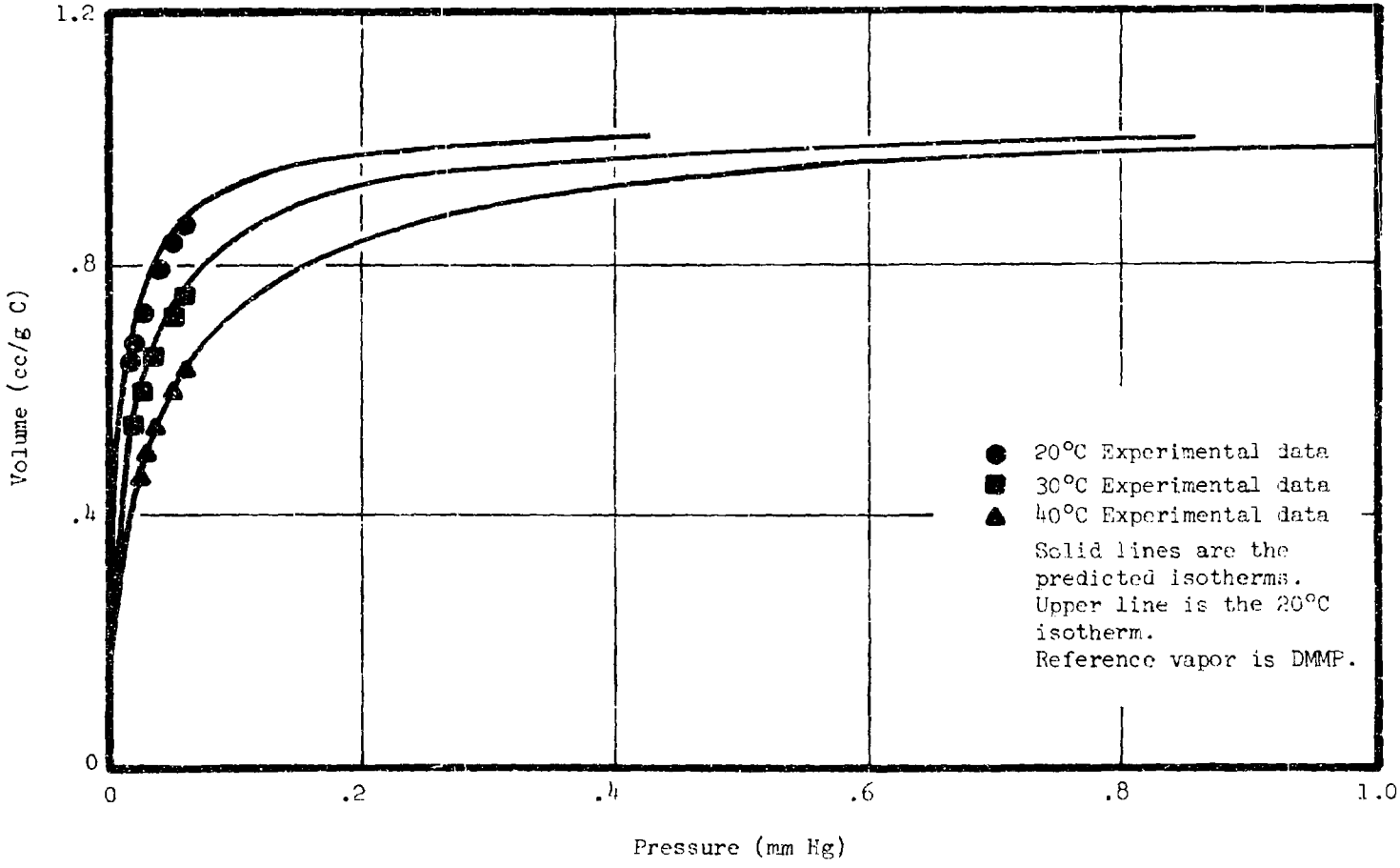

Figure 16b

GB on BC - Medium Pressure Range

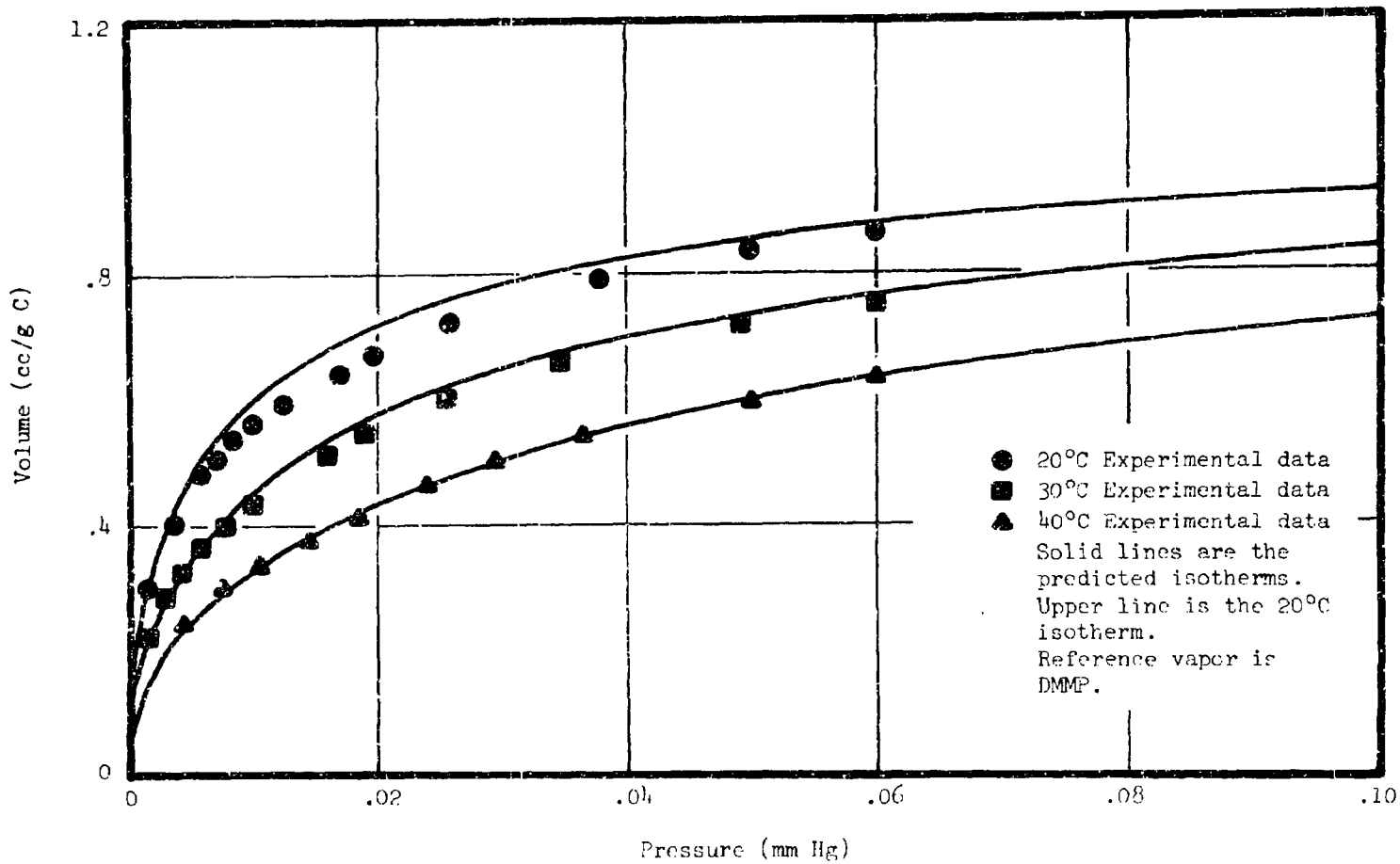

Figure 16c

GB on BC - Low Pressure Range

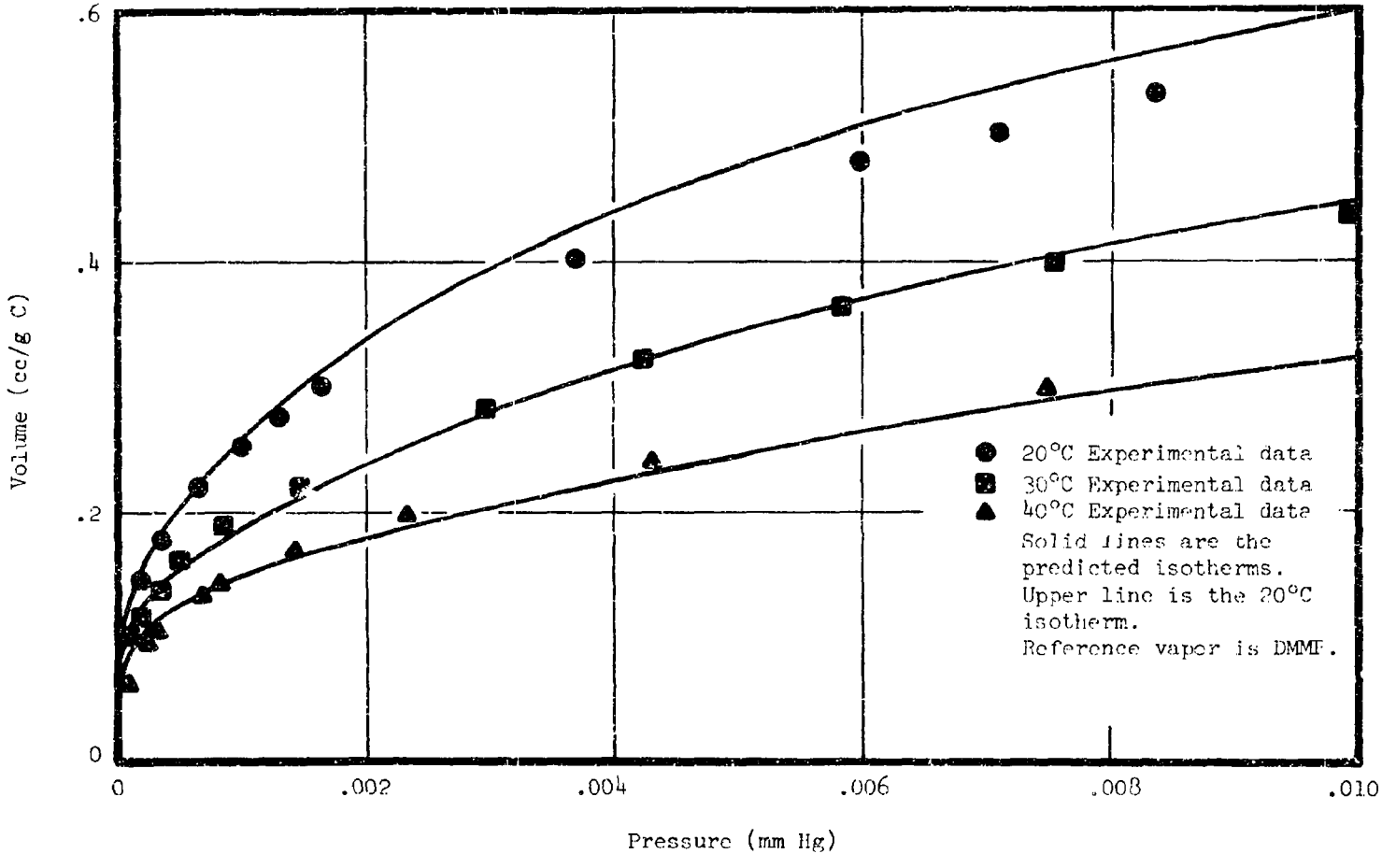

Figure 17a

GA on BC - High Pressure Range

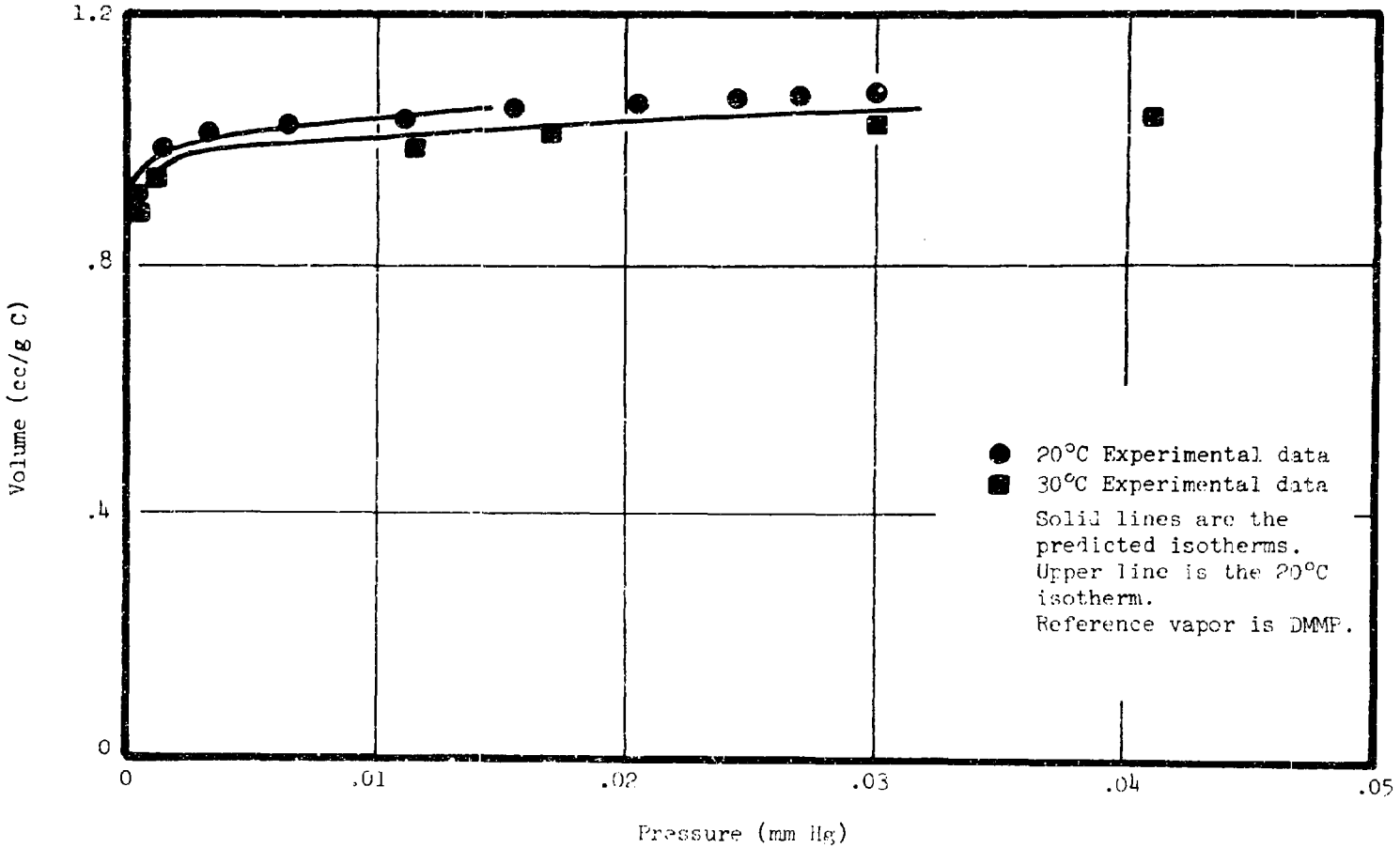

Figure 17b

GA on BC - Medium Pressure Range

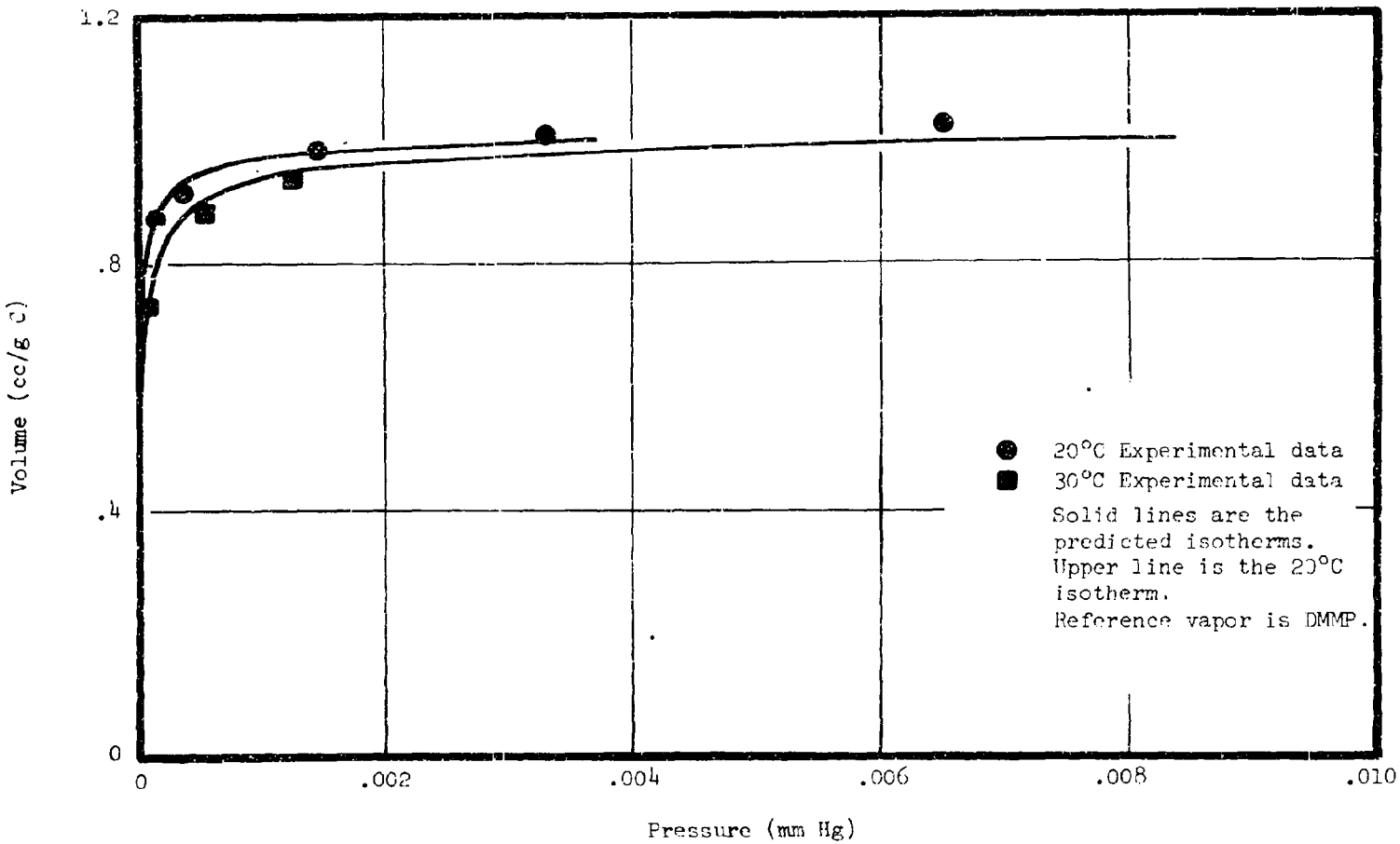

Figure 17c

GA on BC - Low Pressure Range

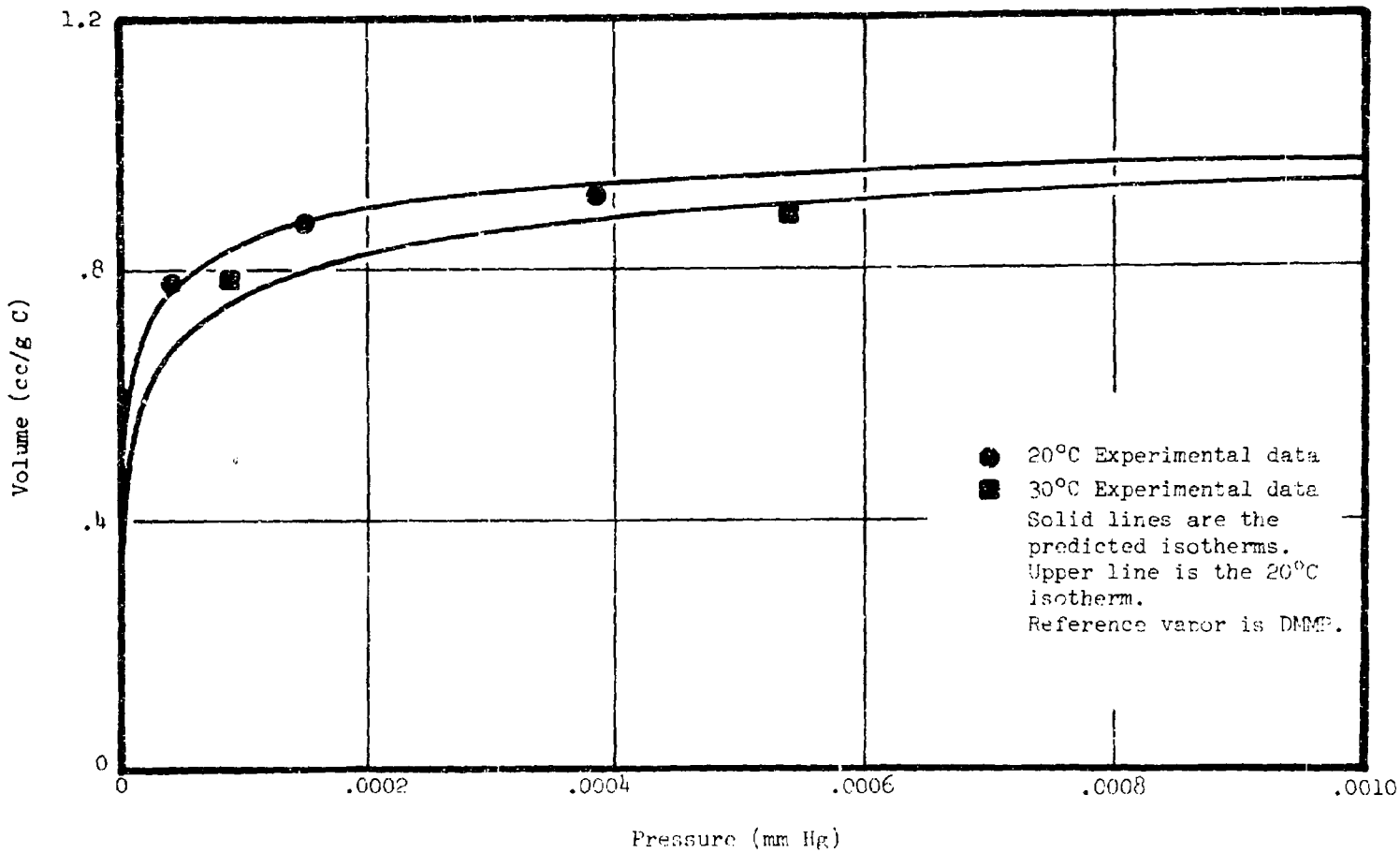

between $CCl_4$ and the G agents, $CCl_4$ is not generally thought of as a simulent. However if there is general validity to the use of the Dubinin method, this vapor might be suitable as far as adsorption is concerned if the degree of nondispersive adsorption interactions is low in agent adsorption. There would be some advantages in using $CCl_4$ as a simulent with respect to ease and accuracy of isotherm measurements. The vapor pressure of the liquid is relatively high so that characteristic curve data corresponding to very low agent pressures could be obtained without actually having to measure these low pressures. Carbon tetrachloride is also easily obtainable at high purity and its physical properties are well defined.

Isotherm predictions made for the PCC carbon using the experimental characteristic curve for $CCl_4$ (Figure 18) are shown in Figures 19 - 22 for DMMP, GB, GA and GF, respectively. The values of $\beta$ used were obtained by finding the relative strength of the interaction between $CCl_4$ and DMMP by matching characteristic curves on the PCC carbon using $CCl_4$ as the reference material. The resulting factor was then used to multiply values of $\beta$ for the other agents determined previously with reference to DMMP. Values of $\beta$ for the $CCl_4$ reference are listed in Table II along with those values calculated from parachors.

TABLE II

VALUES OF $\beta$ WITH REFERENCE TO $CCl_4$

| | Empirical | From Parachors |
|---|---|---|
| $CCl_4$ | 1.00 | 1.00 |
| DMMP | 1.06 | 1.20 |
| GB | 1.10 | 1.32 |
| GA | 1.80 | 1.63 |
| GF | 1.88 | 1.73 |

In Figures 19 - 22, the predicted isotherms are shown as solid lines and the points represent experimental data. It is seen that in general the fits obtained are fairly good with the major deviation occurring at the higher pressures where the $CCl_4$ characteristic curve does not seem to have the same shape as that for DMMP. An exception to this occurs with the data for GA, although these may have been influenced by decomposition.

Predictions were also made for the BC carbon based upon $CCl_4$ data. Values of $\beta$ were independently determined by matching the DMMP data with the $CCl_4$ characteristic curves show in Figure 23 and in this case the $\beta$ for DMMP was 1.05. This value was chosen to fit the data in the low pressure range and the correspondence in other ranges might look better if a slightly higher $\beta$ had been taken. In any case, it is seen that there is

Figure 18

Characteristic Curve for $CCl_4$ on PCC

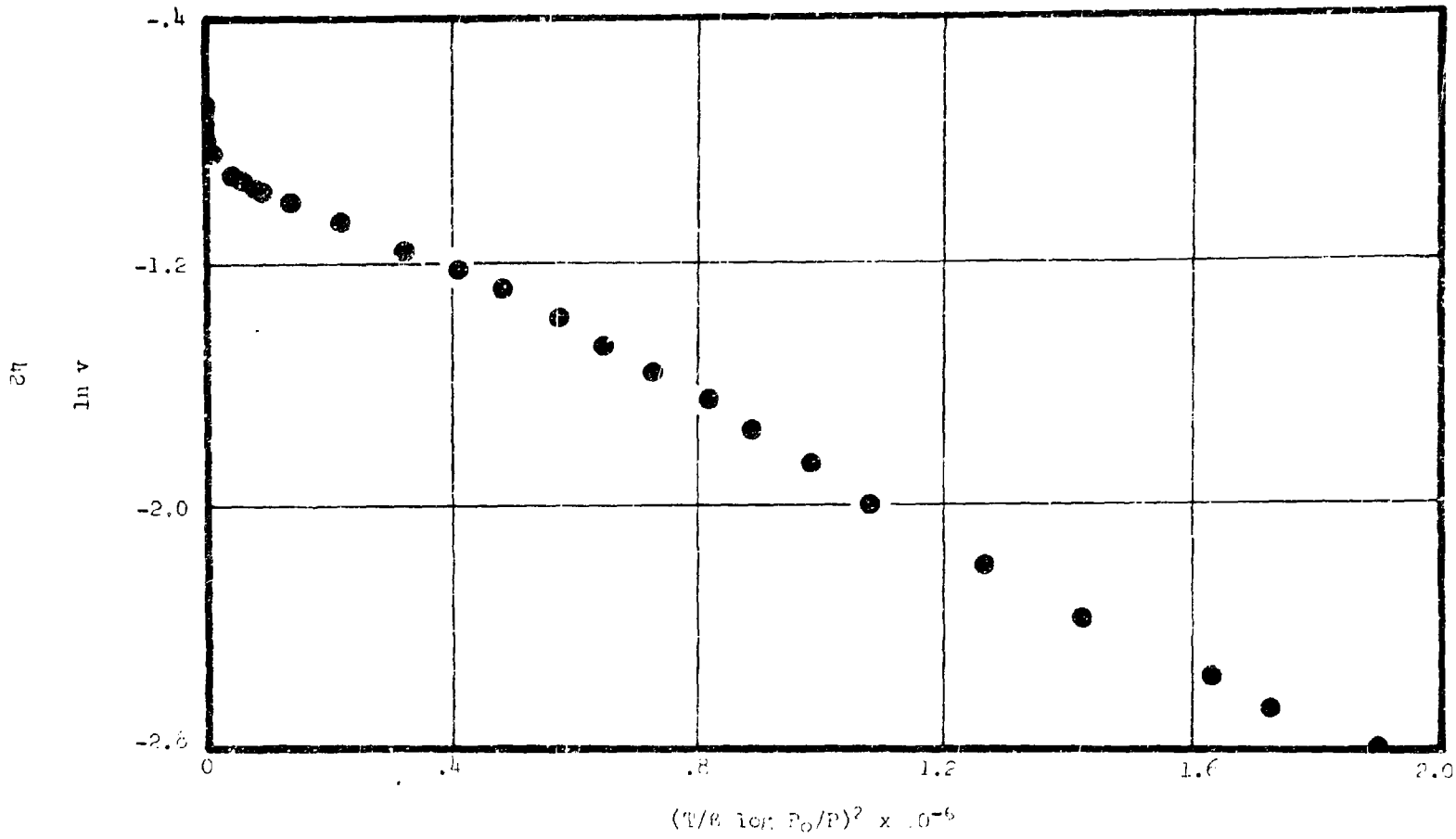

Figure 19a

DMMP on PCC - High Pressure Range

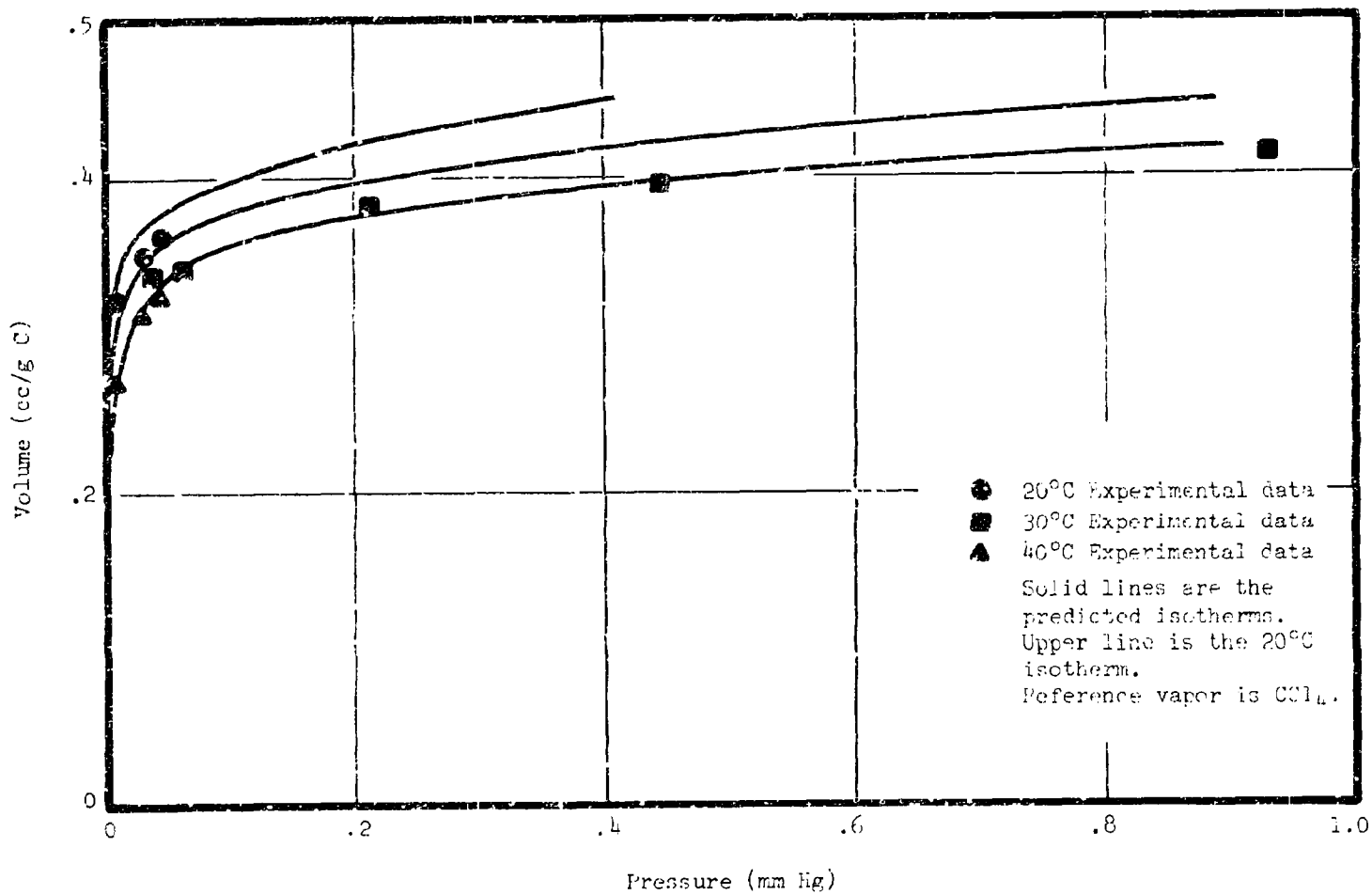

Figure 19b

DMMP on PCC - Medium Pressure Range

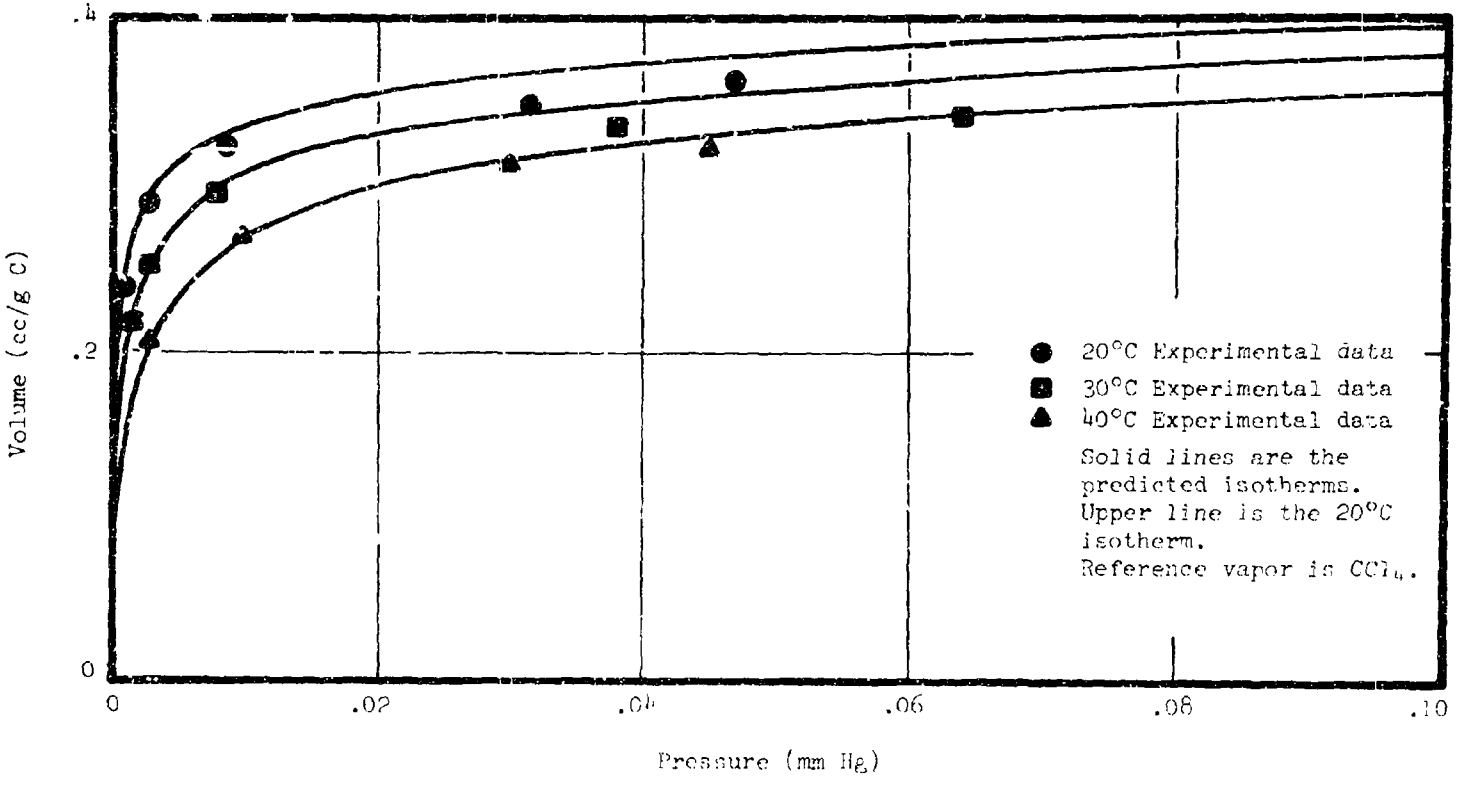

Figure 19c

DMMP on PCC - Low Pressure Range

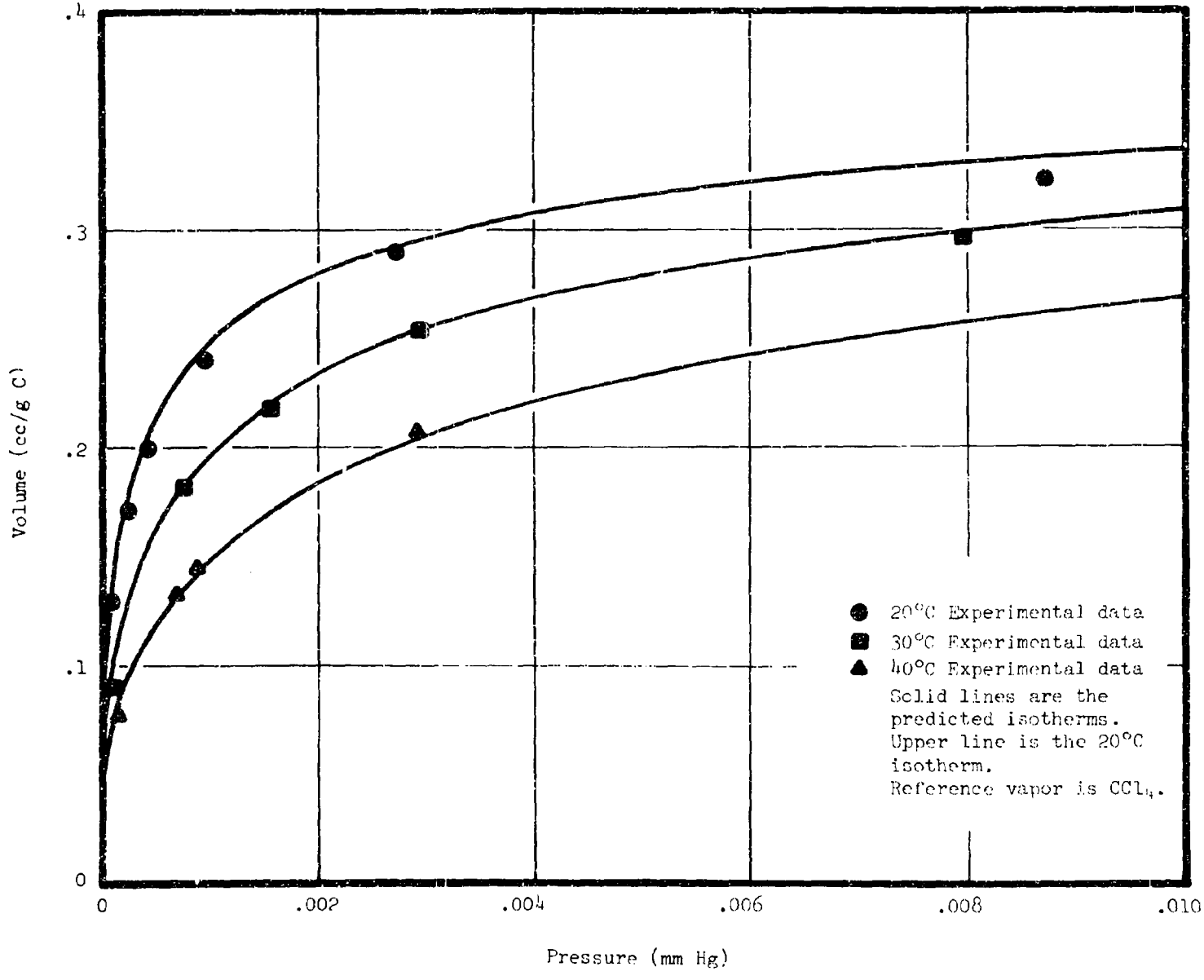

Figure 20a

GB on PCC - High Pressure Range

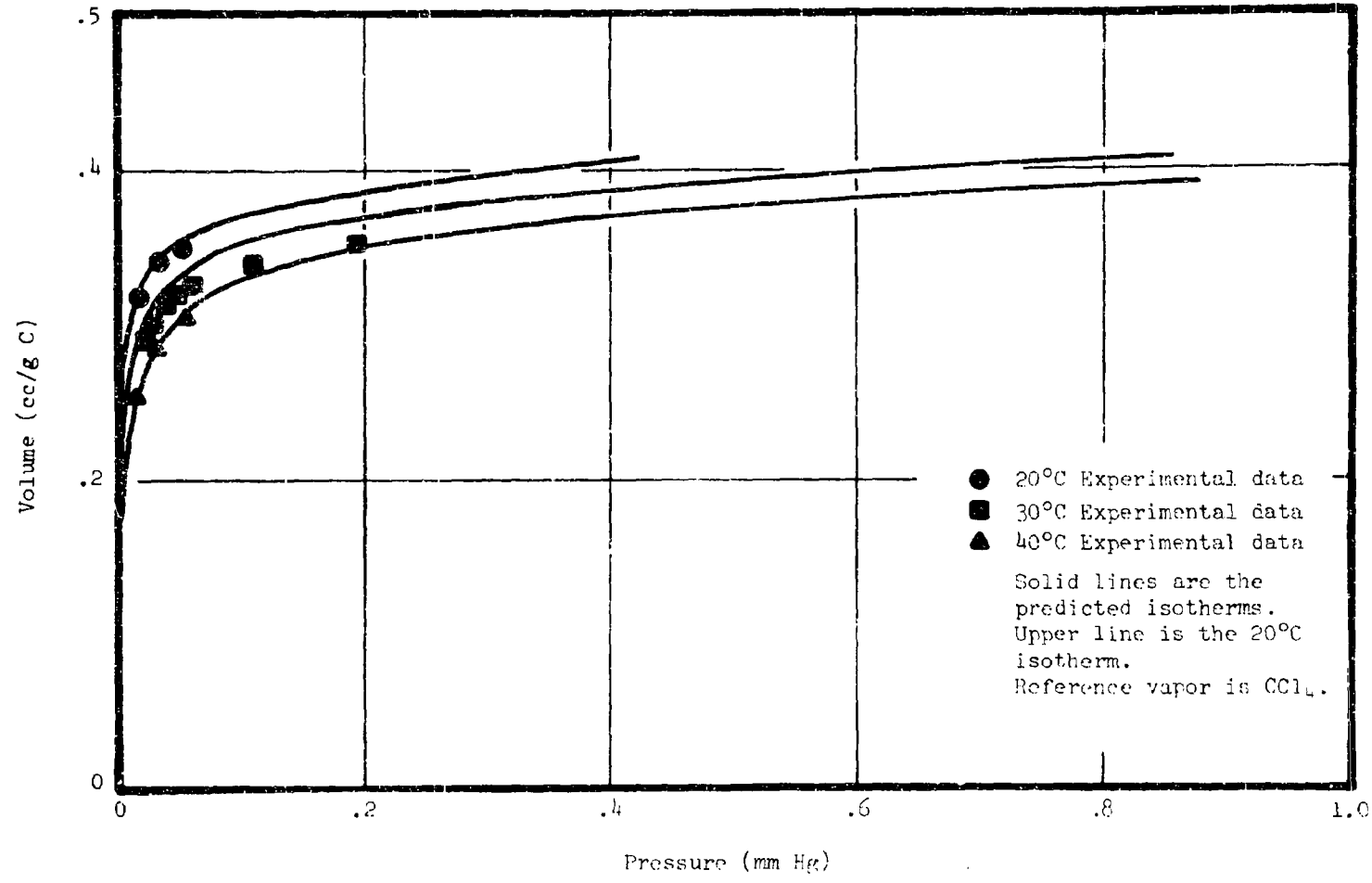

Figure 20b

GB on FCC - Medium Pressure Range

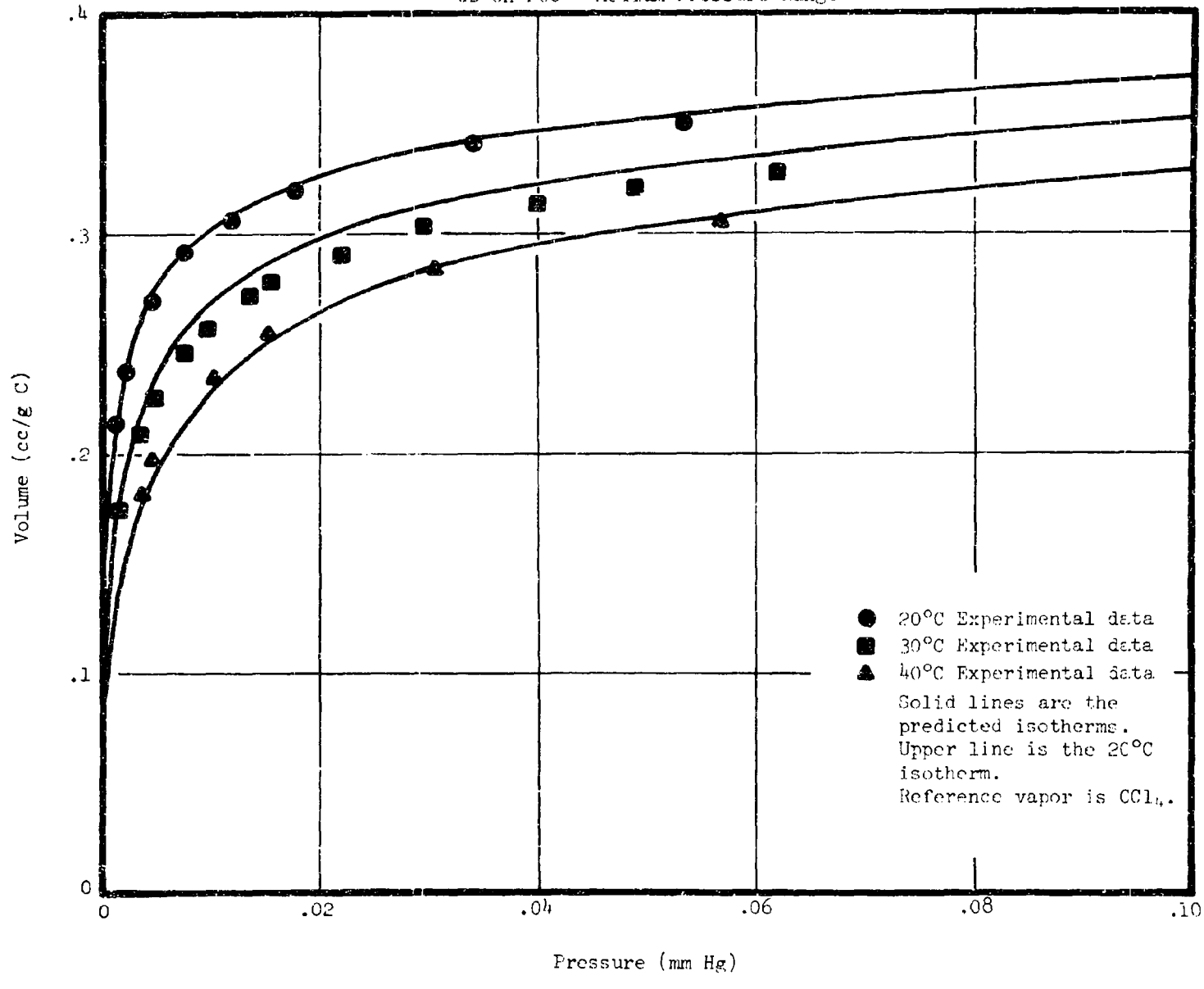

Figure 20c

GB on PCC - Low Pressure Range

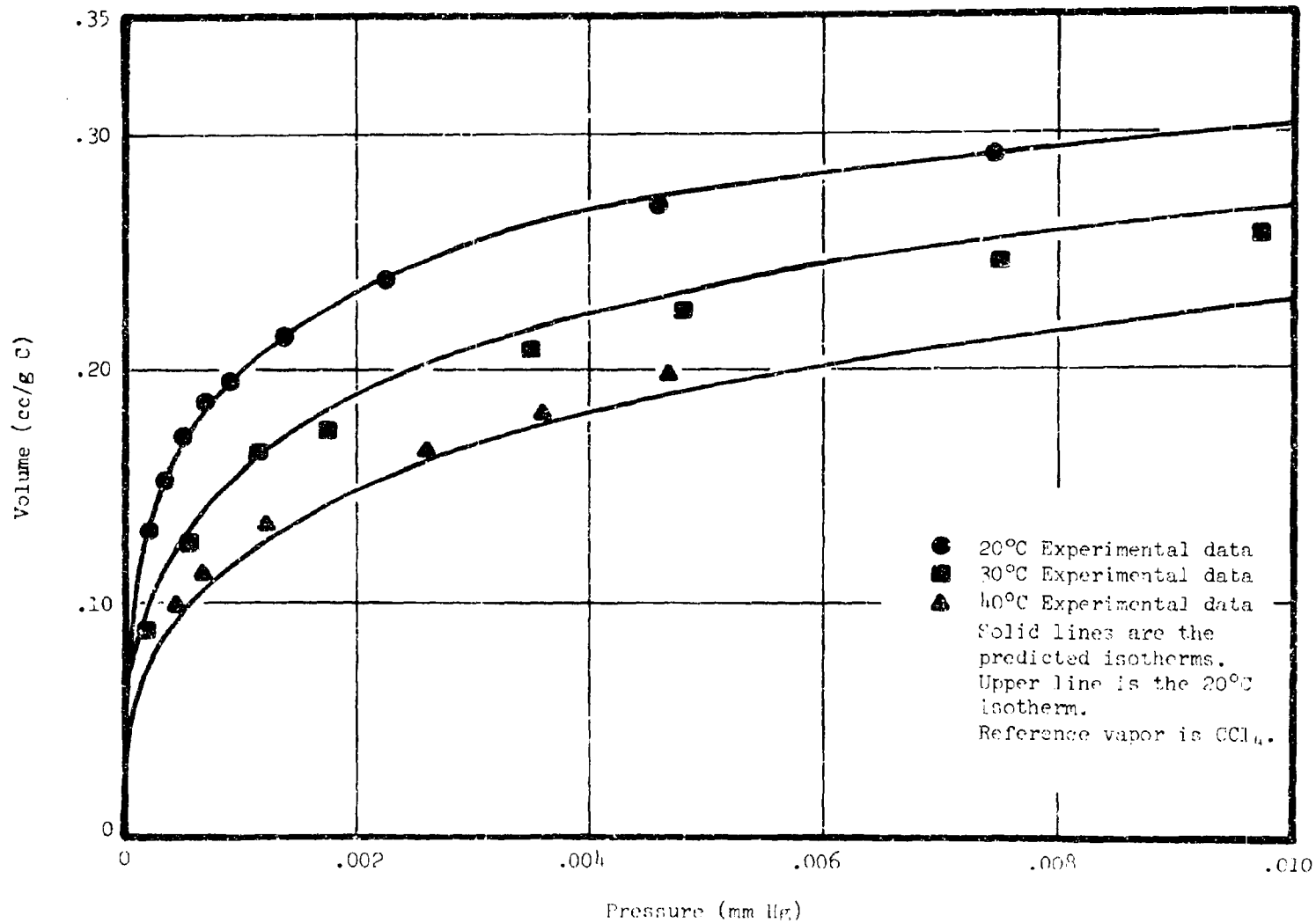

Figure 21a

GA on FCC - High Pressure Range

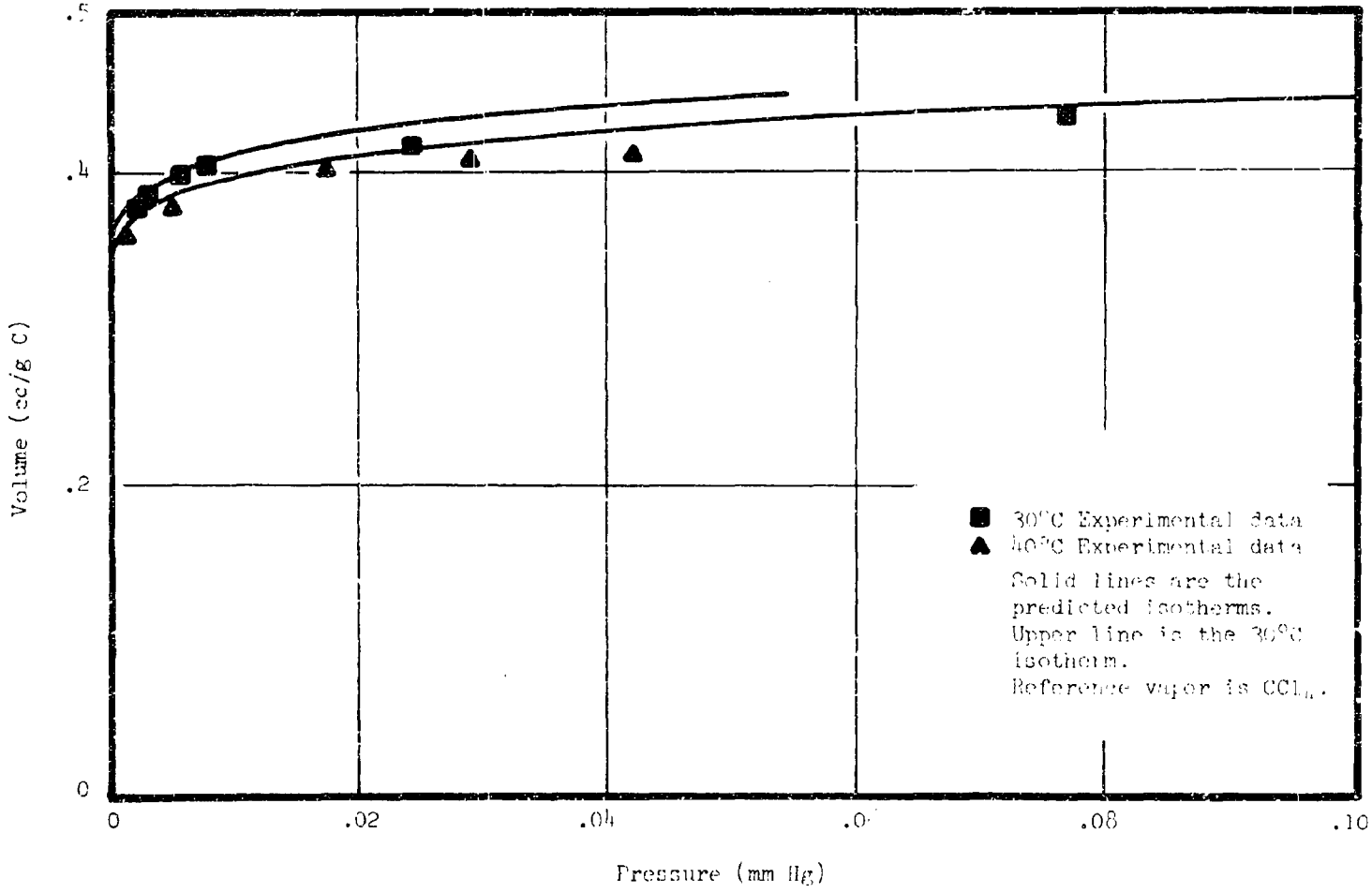

Figure 21b

GA on PCC - Medium Pressure Range

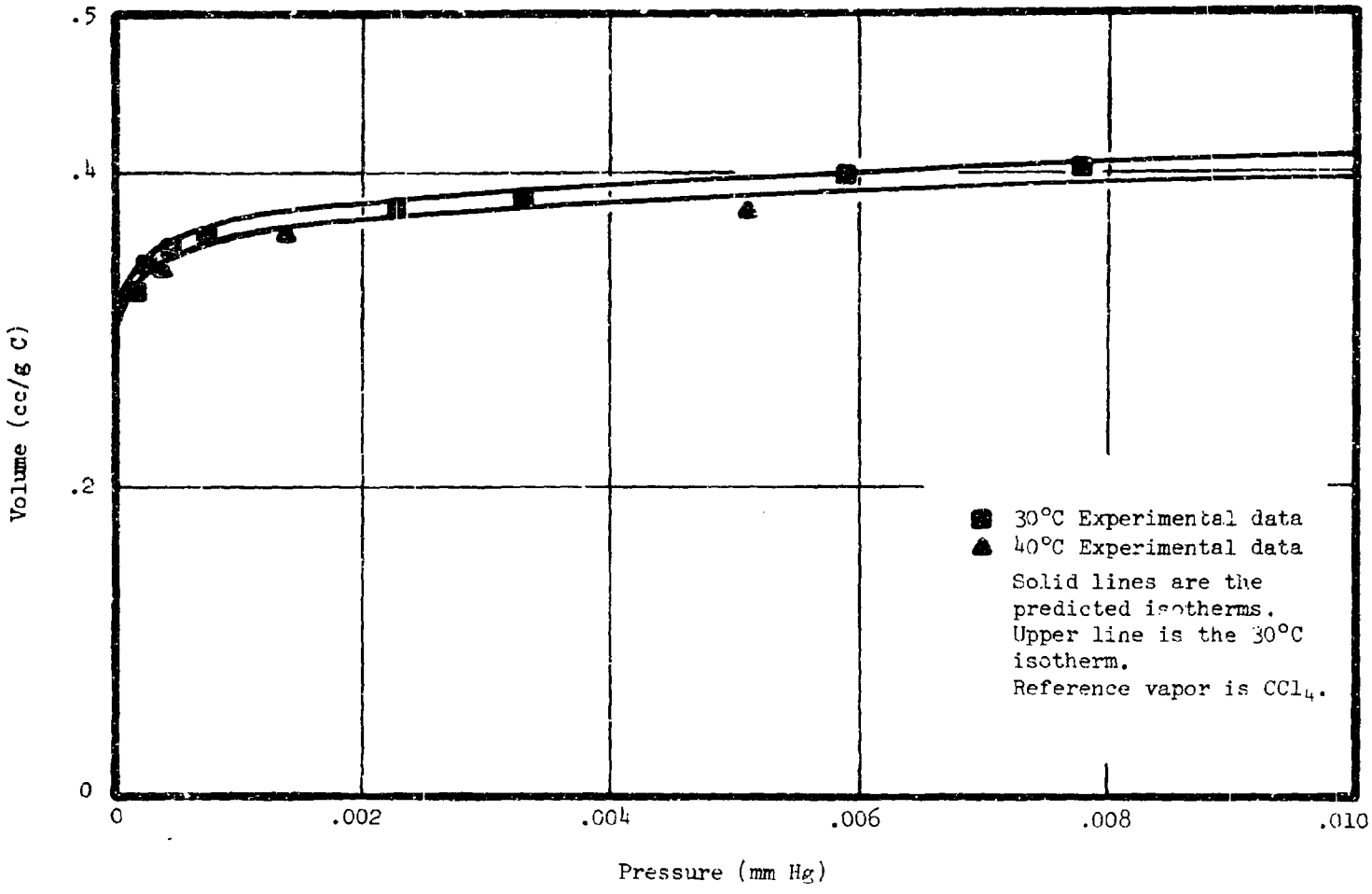

Figure 21c

CA on PCC - Low Pressure Range

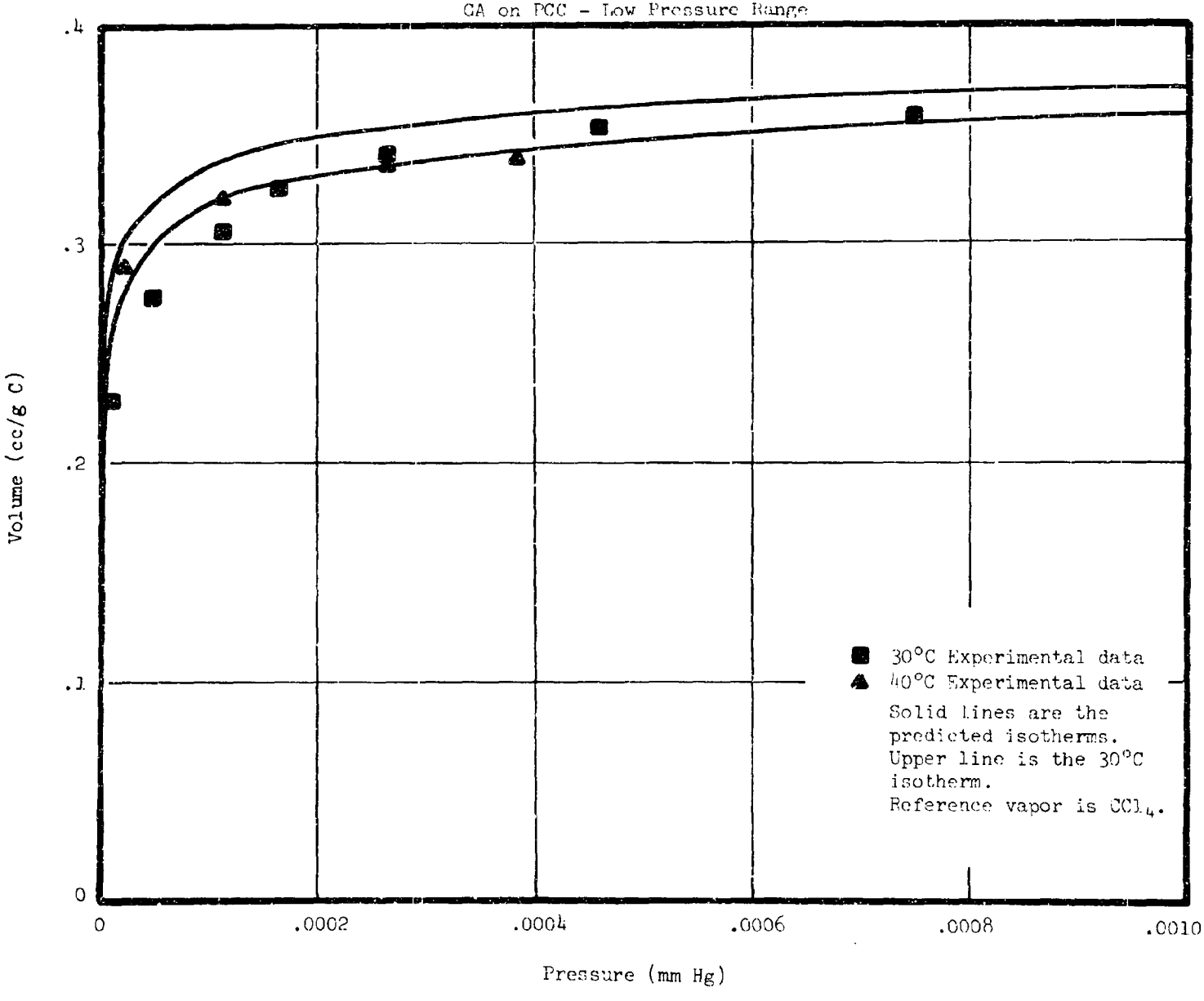

Figure 22a

GF on PCC - High Pressure Range

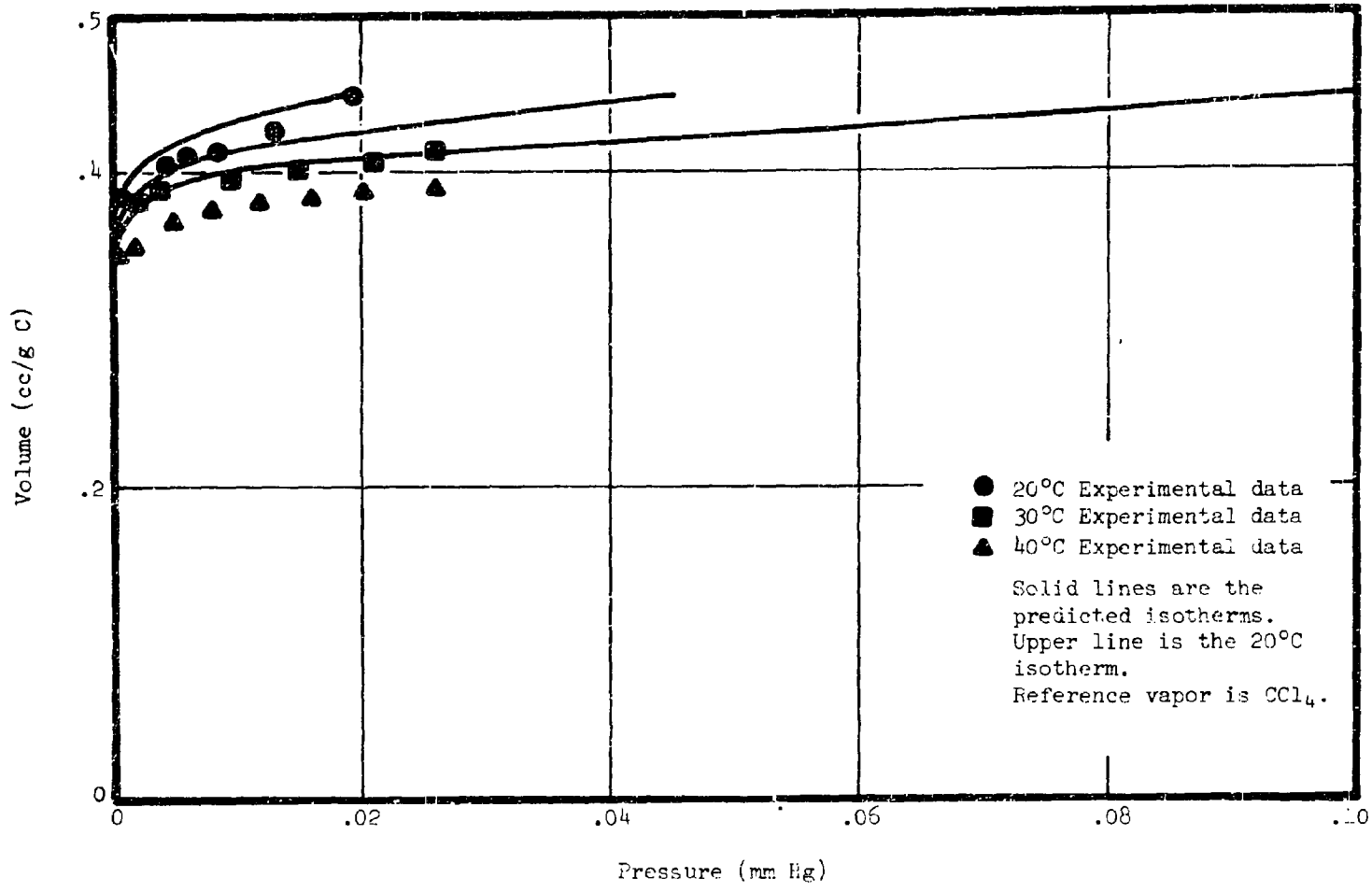

Figure 22b

GF on PCC - Medium Pressure Range

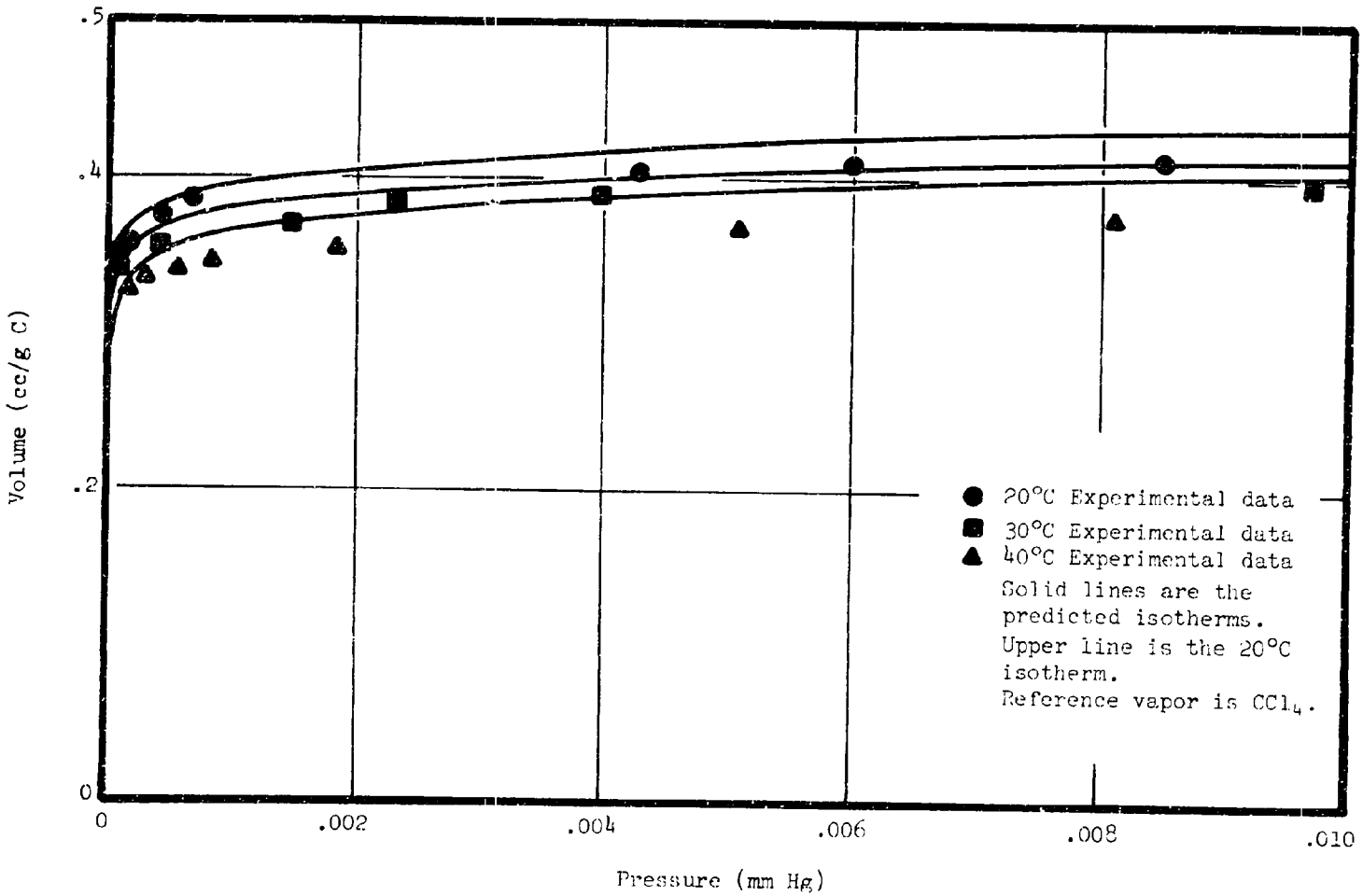

Figure 22c

GF on PCC - Low Pressure Range

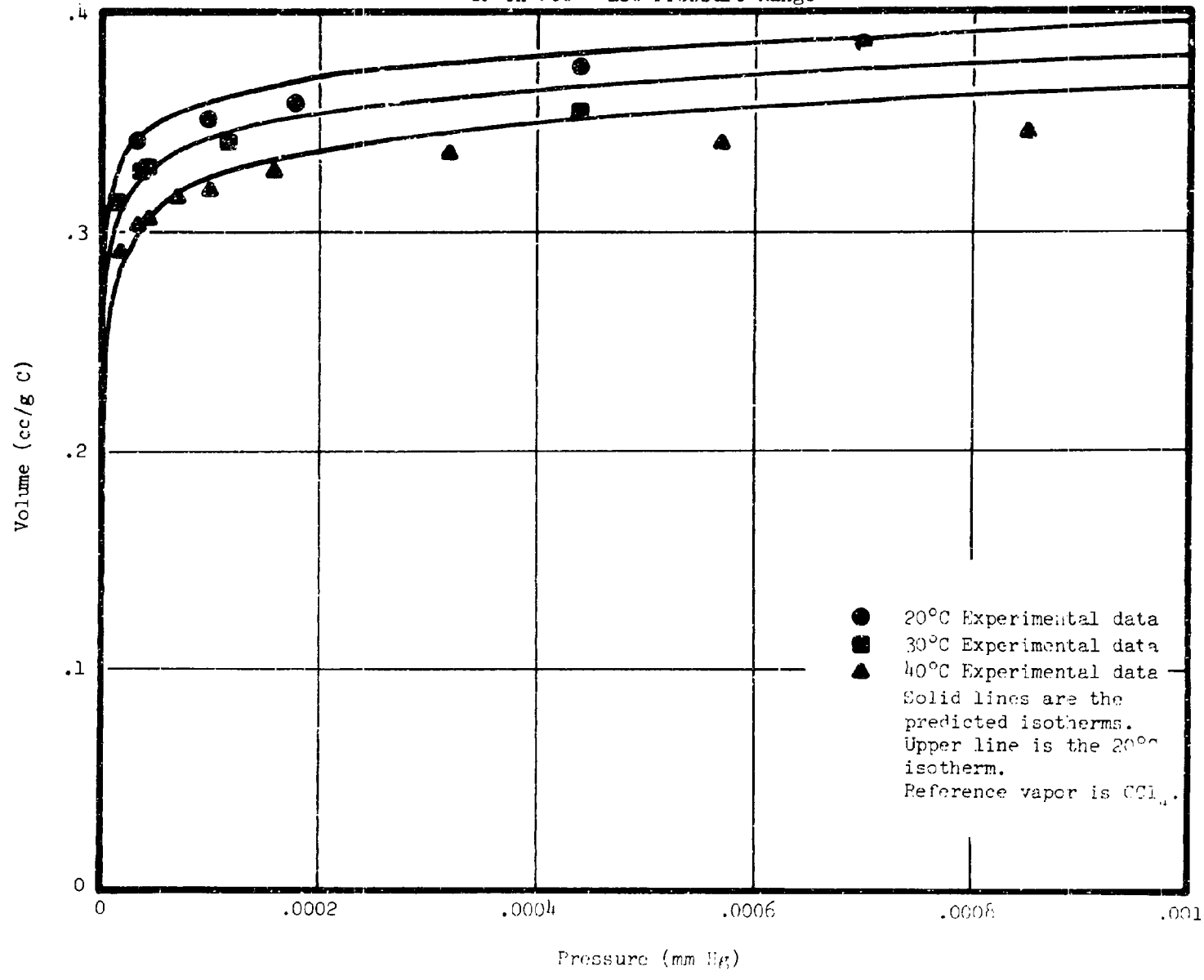

Figure 23

Characteristic Curve for $CCl_4$ on BC

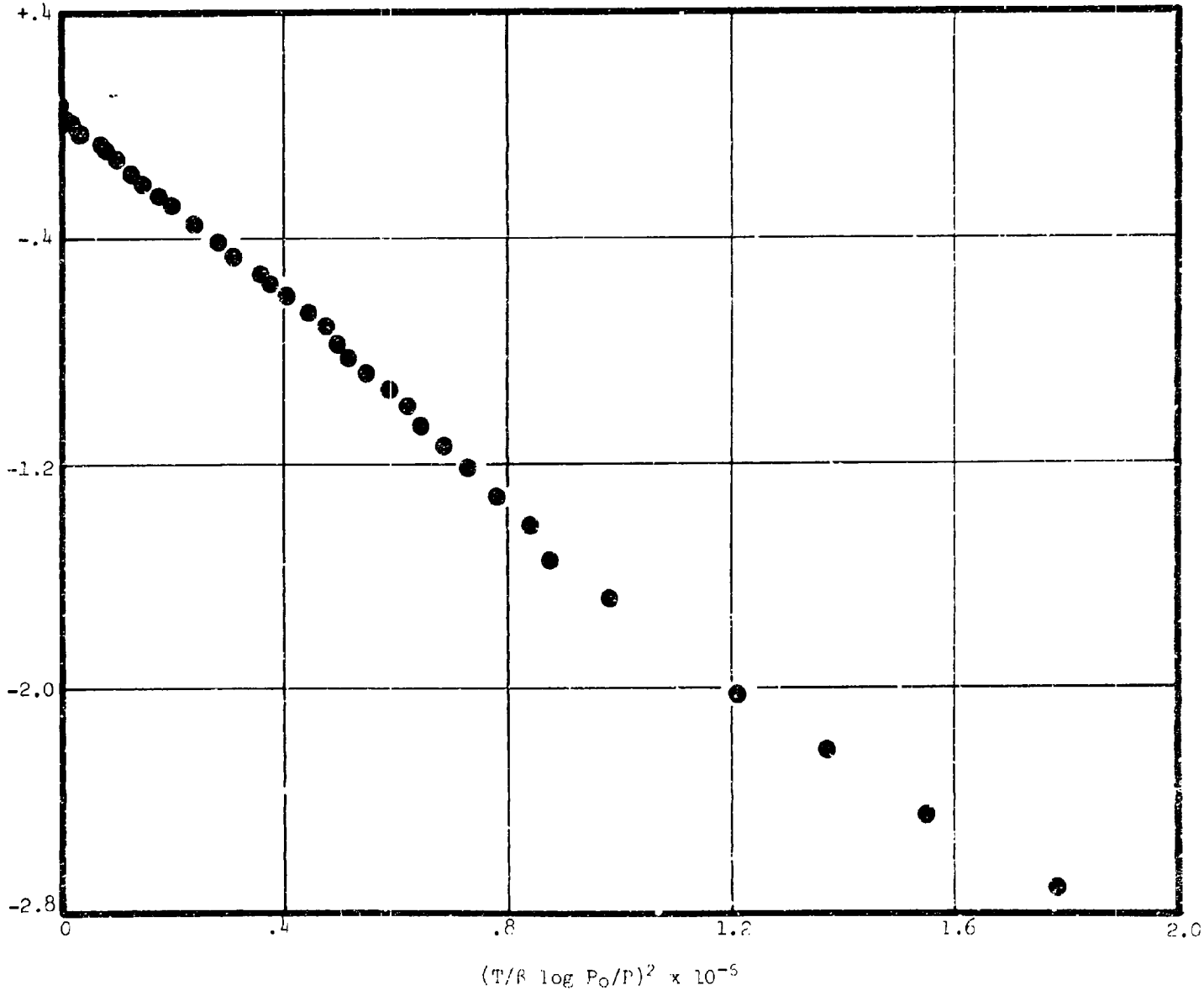

a favorable comparison between the values of β for DMMP as determined from $CCl_4$ data on each of the carbons. Predicted isotherms are shown with the experimental datum points in Figures 24 - 26. β values for GB and GA were calculated to be the same as those shown in Table II. It is seen that except for GB, the predictions are not as good as for the PCC carbon although differences between the predicted and measured amounts adsorbed for the agents are generally less than about 10%.

Attempts made to predict benzene isotherms from $CCl_4$ data were not very successful as seen in Figures 27 and 28 for the PCC and BC carbons. While the shapes of the predicted isotherms for the other adsorbates studied were the same as the actual data and correspondence could therefore be achieved by proper selection of β, the shape of the actual benzene isotherm appears to be considerably different than that predicted from $CCl_4$ data. The reason for this difference is not known although the benzene isotherm has the appearance of isotherms which exhibit hysteresis due to capillary condensation. From this it does not appear that benzene would make a suitable simulent for the adsorption of G agents.

F. Summary of Results of Equilibrium Adsorption Experiments

The agent adsorption isotherms which were measured experimentally could be predicted with fair accuracy by using the entire characteristic curve of a simulent to define the adsorptive properties of the adsorbent and by using an expermentally determined factor to define the relative interaction strength of the adsorbate. At present it does not seem possible to calculate accurate values of β from physical properties of the agents. However, experimental measurement would no doubt be too difficult. The term β can be determined for a particular vapor under test by finding the amount adsorbed at a single pressure. Comparing this pressure to that of the reference vapor at the same volume adsorbed in the following manner yields β:

$$\beta = \left[ \frac{(T \log Po/P)_{test}}{(T \log Po/P)_{reference}} \right]_W \qquad [2]$$

Because the experimentally determined characteristic curves were not linear, the characteristics B and $W_o$ which define the nature of the adsorbent had no meaning in this work. However, where non-linearity occurs it appears possible to work directly from plots of ln W vs. $(T/\beta \log Po/P)^2$ in constructing predicted isotherms.

Figure 24a

DMMP on BC - High Pressure Range

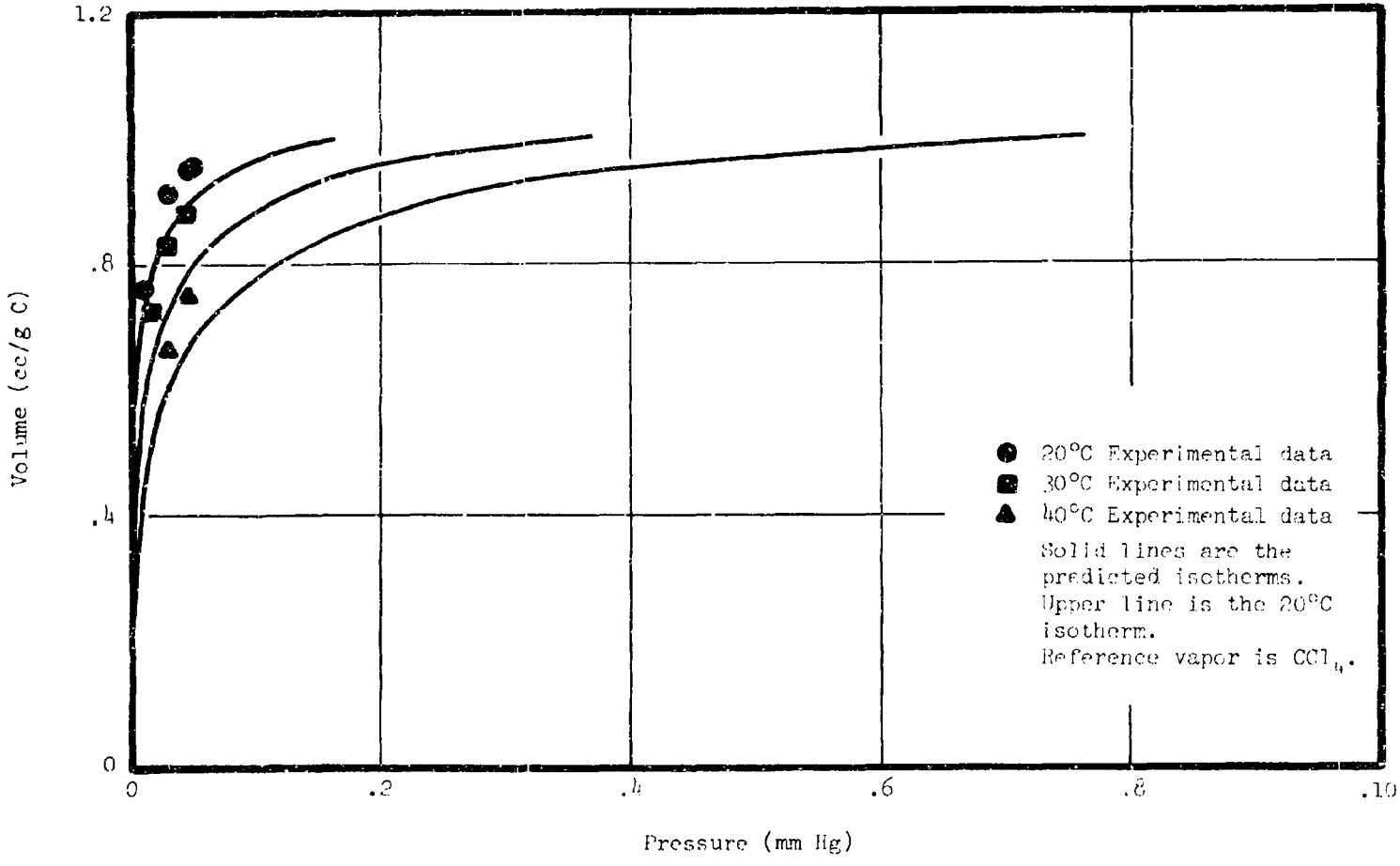

Figure 24b

DMMP on BC - Medium Pressure Range

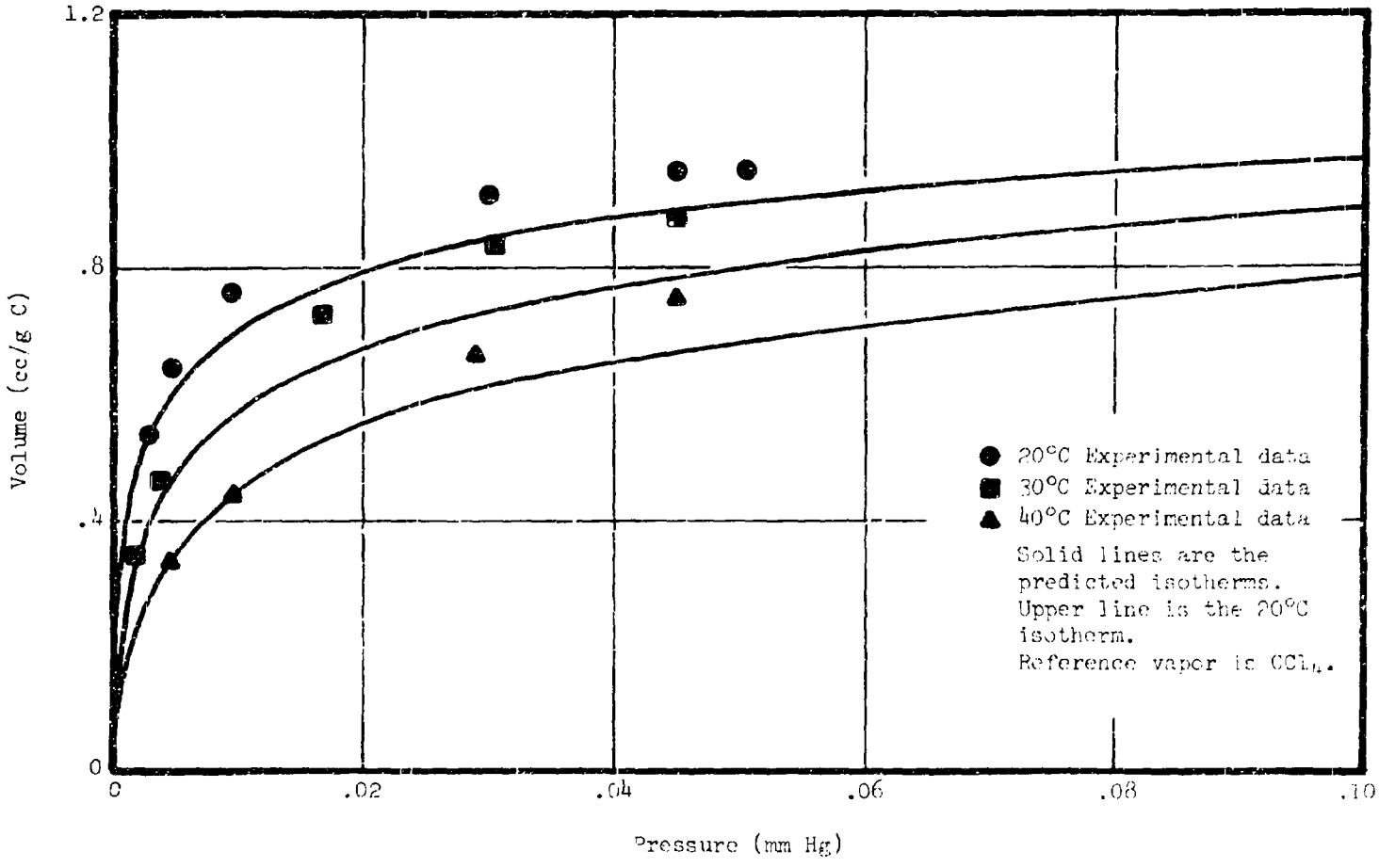

Figure 24c

DMMP on EC - Low Pressure Range

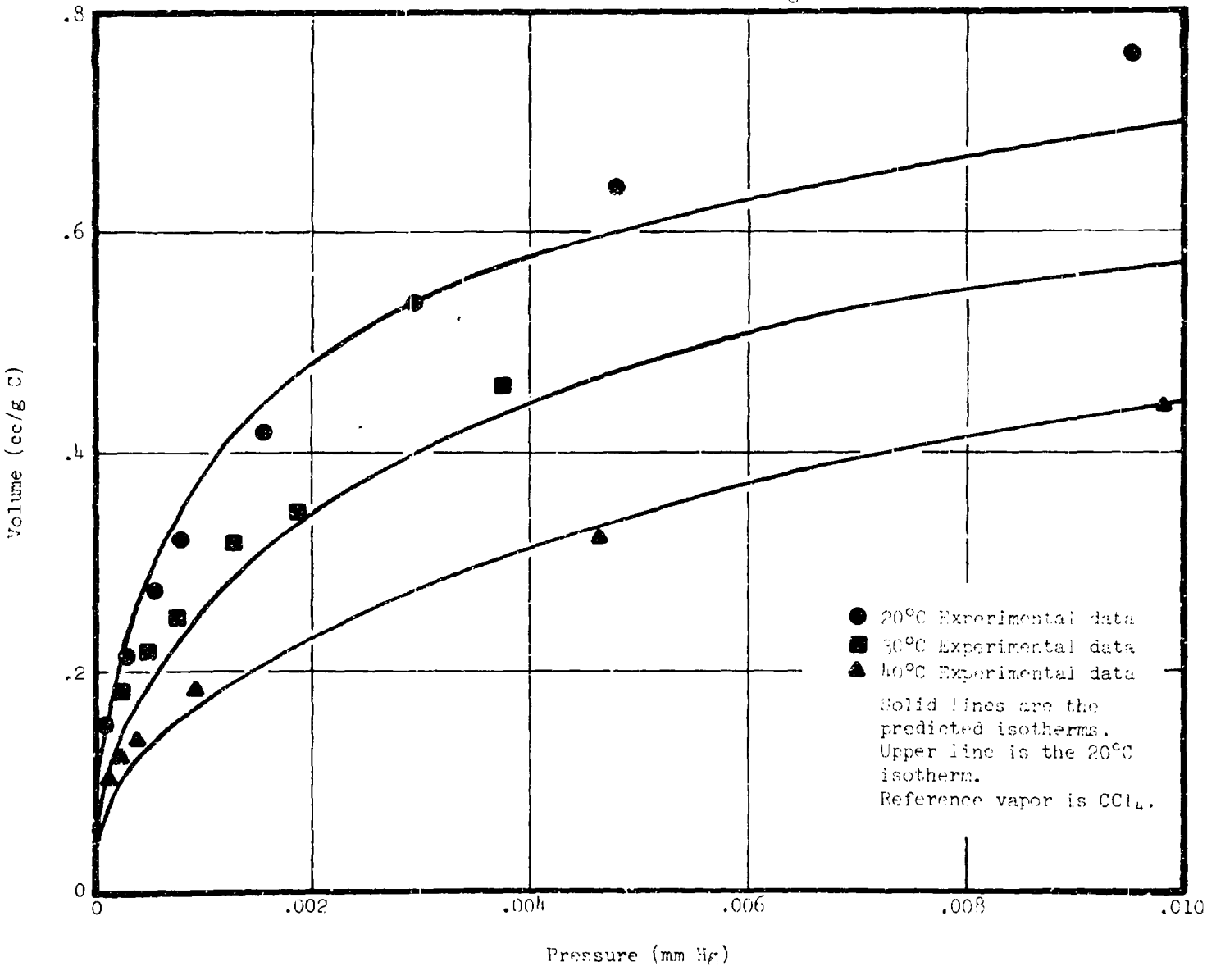

Figure 25a

GB on BC - High Pressure Range

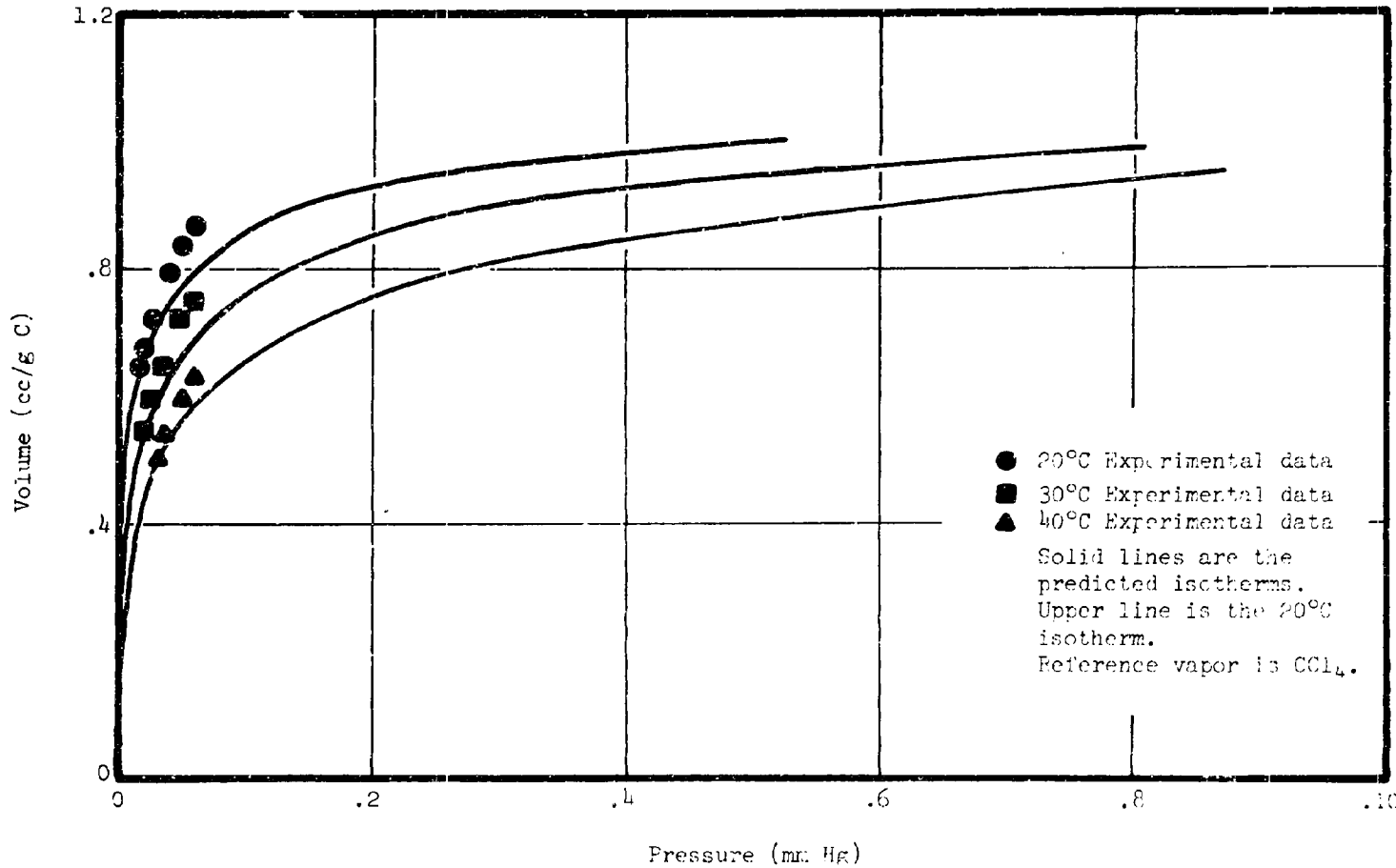

Figure 25b

GB on BC - Medium Pressure Range

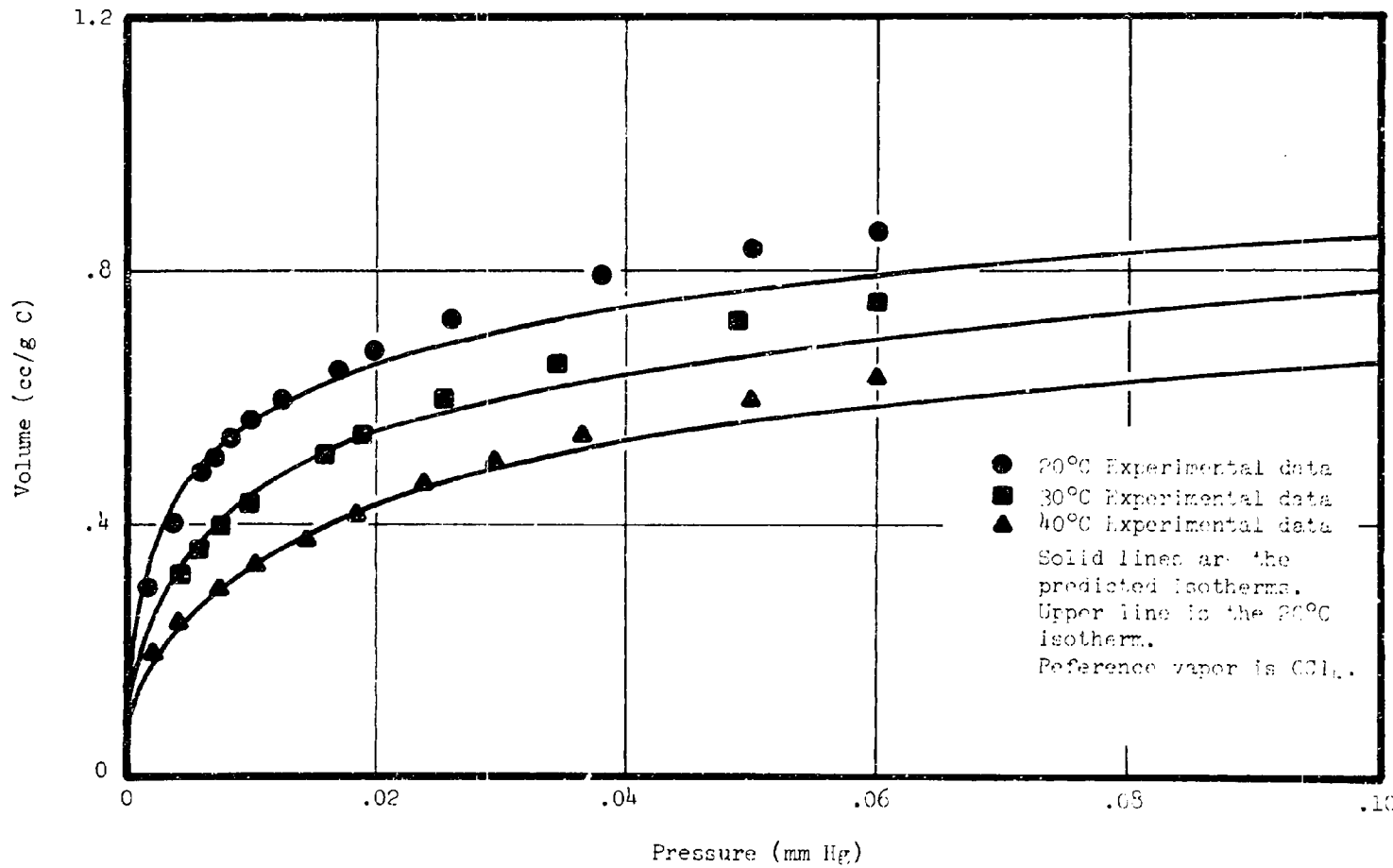

Figure 25c

GB on BC - Low Pressure Range

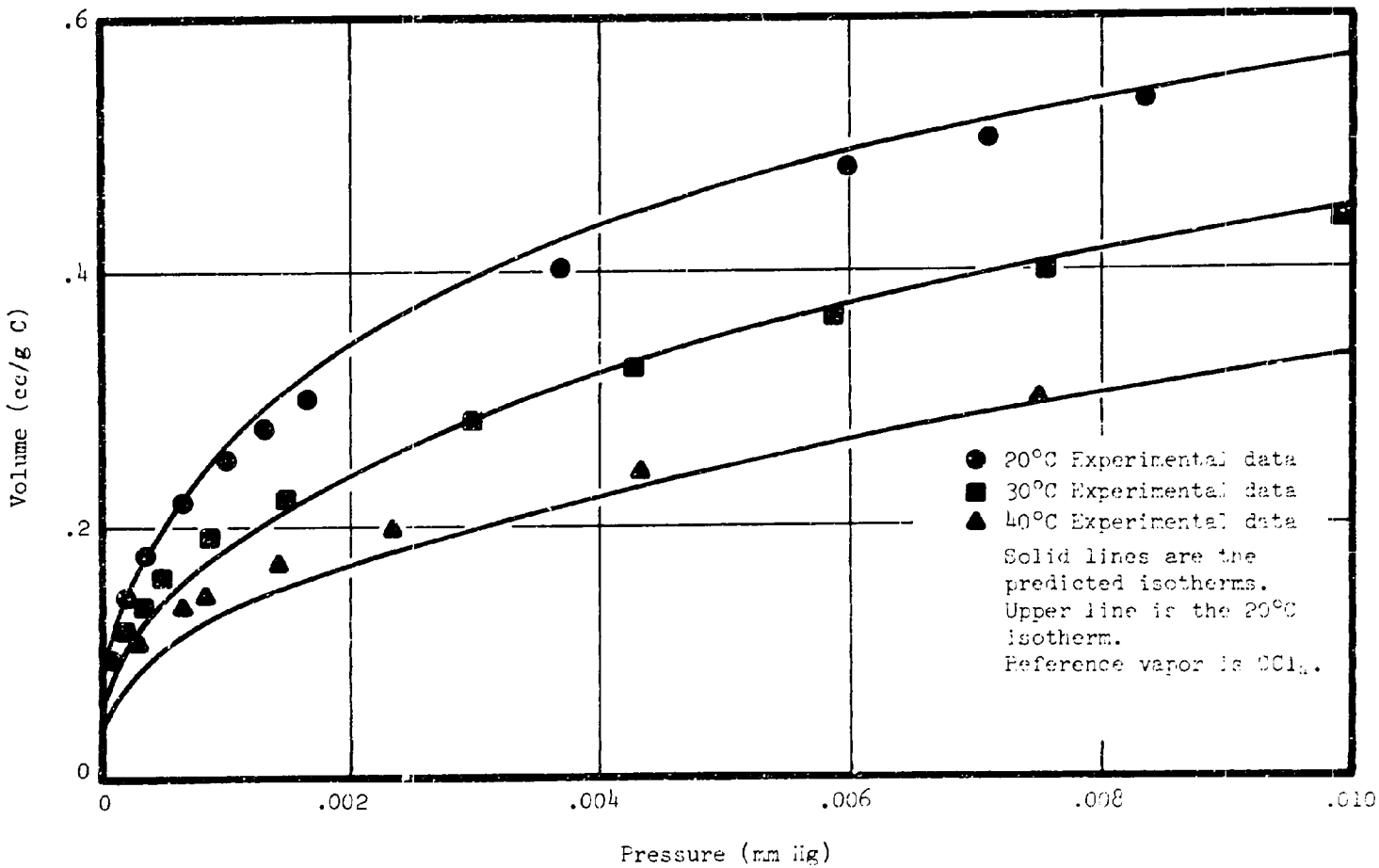

Figure 26a

GA on BC - High Pressure Range

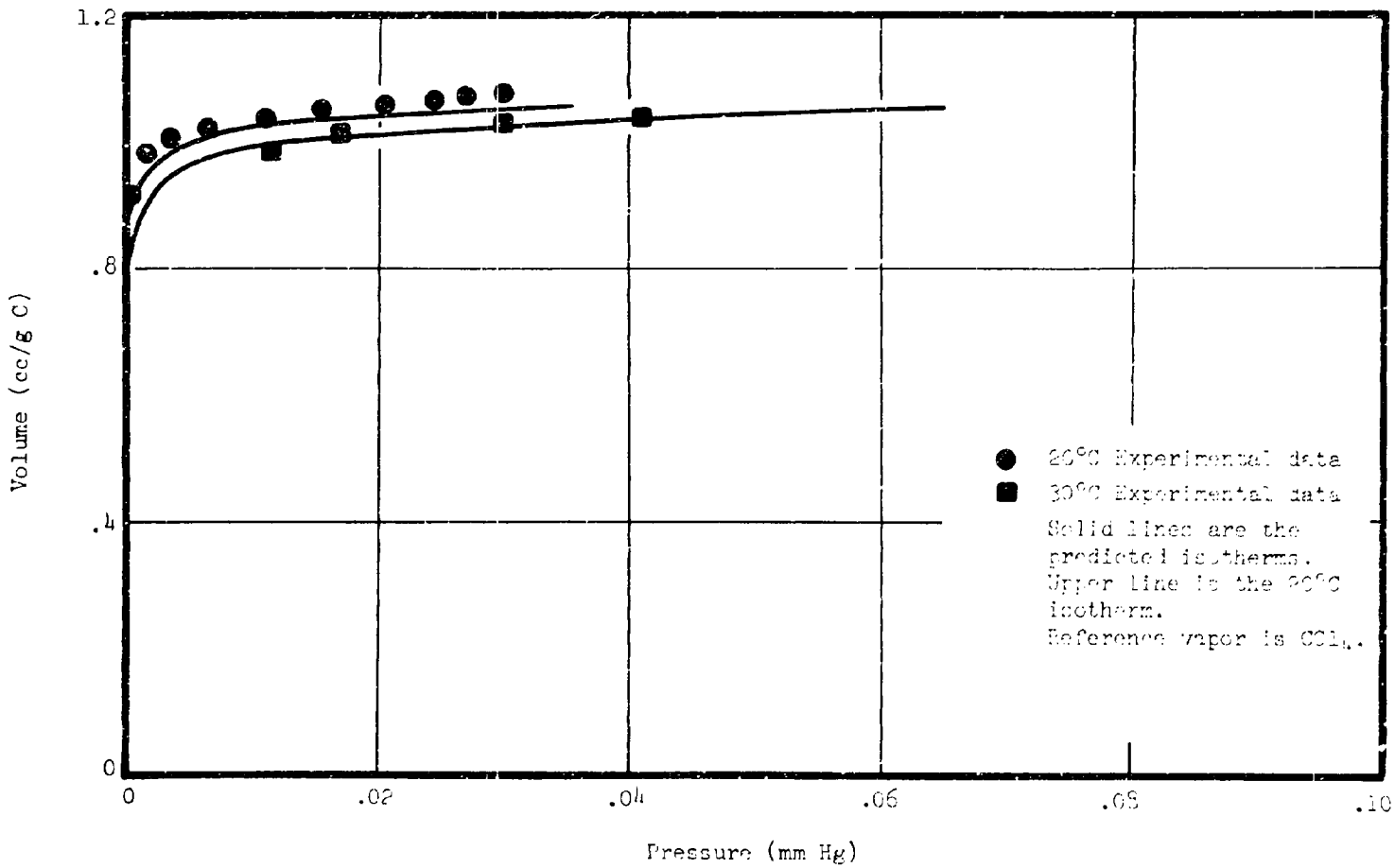

Figure 26b

GA on BC - Medium Pressure Range

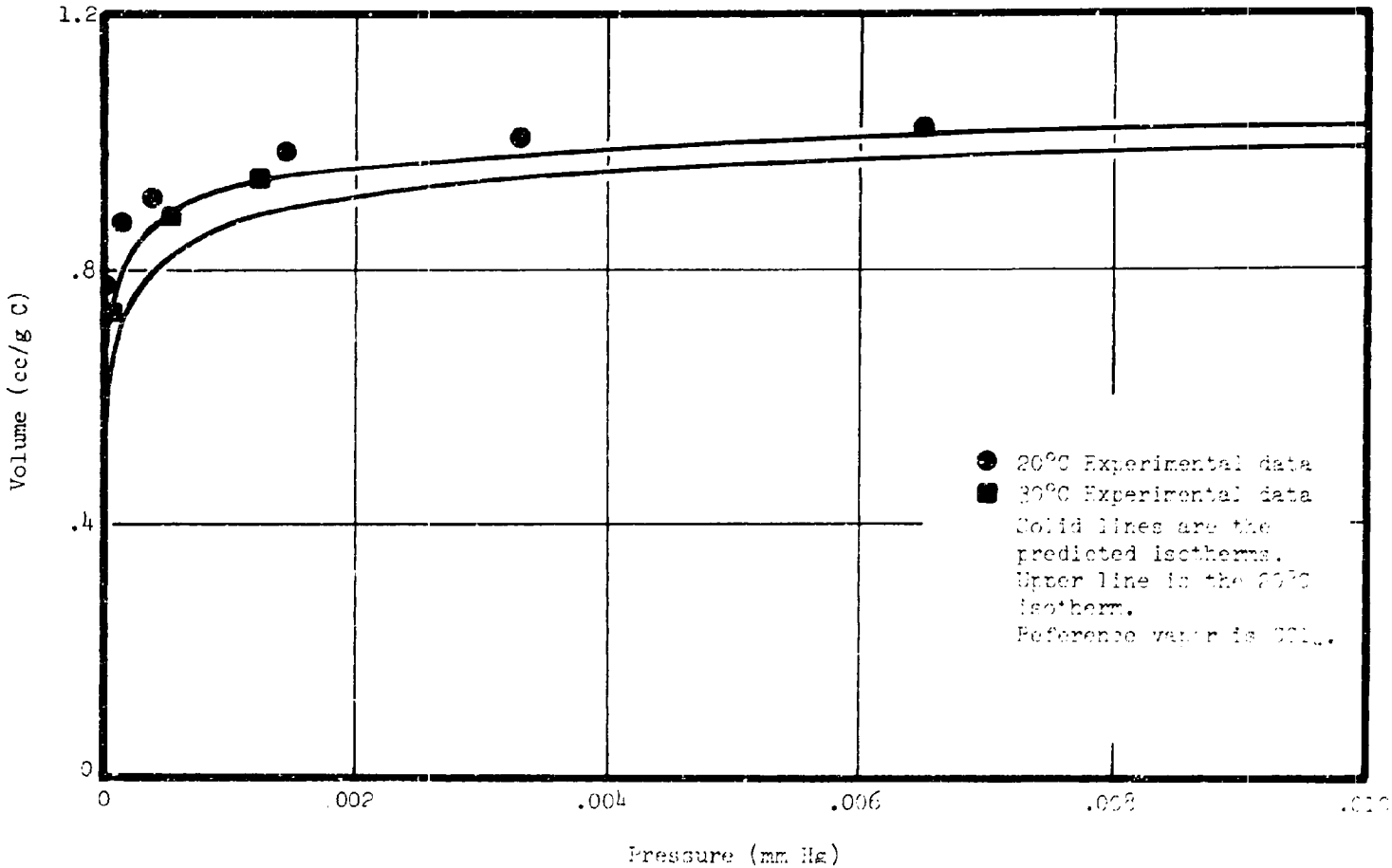

Figure 26c

GA on BC - Low Pressure Range

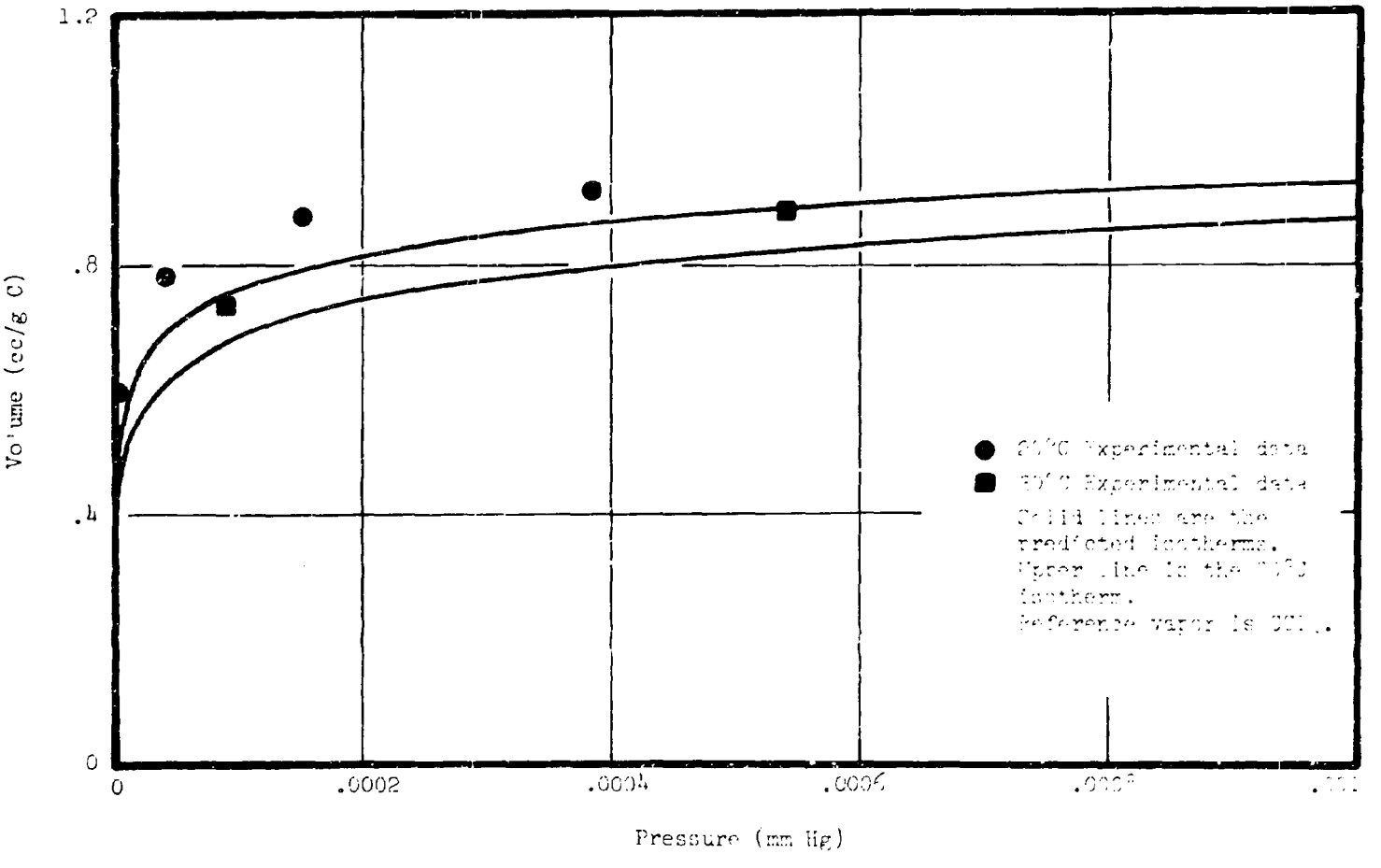

Figure 27a

Benzene on PCC - High Pressure Range
Solid Circles - Experimental Data; Solid Line - Predicted Isotherm;
Reference Vapor - $CCl_4$

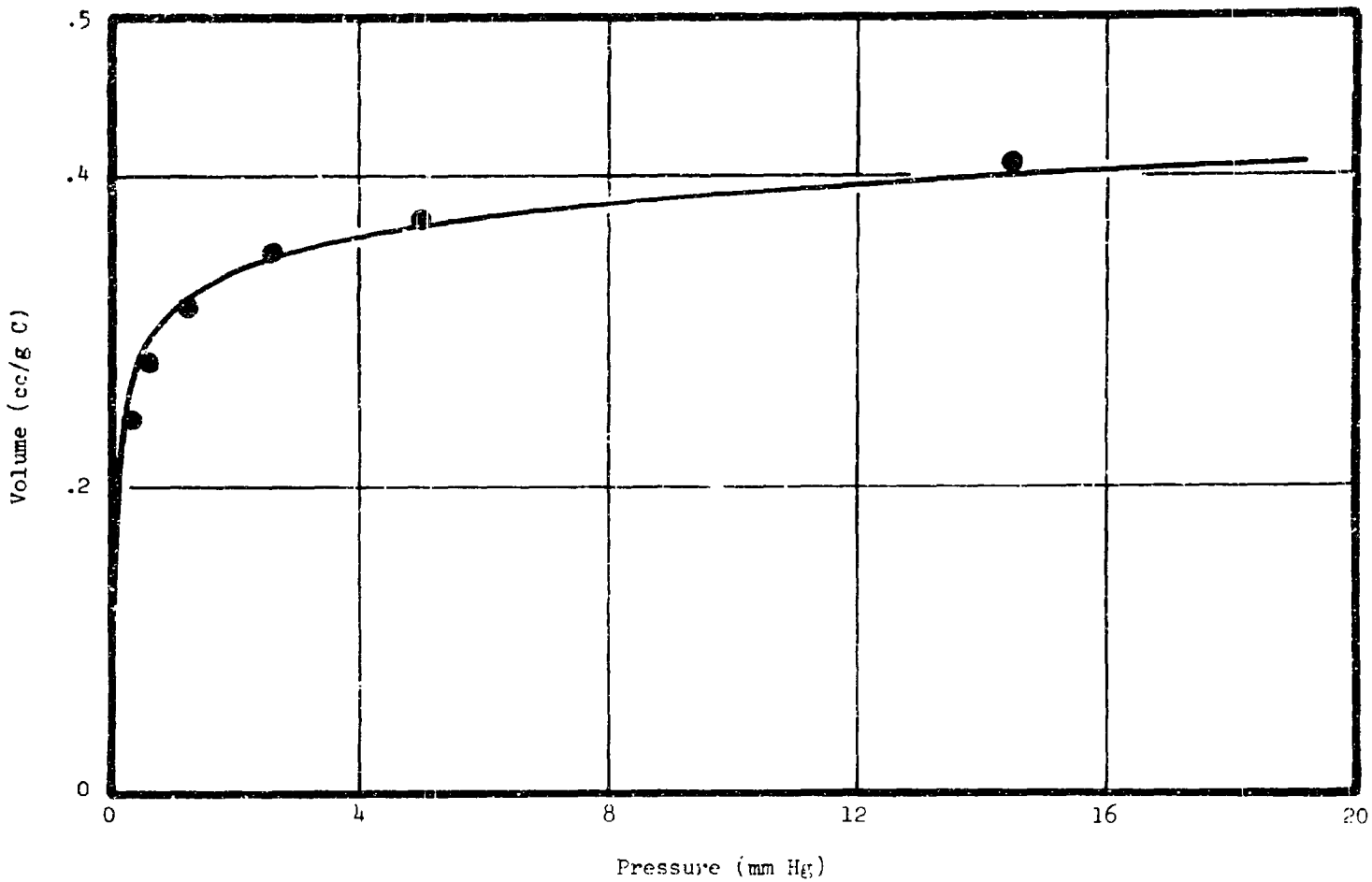

Figure 27b

Benzene on PCC - Medium Pressure Range
Solid Circles - Experimental Data; Solid Line - Predicted Isotherm;
Reference Vapor - $CCl_4$

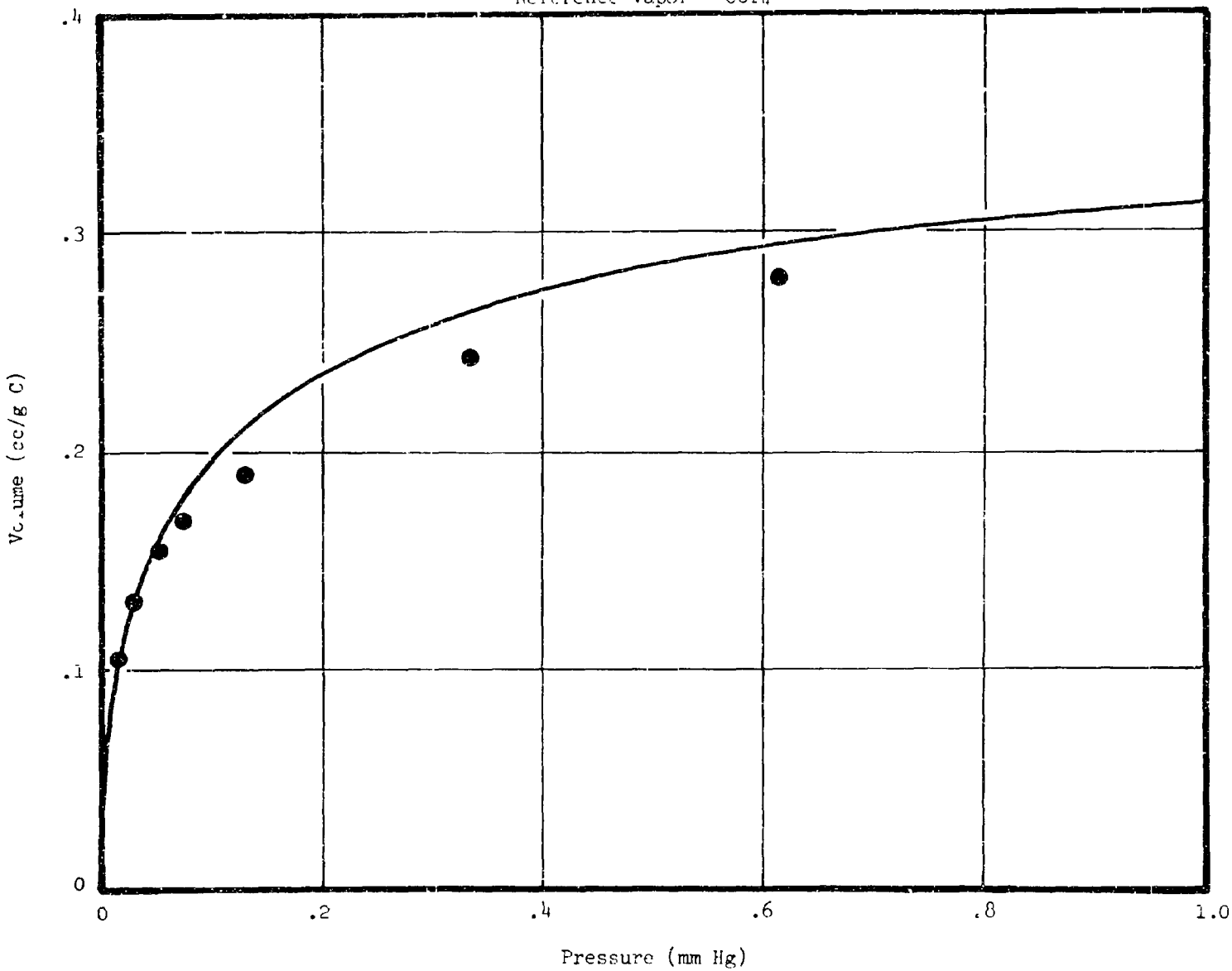

Figure 27c

Benzene on PCC - Low Pressure Range
Solid Circles - Experimental Data; Solid Line - Predicted Isotherm;
Reference Vapor - $CCl_4$

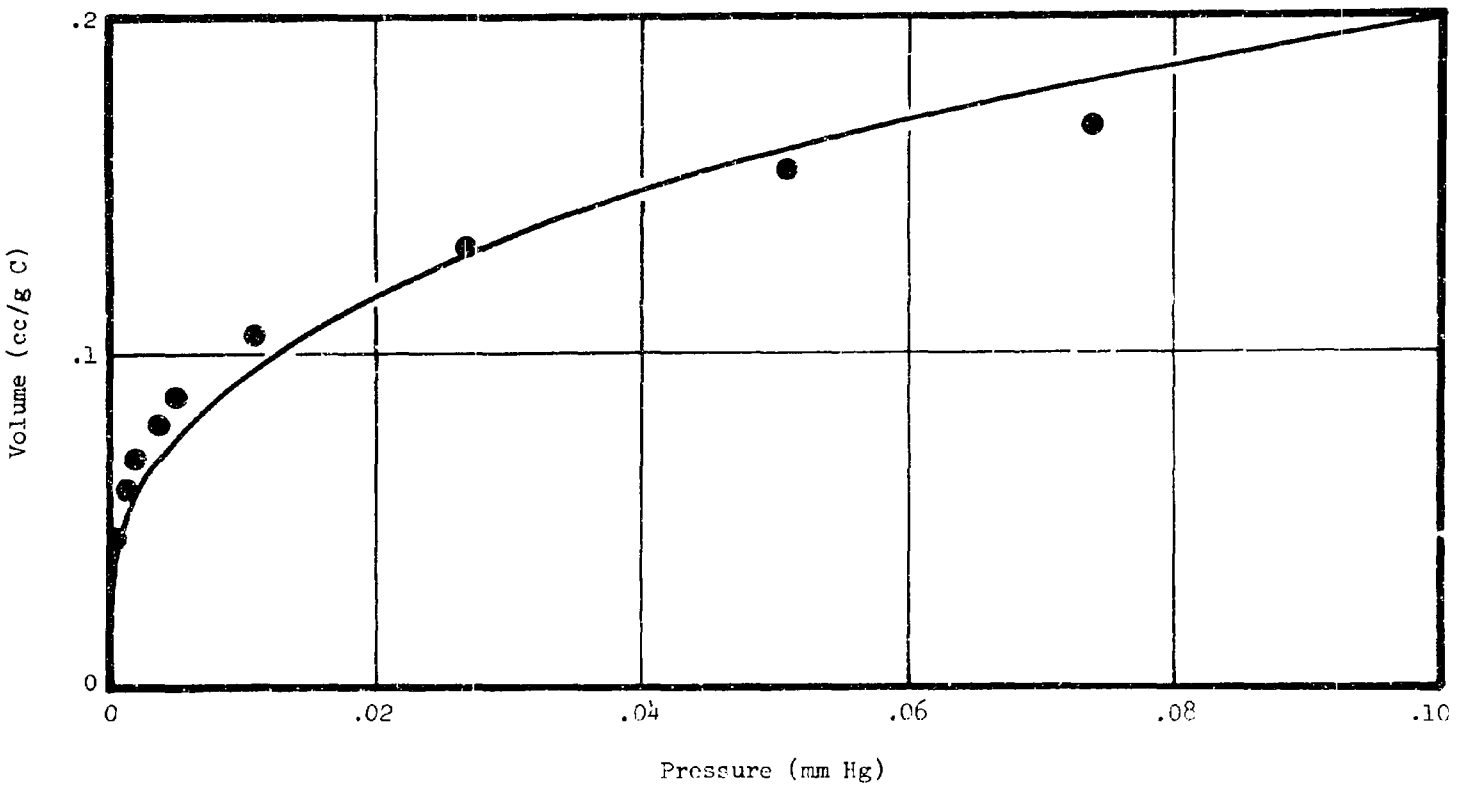

Figure 28a

Benzene on BC - High Pressure Range
Solid Circles - Experimental Data; Solid Line - Predicted Isotherm;
Reference Vapor - $CCl_4$

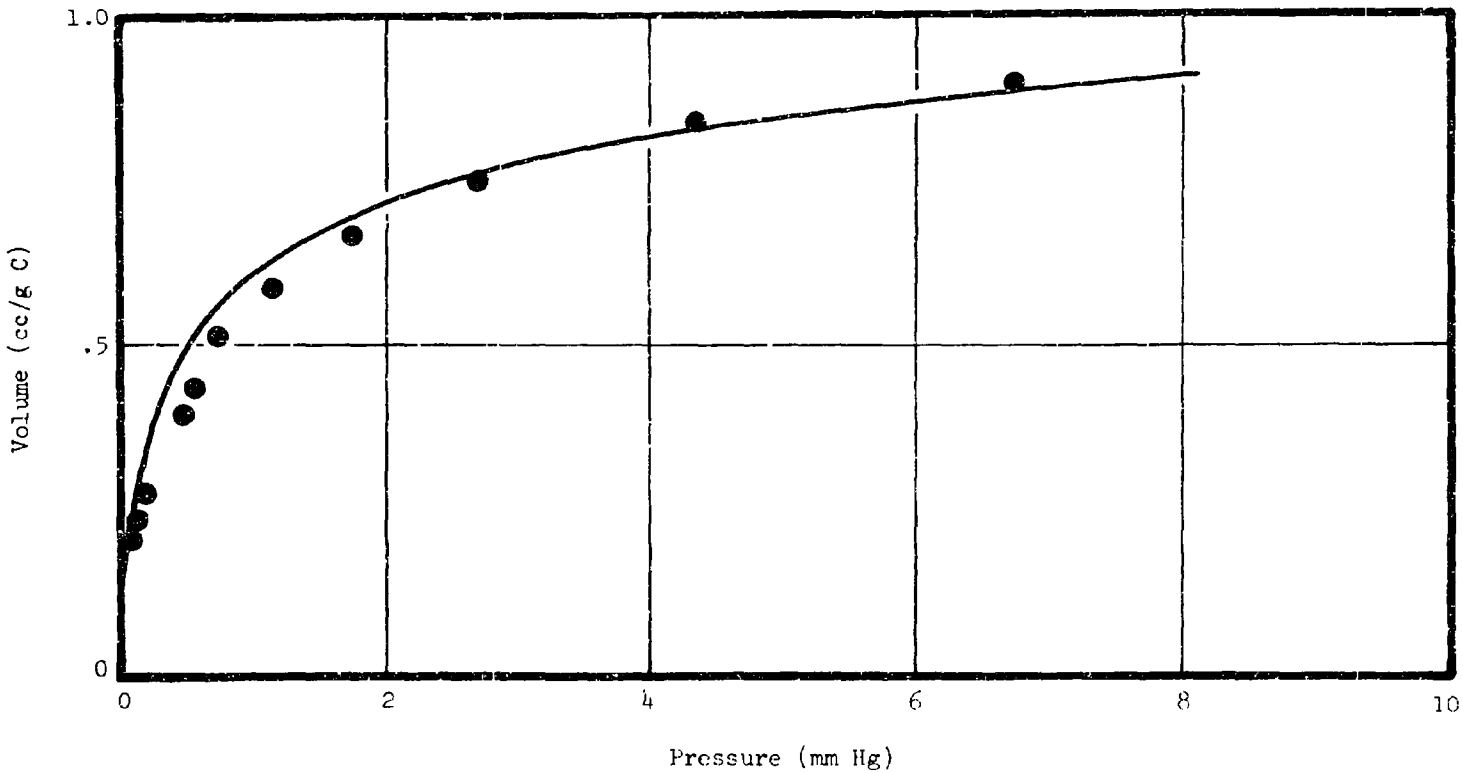

Figure 28b

Benzene on BC - Medium Pressure Range
Solid Circles - Experimental Data; Solid Line - Predicted Isotherm;
Reference Vapor - $CCl_4$

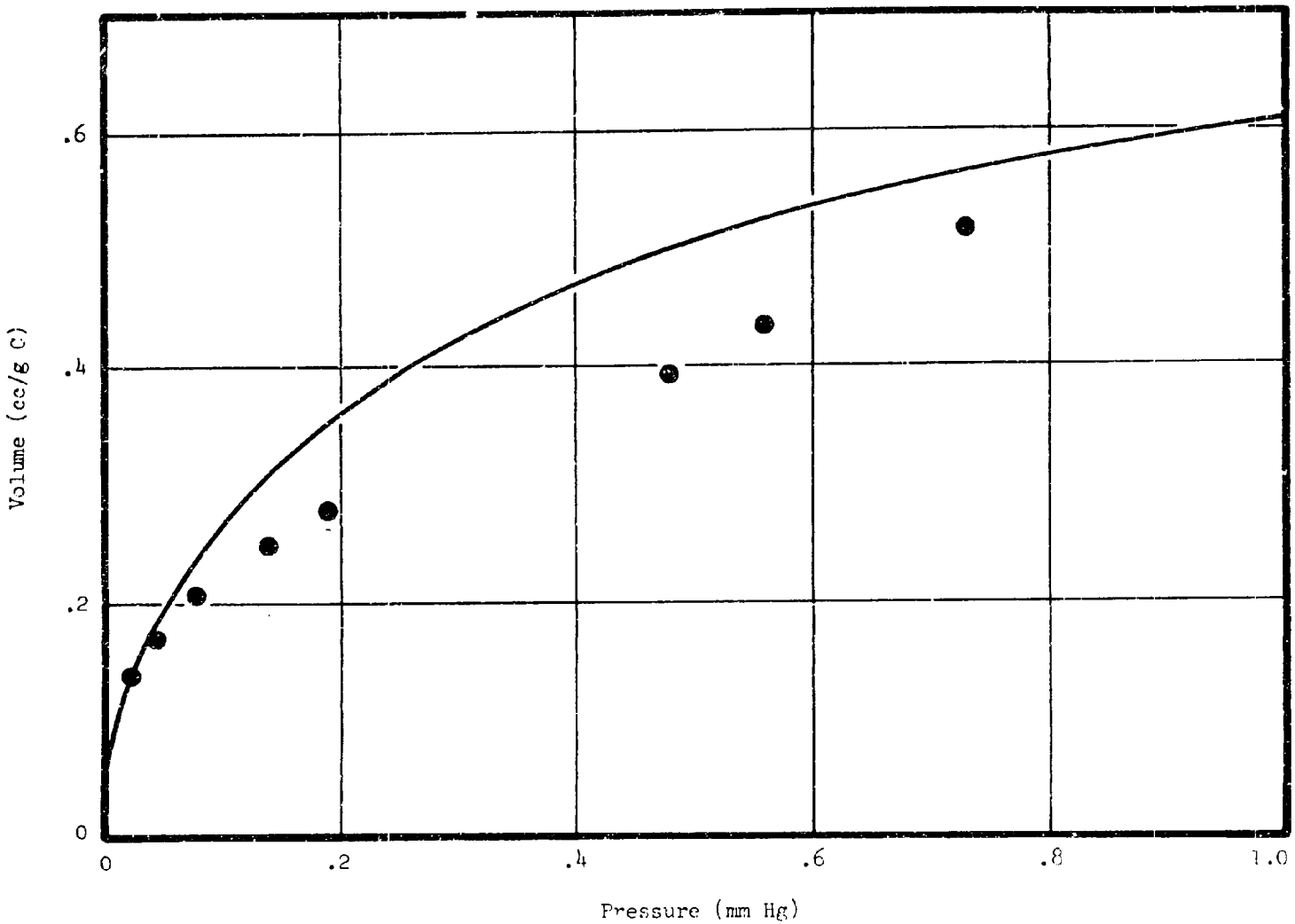

Figure 28c

Benzene on BC - Low Pressure Range
Solid Circles - Experimental Data; Solid Line - Predicted Isotherm;
Reference Vapor - $CCl_4$

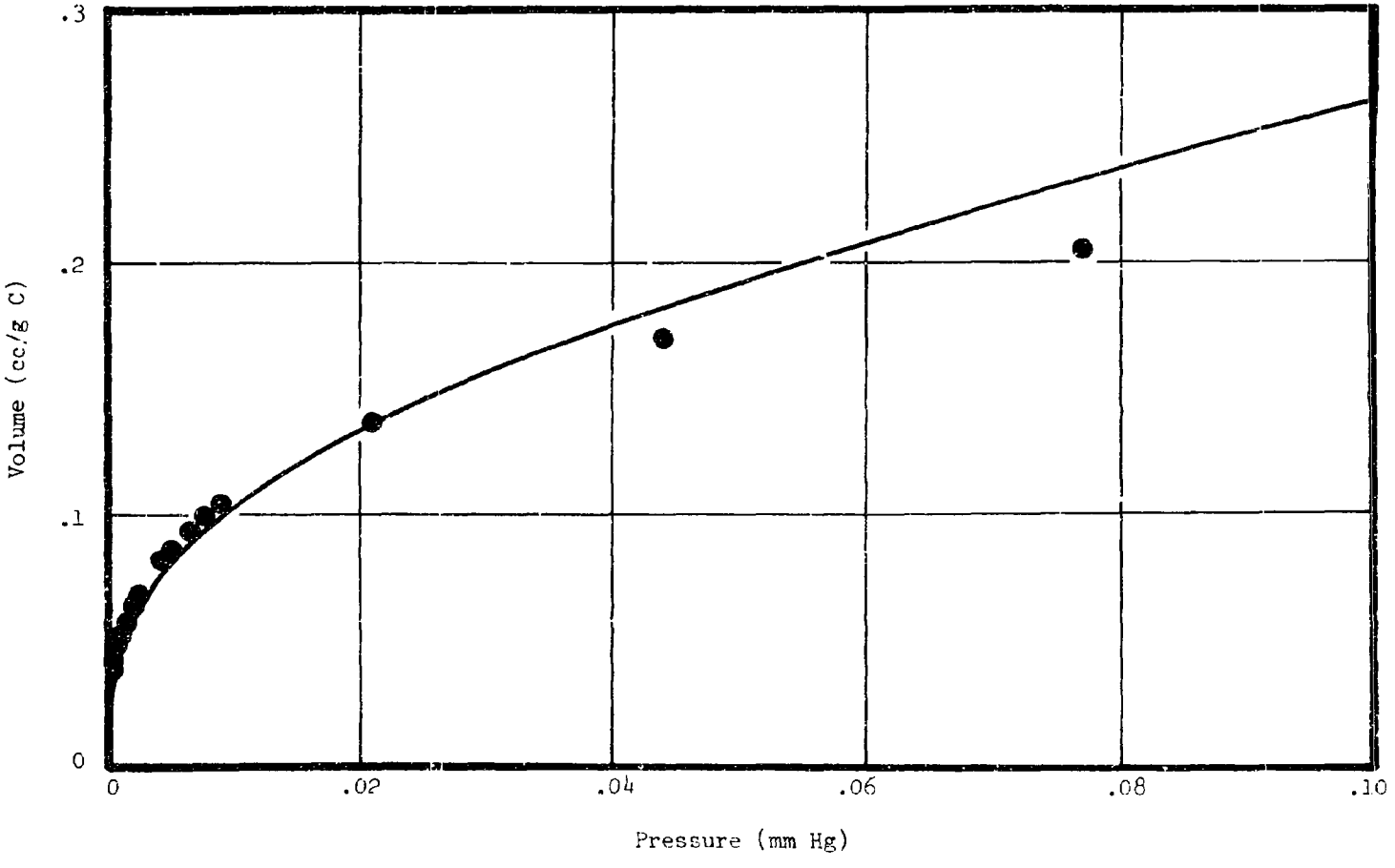

## III. PHYSICAL AND ADSORPTIVE PROPERTIES OF IMPREGNATED CARBONS

Samples of the PCC carbon which had been impregnated with siloxane polymers to alter its water adsorption properties were characterized by the following methods:

1. Carbon tetrachloride activity
2. Surface area and pore size distributions by nitrogen adsorption
3. Pore-size distributions by mercury penetration
4. Water adsorption and desorption isotherms.

The samples investigated included "Sample 9" impregnated with 0.133 gm methyl trichlorosiloxane per gram carbon, and "Sample 11" containing about 0.17 gm of a 2:1 weight ratio mixture of dimethyl dichlorosiloxane and methyl trichlorosiloxane. These samples, which were prepared by Mr. A. C. Oglesby at Edgewood Arsenal are compared with the unimpregnated 50x150 mesh base material.

### A. Effect on Activity

The effect of impregnation on two of the standard measures of activity, carbon tetrachloride value and surface area are shown in Table III.

TABLE III

EFFECT OF IMPREGNATION ON ACTIVITY

| | $CCl_4$ Activity (%) | BET Surface Area ($m^2/gm$) |
|---|---|---|
| Control | 63 | 1058 |
| Sample 9 | 38 | 651 |
| Sample 11 | 42 | 499 |

From this it is seen that impregnation produced a considerable loss in adsorbent activity.

### B. Porosity Measurements

In an effort to determine how the resins were distributed within the carbon pore structure, pore volume measurements were made both by nitrogen adsorption and by mercury intrusion. The results were not conclusive but it is suspected that most of the resin is contained in the macropores and larger transitional pores which are not specifically involved in the adsorption vapors. The observed loss in surface area is thought to be largely due to blockage of the micropores.

An analysis of the mercury porosimeter data was made in the following way:

(1) The pore volumes in a range of pore sizes from 60 to 0.012 micron was determined per gram of resin treated sample.
(2) From similar porosimeter data using the untreated carbon, the pore volume distributions for the amount of carbon in a gram of the impregnated sample was calculated.
(3) The differences between the above items were calculated and the total difference compared with the volume of resin present in a gram of the impregnated material.

Table IV shows these calculations for Sample 9 containing 0.133 gm resin/gm carbon.

TABLE IV

ANALYSIS OF MERCURY POROSIMETER FOR SAMPLE 9

| Pore Size Range (microns) | Volume* in Treated Sample (cc) | Volume* in Carbon Alone (cc) | Difference (cc) |
|---|---|---|---|
| 0.012 | 0.024 | 0.030 | + 0.006 |
| .020 | .057 | .070 | .013 |
| .100 | .029 | .029 | .000 |
| .200 | .100 | .134 | .034 |
| 1.00 | .042 | .049 | .007 |
| 4.00 | .021 | .028 | .007 |
| 10.00 | .036 | .041 | .005 |
| 20.00 | .173 | .107 | - .066 |
| 40.00 | .218 | .267 | .049 |
| 60.00 up | .253 | .265 | .012 |
| | | | .067 TOTAL |

*Volume between stated size and next higher size.

The total difference of 0.067 cc obtained in this way is at least similar to 0.078 cc, the volume of resin in the sample assuming a resin density of 1.50 gm/cc.

When the same kind of analysis was attempted for Sample 11, however, it was found that in each pore size range the treated sample had more volume than the predicted amount of carbon in the sample based upon a 17% loading. These are some possible reasons for this:

(1) The porosimeter data cannot be trusted.
(2) Surface coating outside the pore-size range investigated might have resulted in partial blockage of very large pores which would then have been observed as smaller pores within the instrument range.
(3) The amount of resin present was less than 17%. In order to account for the error the resin loading here would have had to be less than on Sample 9.

It is suspected that each of these is true to some extent.

An analysis was also made of pore-size distributions obtained from nitrogen adsorption data by the method of Roberts. (3) In this case the volumes in a series of pore radius ranges from 1000 Å to 10 Å were compared as ratios on the basis of equal activated carbon content. It was found that in each range below about 500 Å the ratio of the volume of the treated sample to that in the untreated carbon was roughly constant. This was true for both impregnated samples and indicates that nitrogen was denied access to a fraction of the smaller pores because of blockage in the larger pores to which they were connected.

A clear case for pore blockage can also be seen by comparing the volumes of nitrogen adsorbed near saturation for the treated and untreated samples. Table V shows the volumes obtained for Samples 9 and 11, the volume in the same amount of untreated carbon as contained in these samples, and the volume of resin actually present. The resin volume is considerably less than the loss in pore volume due to impregnation.

TABLE V

NITROGEN VOLUMES NEAR SATURATION

| Sample | Measured Volume | Carbon Volume | Difference | Resin Volume |
|---|---|---|---|---|
| 9 | 0.361 | 0.524 | 0.163 | 0.078 |
| 11 | .281 | .508 | .227 | .097 |

C. Water Adsorption

The interaction between water molecules and a pure carbon surface is relatively weak at normal temperatures. However, activated carbon always contains chemical groups which are polar or able to form hydrogen bonds with water and thus interact much more strongly than pure carbon. Water adsorption may

therefore be viewed as an initial adsorption on specific sites followed by intramolecular interactions between water molecules to form clusters. With increasing pressure, these clusters grow and finally merge to coat capillary walls continuously. Capillary condensation effects are then observed since the contact angle between liquid water and the water coated walls is zero.

An indication of the extent of surface coverage by hydrophilic sites may be obtained by observing the amount of water adsorbed at a relative pressure of 0.50. (4) From the adsorption/desorption isotherms shown in Figure 29 for Sample 9, Figure 30 for Sample 11 and Figure 31 for the untreated control sample, it can be seen that impregnation had little effect on the amount adsorbed at $P/P_o = 0.50$, and in fact produced a slight increase in Sample 9. The overall reduction in the amount adsorbed at saturation is due to a reduction in available pore volume.

It must be pointed out that while siloxanes will react with hydroxyl groups which would indeed be hydrophilic sites, other oxygen complex groups which do not react with siloxane also act as nucleation centers for water adsorption. There are other chemical methods of inhibiting water vapor adsorption which offer more promise than resin impregnation although such treatment might have value in surface coating of granules to prevent drenching by bulk water.

## IV. DYNAMIC ADSORPTION STUDIES

Efforts were made to test experimentally two methods which have appeared in the literature which are designed to predict the breakthrough of adsorbates from packed beds.

### A. Apparatus

The apparatus used in this work has been fully described previously (5) but its basic elements are shown in Figure 32. High quality air was obtained by passage through mechanical and molecular sieve dryers, a carbon bed, and a particulate filter. The main air flow was metered into the system through rotameter 1. DMMP vapor was produced by bubbling air through the liquid held at 20°C and then passing this over a saturated aludnum wick held at the same temperature. The air/DMMP mixture, held at 2.5 psig by a controller, was admitted to the column section through rotameter 3. After passing through the bed most of the gas escaped through a low pressure regulator valve but a small amount was admitted to a gas sampling valve through rotameter 4. By means of this valve, samples of the effluent mixture were injected into the chromatograph for analysis. The chromatograph used a flame ionization detector.

Figure 29

$H_2O$ on Resin Impregnated Sample # 9 at 20°C

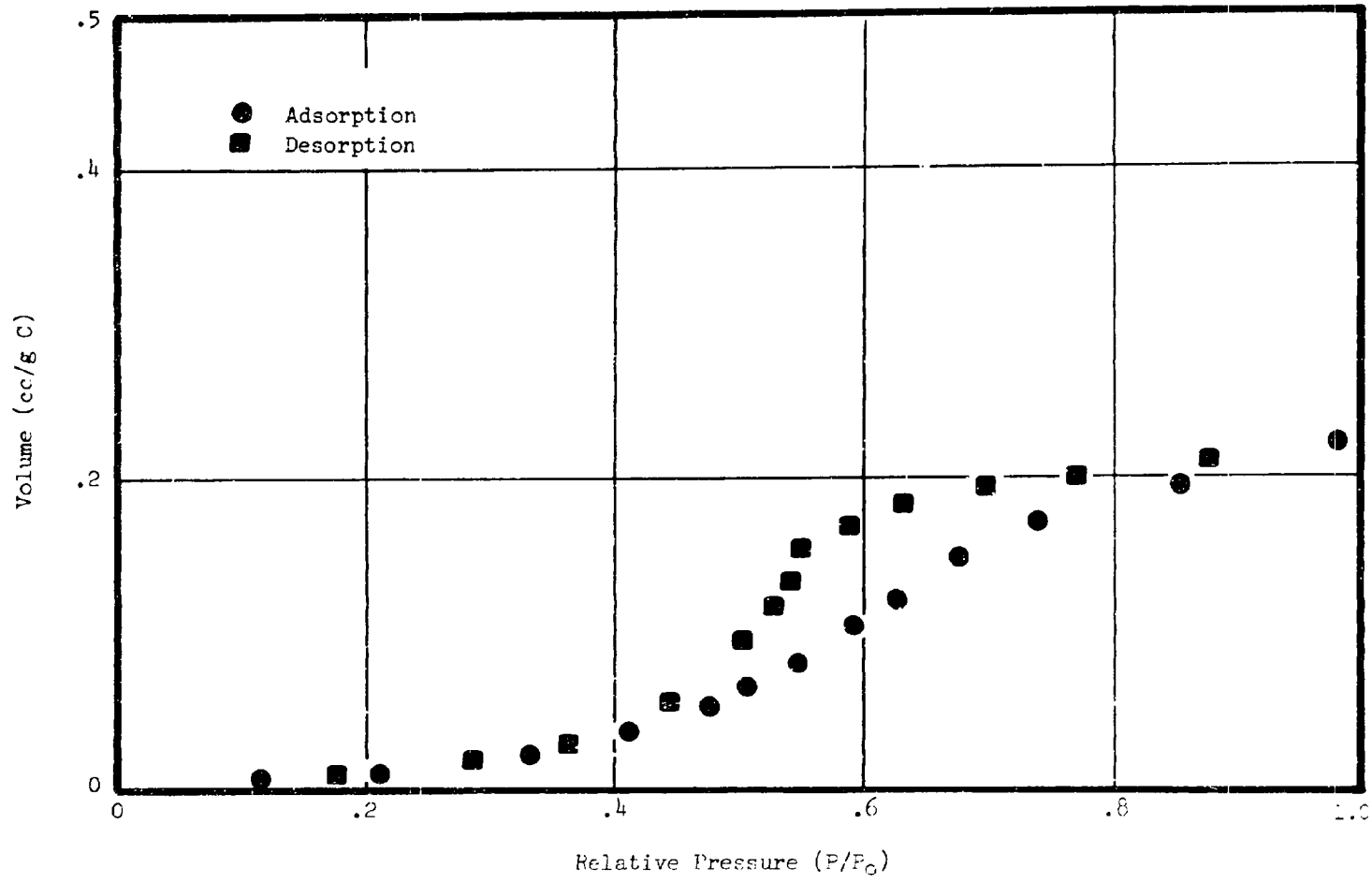

Figure 30

$H_2O$ on Resin Impregnated Sample # 11 at 20°C

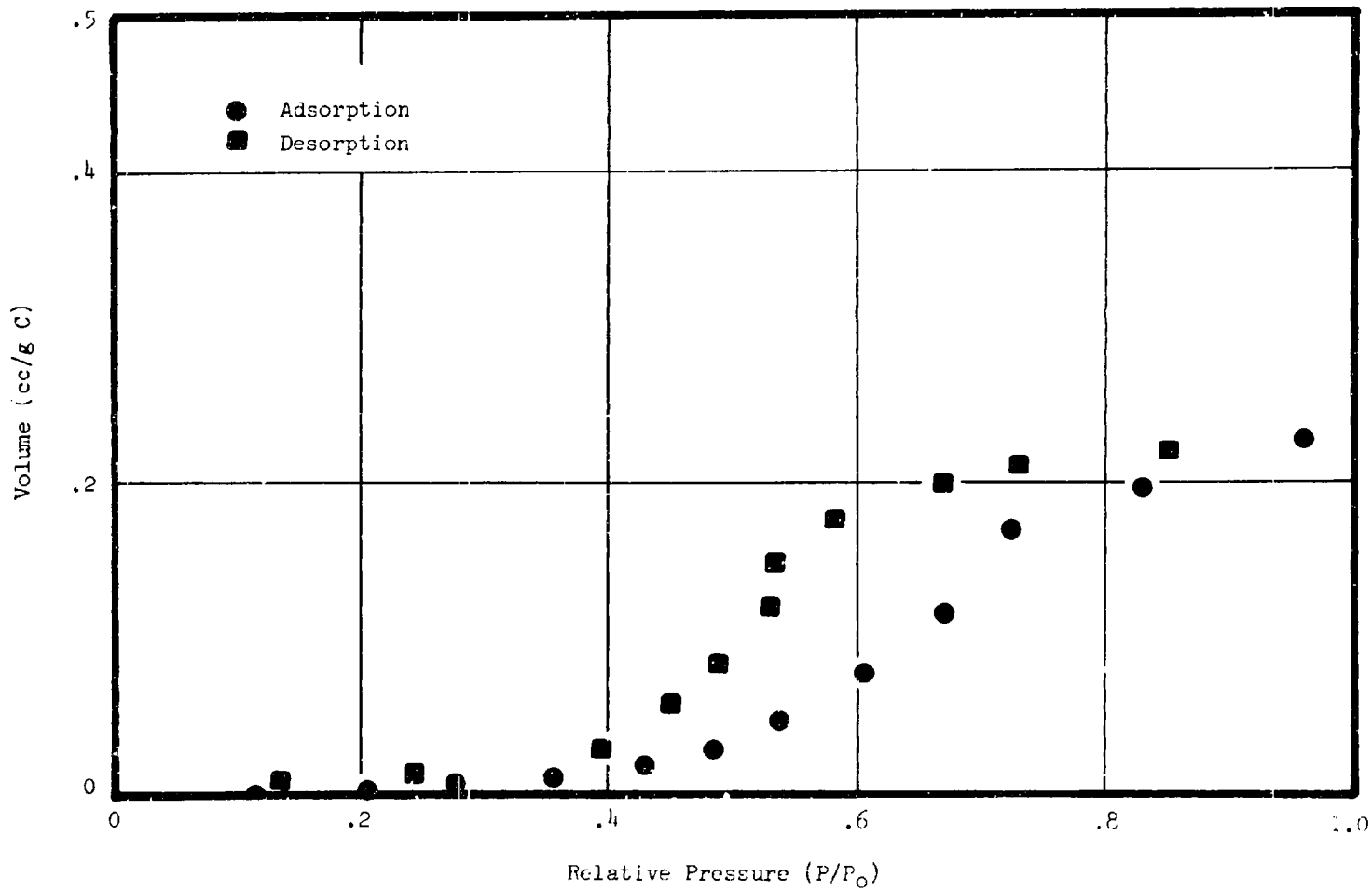

Figure 31

$H_2O$ on Control Sample at 20°C

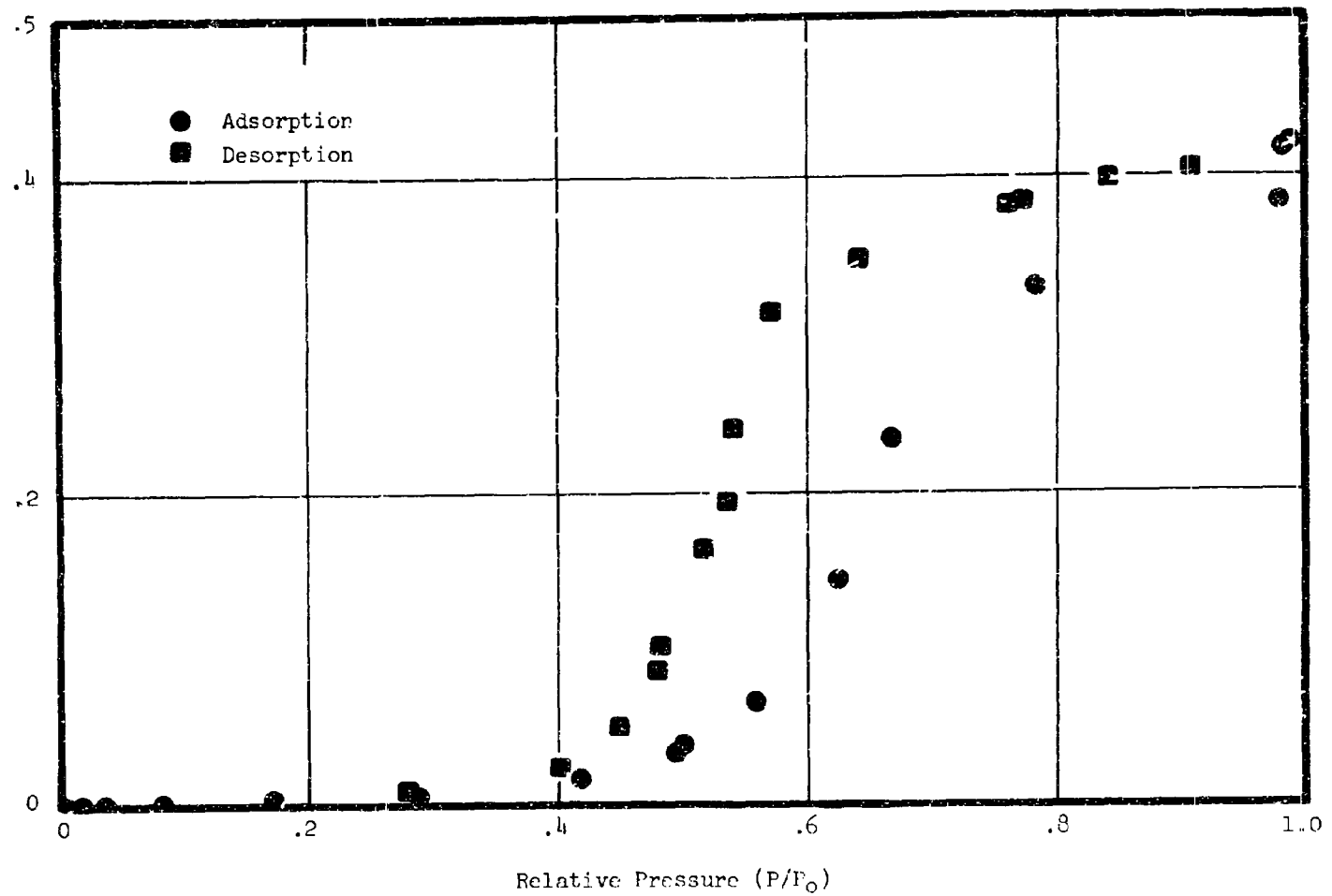

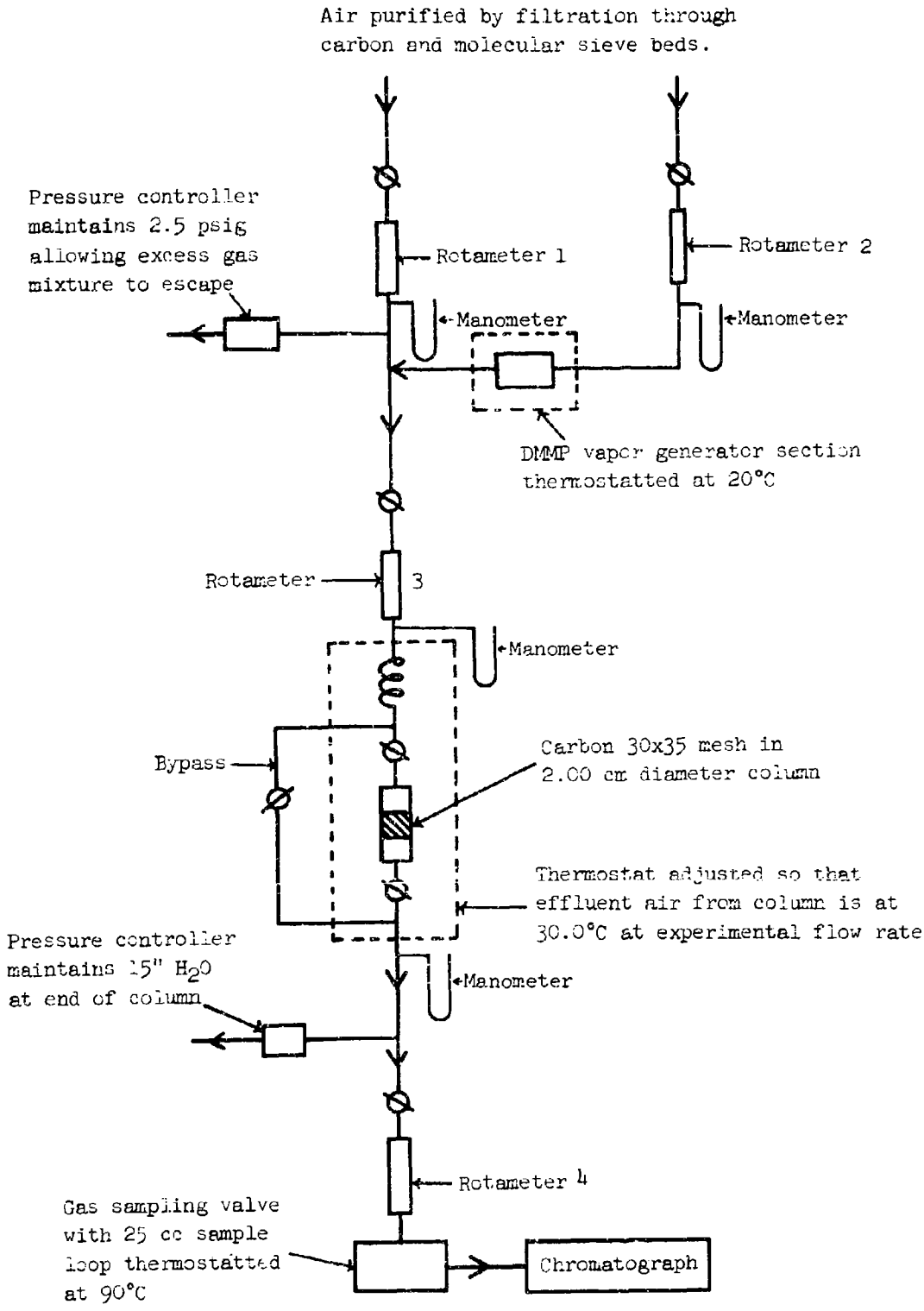


FIGURE 32

Elements of Flow Adsorption Apparatus

B. Experimental Procedure

A column 2.00 cm. in diameter was packed with 30x35 mesh PCC carbon. The top of the bed, which tended to be a little rounded because of vibration during packing, was leveled by gently tapping with a metal disk, and the length of the bed was measured using a cathetometer. This particular mesh size was used to maintain a 30:1 column diameter to partial size ratio in order to minimize velocity gradients near the column wall. (6) Pretreatment of the carbon involved outgassing at 35°C under 1 x $10^{-5}$ torr vacuum and storage in a partially evacuated dessicator.

With the packed column in place in the apparatus, air was passed through at the experimental flow rate and the thermostat bath controlling the temperature of the influent gas preheater and the column jacket was adjusted until the effluent air was at 30.0°C. The bed flow characteristics were then investigated to determine the approximate transition velocity between flow regions. Pressure drop vs. linear velocity plots are shown in Figure 33 and demonstrate that the flow rates used in the present experiments are within the turbulent regime.

Following the above measurements, the column was bypassed and its presence in the system simulated by a partially closed stopcock. All flows were then established to provide the proper gas mixture and influent flow rate, and the temperature in the vapor generator was allowed to equilibrate for 1/2 to 3/4 hour. In the present runs all of these parameters were intended to be identical.

The column was then switched into the line and the bypass closed off. 25 cc. samples of the effluent were taken at regular intervals by means of a gas valve and chromatographed on an 18 inch 10% Tween 80 on Anakrom ABS column held at 95°C. Sampling was begun 1 to 2 hours before the expected breakthrough in order to establish baseline characteristics. The limit of detectability depends upon baseline noise but on the average it is about 0.5 µg/l. This assumes the concentration to be proportional to peak height and the response directly proportional to the response at 8 µg/l.

After initial breakthrough, samples were taken at 20-minute intervals until breakthrough was complete. Sampling was then continued up to three hours longer.

The column was then bypassed, and the carbon removed and weighed to determine the amount of DMMP adsorbed.

At the end of each experimental run the chromatograph detector sensitivity was recalibrated. This calibration was based upon

FIGURE 33

Bed Flow Characteristics

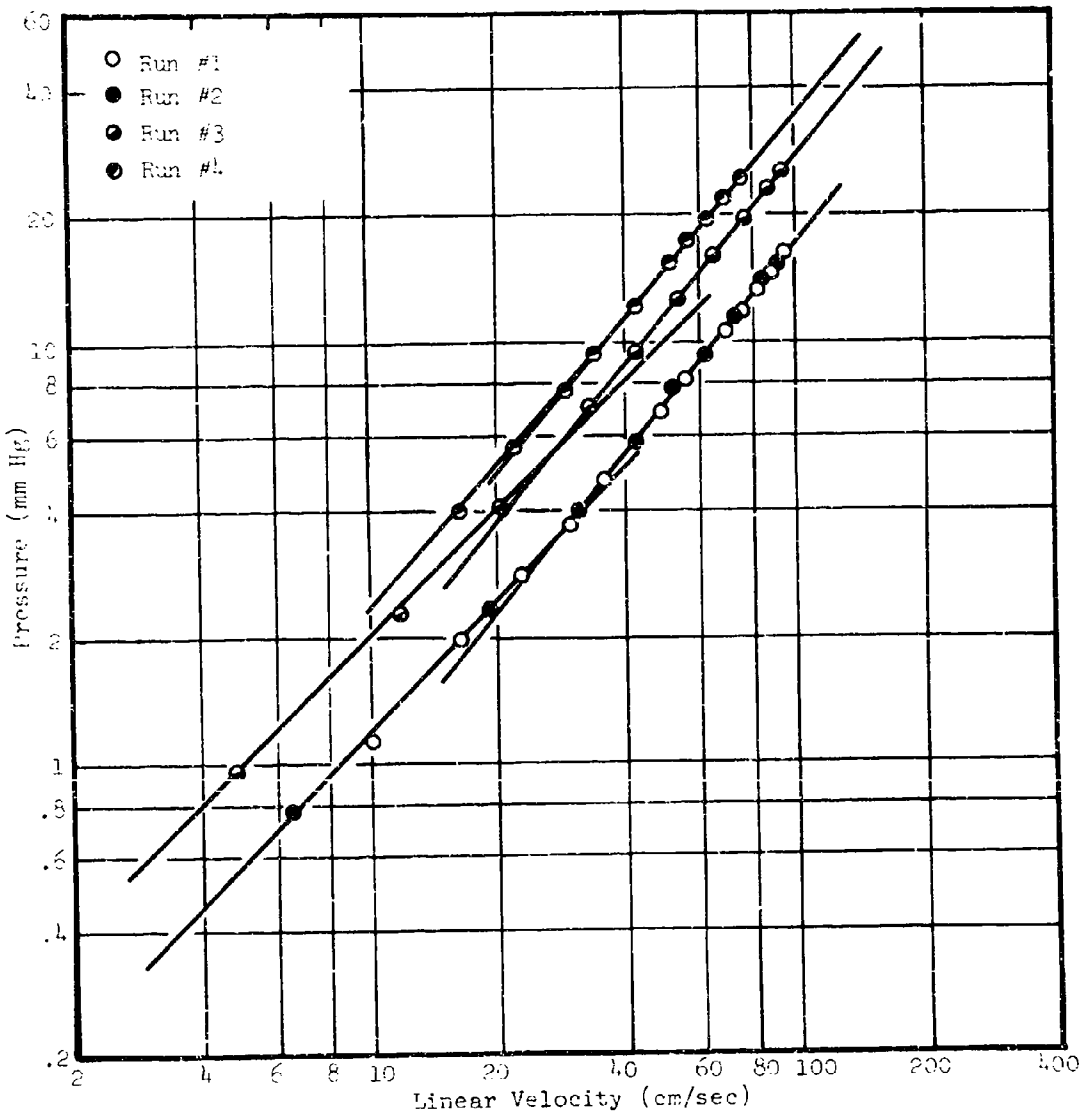

a prior determination of the DMMP generator output vs. the generator air flow rate. The relationship was established by determining the output over a range of flow rates by trapping the DMMP on a carbon bed and weighing the amount picked up. Using this generator calibration, specific concentrations could be made up by mixing the generator output with pure air flowing at an accurately known rate. When this method was used to calibrate the chromatograph, response curves, such as those shown in Figure 34, were obtained. It can be seen from the different observed sensitivities why it was necessary to recalibrate each time the detector flames were relighted.

Some features relevant to calculating concentrations produced in flow systems are noted below for reference purposes:

(1) The calibration of rotameter type flowmeters is dependent upon the particular pressure of gas in the rotameter during calibration. Assuming a rotameter has been calibrated at pressure $P_c$ and a calibration curve showing meter reading vs. gas volume per unit time is at hand, the flow rate, $V_2$, passed through the meter at a pressure, $P_2$, can be calculated by

$$V_2 = V_c \sqrt{P_2/P_c} \qquad [3]$$

$V_c$ is the flow rate read from the calibration curve at the observed rotameter reading. This flow rate is usually in terms of some standard conditions, e.g., 1 atmosphere pressure and 70°F. $V_2$ is, therefore, also a standard flow rate.

(2) The actual rate in the flow system obviously depends upon the temperature and pressure in the apparatus and must be calculated from the standard rate by application of the gas laws.

(3) The concentration produced by injecting a vapor into a flow system is given by dividing the gravimetric flow rate of the vapor by the actual flow rate of the carrier.

C. Systems Studied

Experimental runs were made with the PCC carbon for several different bed lengths and influent concentration levels of DMMP in air. These systems are summarized in Table VI.

D. Results of Flow Adsorption Experiments

Breakthrough curves were determined by the methods given above for the six systems outlined in Table VI.

FIGURE 34
Typical Detector Response Curves

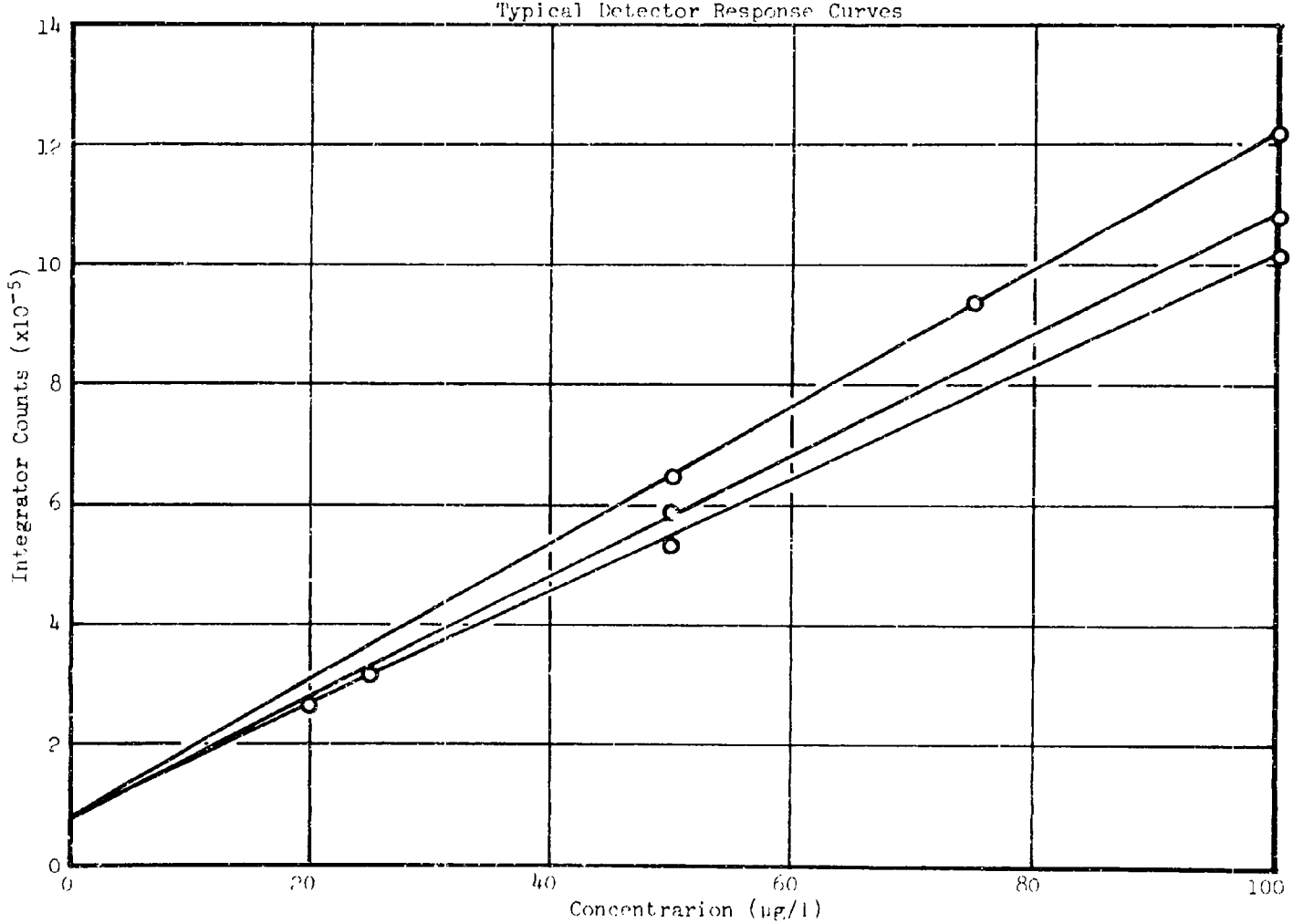

TABLE VI

EXPERIMENTAL PARAMETERS FOR FLOW ADSORPTION MEASUREMENTS

| | |
|---|---|
| Carbon Type | PCC |
| Mesh Size | 30 x 35 |
| Column Diameter | 2.00 cm |
| Temperature | 30.0°C |

| | | | | | | | |
|---|---|---|---|---|---|---|---|
| 1. | Run Number | 1 | 2 | 3 | 4 | 5 | 6 |
| 2. | Column Length (cm) | 1.555 | 1.479 | 2.474 | 3.066 | 1.527 | 1.104 |
| 3. | Bulk Density ($gm/cm^2$) | 0.417 | 0.435 | 0.424 | 0.431 | 0.420 | 0.428 |
| 4. | Weight of Carbon in Bed (gm) | 2.039 | 2.023 | 3.297 | 4.152 | 2.013 | 1.484 |
| 5. | Influent Concentration (µg/l.) | 102.4 | 102.5 | 103.6 | 104.5 | 93.0 | 78.5 |
| 6. | Influent Linear Velocity (cm/sec.) | 88.8 | 88.7 | 88.2 | 87.9 | 88.6 | 89.1 |
| 7. | Influent Volumetric Flow (l./min.) | 16.73 | 16.72 | 16.62 | 16.57 | 16.70 | 16.79 |

In order to check the internal consistency of these data, the amount of DMMP which was adsorbed on each bed at saturation was determined by weighing after each run. It should have been possible to calculate these amounts from the areas over the experimental breakthrough curves if all of the experimental parameters were well defined and accurately known. As shown in Table VII, reasonably good results were obtained with the exception of run No. 1.

We also attempted to calculate the amount adsorbed using the Characteristic equation [1]. Constants $W_o$ and B were determined from earlier attempts at describing the characteristic plot as a straight line. The results were so poor that a new characteristic curve (shown in Figure 35) was determined using the flow system. A straight line was drawn through this short section of data and the B and $W_o$ parameters determined from it were used to calculate amounts adsorbed in the experimental breakthrough runs. Table VII shows that the agreement was very close.

It should not be concluded from this that there are real differences in capacity between equilibrium and flow adsorption measurements at equivalent adsorbate concentrations. Because the Characteristic curve is not really straight, the assumption of linearity for all of the equilibrium data (shown by the dotted line in Figure 35) did not give a good fit to the data in the region of interest. The remaining difference may have been due to real differences in capacity due to the mesh size change, errors in assuming that DMMP gives an ideal solution in air and behaves as an ideal gas when computing equivalent pressures from concentrations, or to fluctuations in the capacities of individual samples.

E. Methods of Analysis of Breakthrough Data

Relationships have been sought which would allow the prediction of breakthrough curves from a knowledge of various system parameters and empirically determined adsorption rate constants.

One of the methods tested was that of Allen and Joyce (7) in which the rate controlling step is assumed to be intraparticle diffusion and in which the assumption of neither steady state conditions nor linear adsorption isotherms is required. In this method the adsorption bed is taken to be made up of a series of small segments and the adsorbate bearing gas is mathematically passed through each of these segments in turn in small volume increments. The concentration of vapor entering the first bed segment is the influent concentration. The effluent concentration from this segment after the first volume increment has passed through is calculated using the equation:

TABLE VII

EXPERIMENTAL AND CALCULATED AMOUNTS ADSORBED IN BREAKTHROUGH RUNS

| | Run Number | | | | | |
|---|---|---|---|---|---|---|
| | 1 | 2 | 3 | 4 | 5 | 6 |
| 1. Wt. DMMP Adsorbed (gm) (By weighing bed) | 0.790 | 0.788 | 1.29 | 1.62 | 0.795 | 0.567 |
| 2. Wt. DMMP Adsorbed (gm) (By area over breakthrough curve) | 0.848 | 0.824 | 1.30 | 1.64 | 0.771 | 0.580 |
| 3. Wt. DMMP Adsorbed (gm) (Predicted from dynamic characteristic curve data) | 0.809 | 0.809 | 1.32 | 1.67 | 0.793 | 0.568 |

FIGURE 35

Characteristic Curves for Adsorption of DMMP on PCC

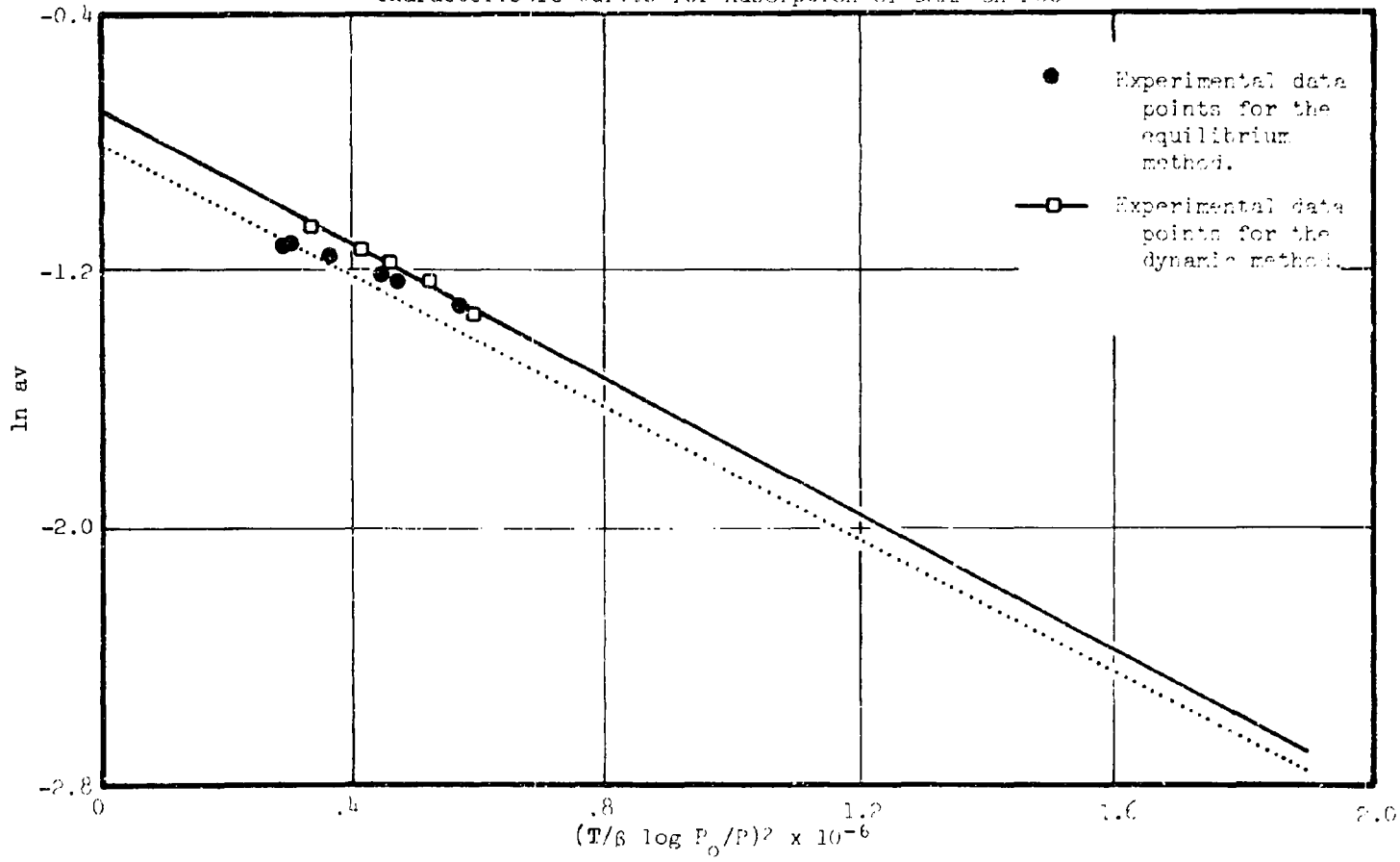

$$\ln C_{in}/C_{eff} = \frac{T_r K Q W_s}{V} \ln y \qquad [4]$$

This equation has only one unknown parameter, the rate constant, K. The other symbols are identified below under "Nomenclature."

The effluent concentration from the first bed segment is then taken as the influent to the next segment and the calculation repeated until the first volume increment has been passed through all bed segments. Further volume elements are then passed through the bed in the same manner until the effluent from last bed element approaches the influent concentration to the first element.

The rate constant for a particular system is found by using trial values K to generate trial breakthrough curves. The curve providing the best match with the experimental data serves to define K for that system.

Using an IBM 1130 Computer, theoretical breakthrough curves have been calculated for six experimental runs, the conditions of which are outlined in Table VI. The rate constant was determined by matching using the data of Run 2 and applied to all other runs. A comparison between the computed breakthrough curves (solid lines) and the experimental data (points) is shown in Figures 36A - 41A.

The analysis of Wheeler, which is well described elsewhere, (8) has also been applied to the experimental data obtained in the present work. This method utilizes a generalized adsorption equation in which the kinetic model can be altered by using various forms of a "$\psi$ - function" which describes the manner in which the rate of adsorption is affected by the accumulation of adsorbate on the bed. Three forms of the $\psi$ - function are considered here.

$$\psi\ (C/C_o) = 1 - C/C_o,\ (1 - C/C_o)^{1/2},\ \text{and}\ (1 - C/C_o)^{3/2}.$$

The corresponding linearized breakthrough equations are, respectively,

I $$\ln \frac{C_o - C_b}{C_b} = -\frac{K_v M C_o^*}{W_e \rho} t_b + \frac{K_v L}{V_L} \qquad [5]$$

II $$\ln \frac{1 + A}{1 - A} \cdot \frac{1}{e^2} = -\frac{K_v M C_o^*}{W_e \rho} t_b + \frac{K_v L}{V_L} \qquad [6]$$

FIGURE 36
Breakthrough Curves for LMMP on PGC
Run 1

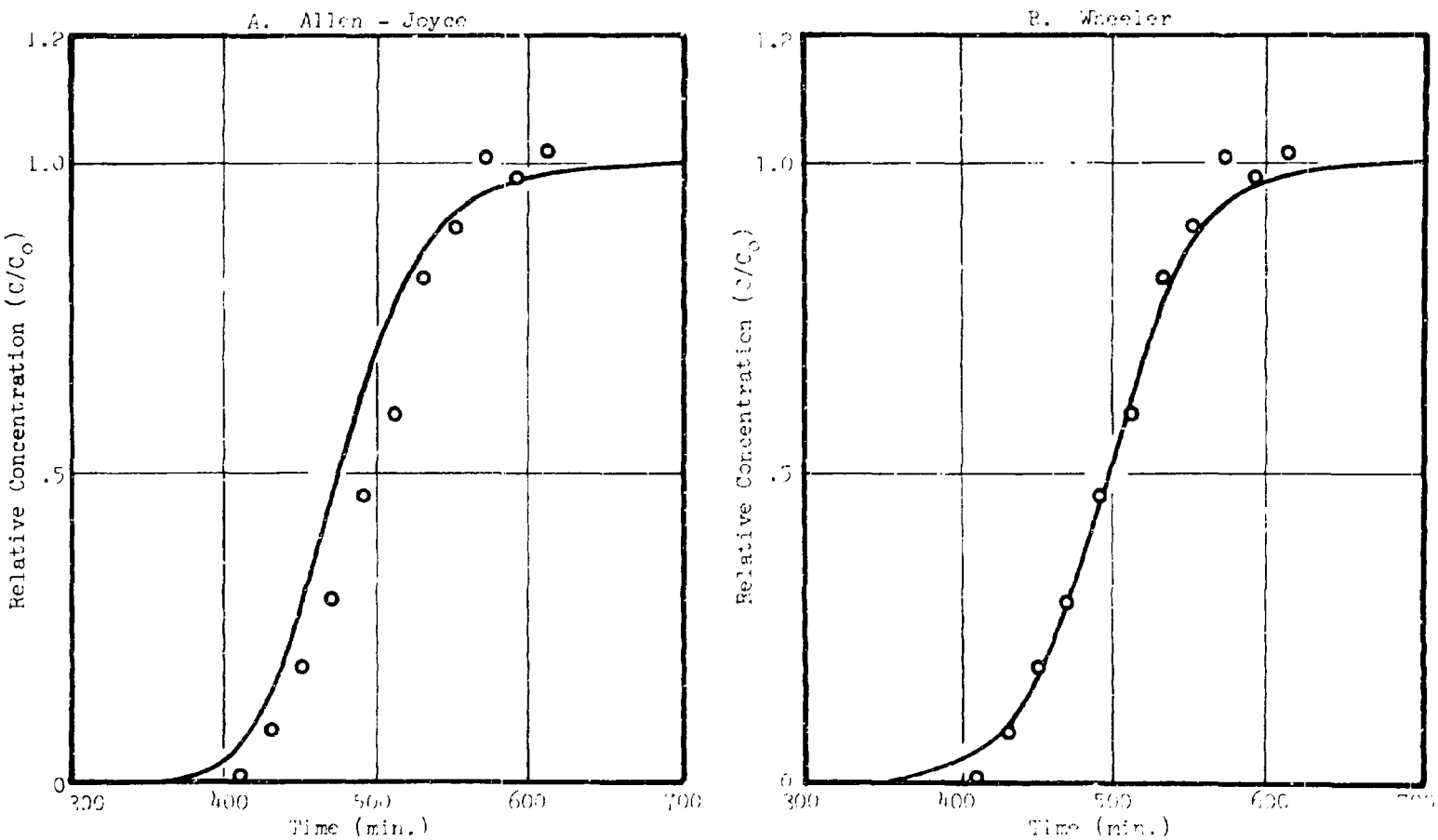

FIGURE 37

Breakthrough Curves for DMMP on PCC
Run 2

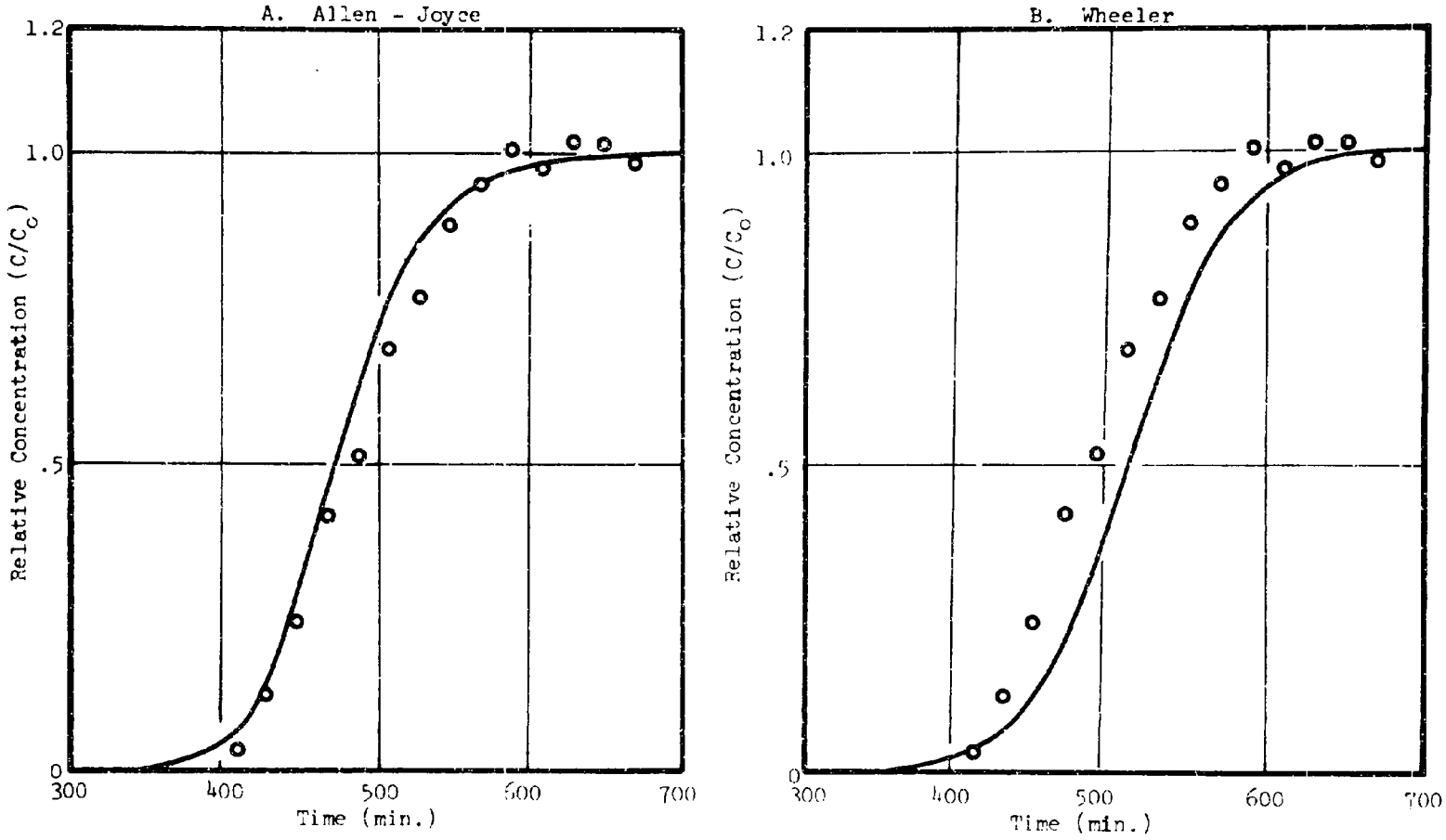

FIGURE 38
Breakthrough Curves for DMMP on PCC
Run 3

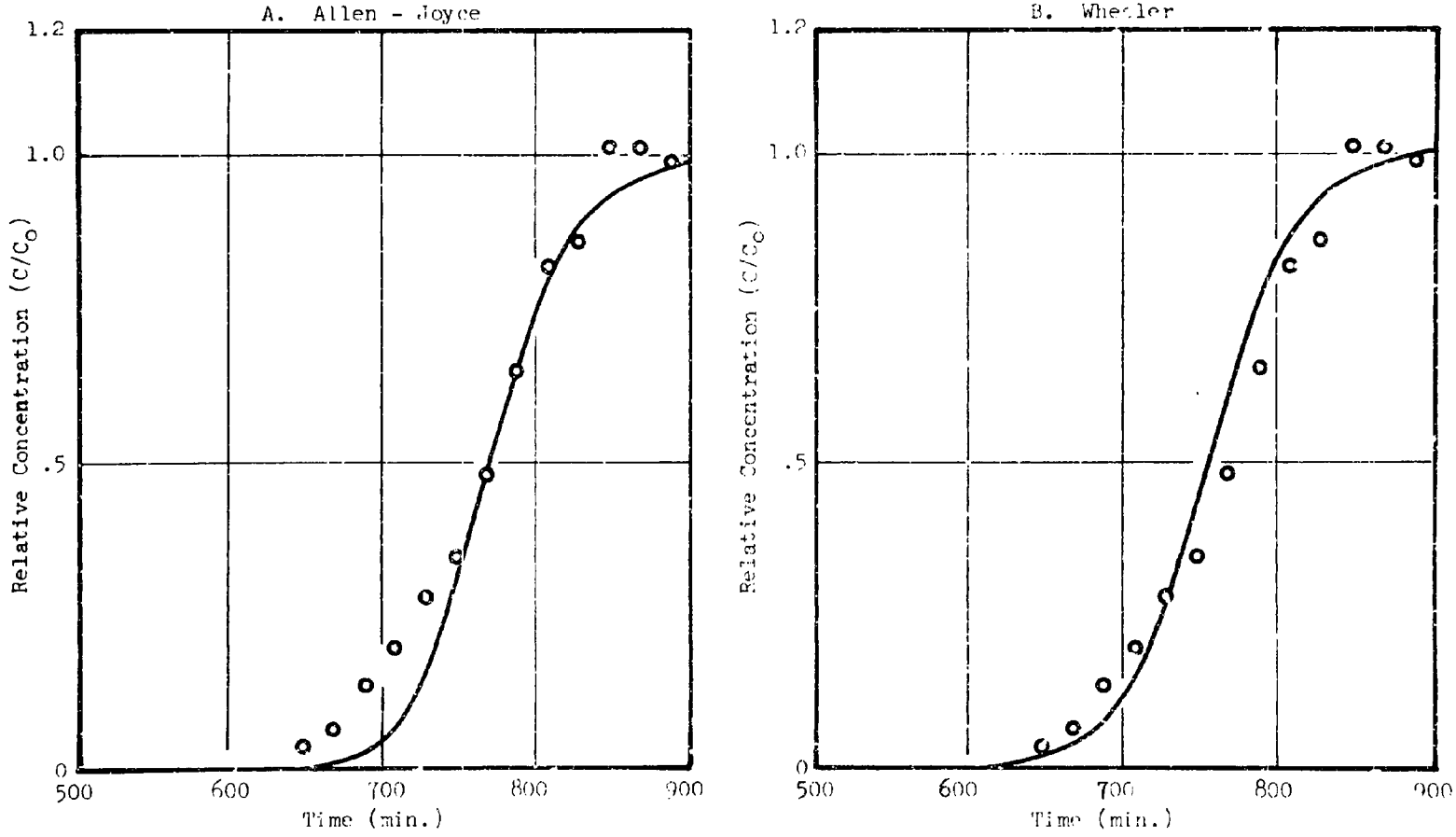

FIGURE 39
Breakthrough Curves for DMMP on PCC
Run 4

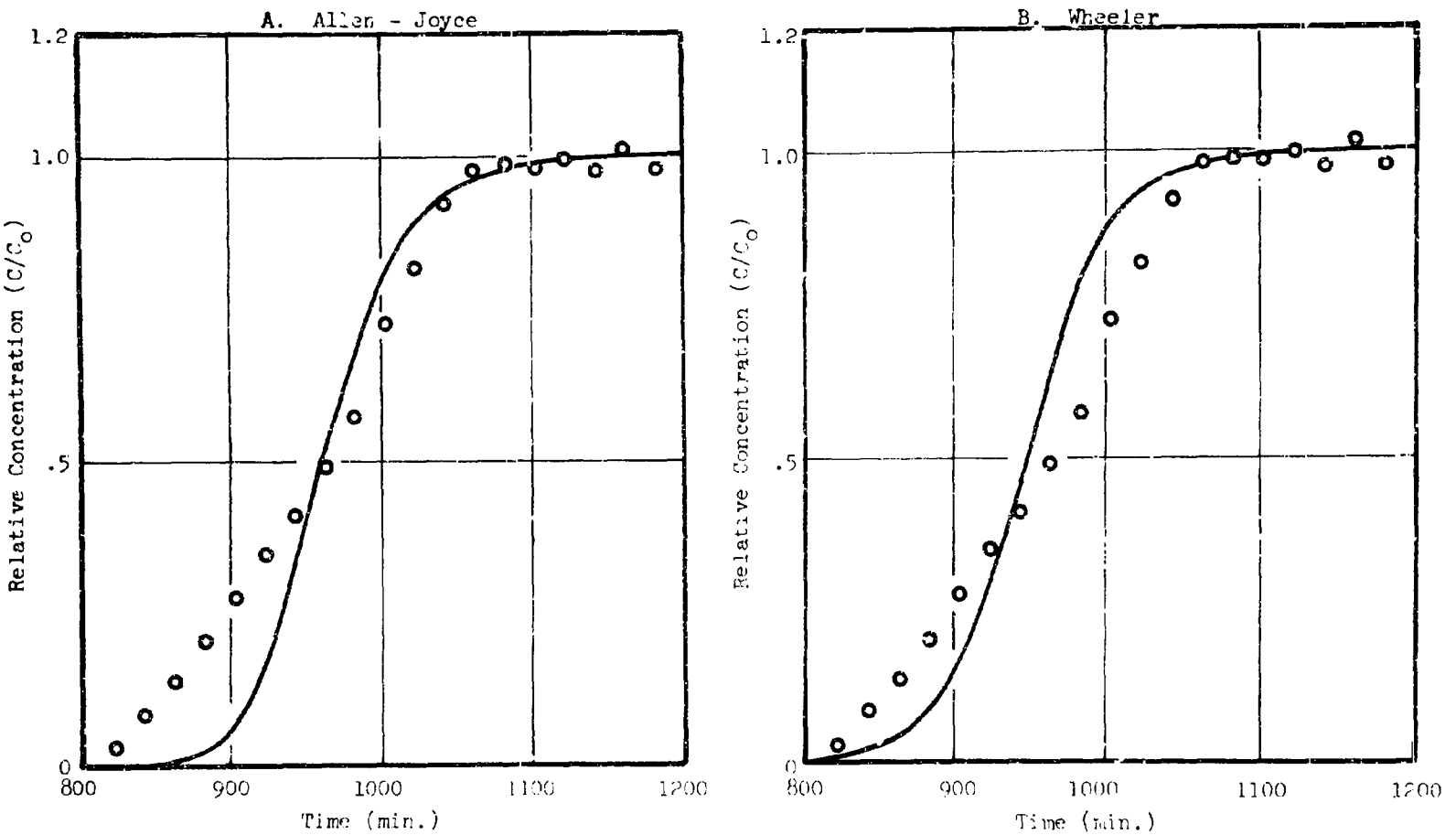

FIGURE 40

Breakthrough Curves for DMMP on PCC

Run 5

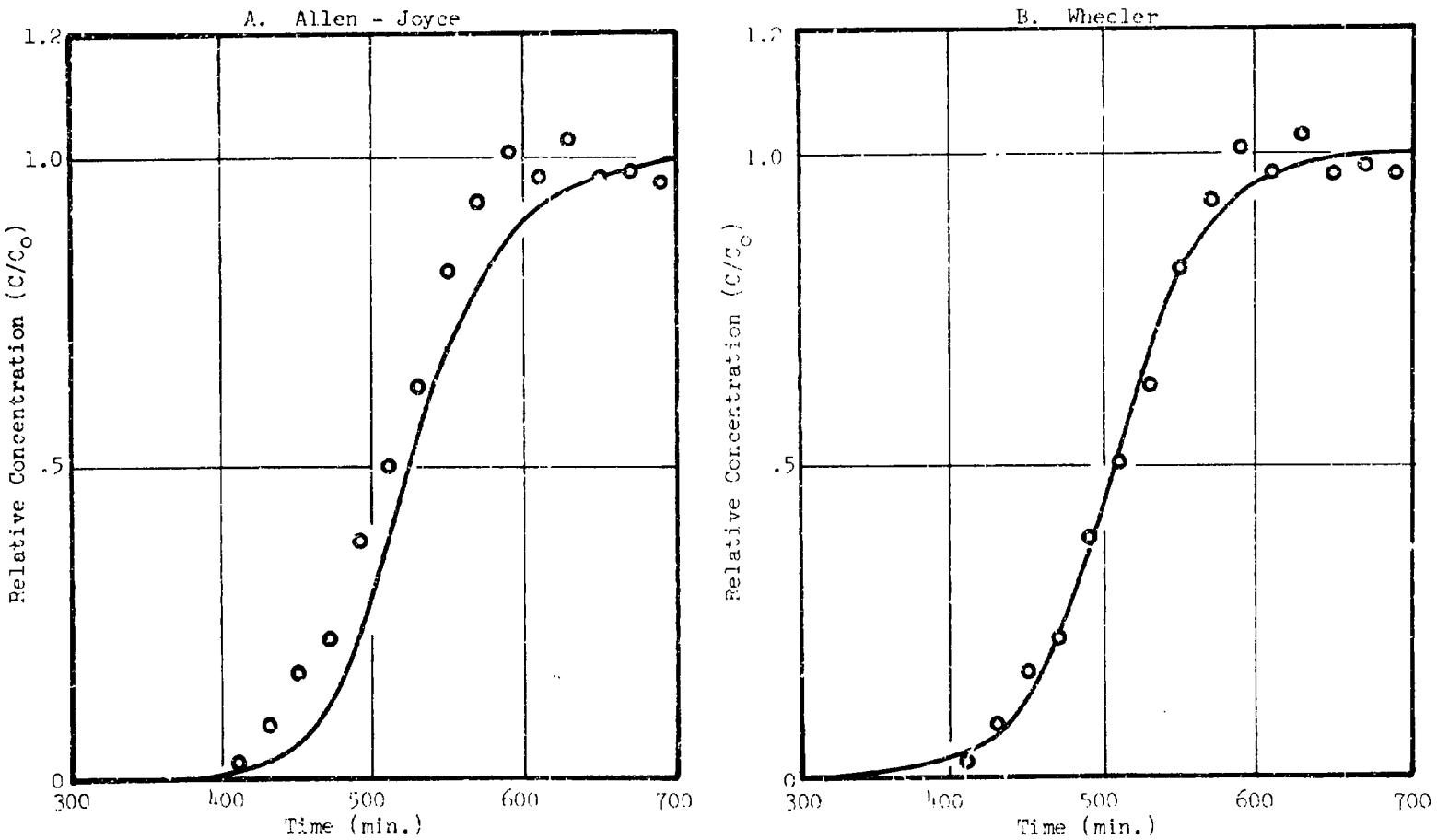

FIGURE 41

Breakthrough Curves for DMMP on PCC

Run 6

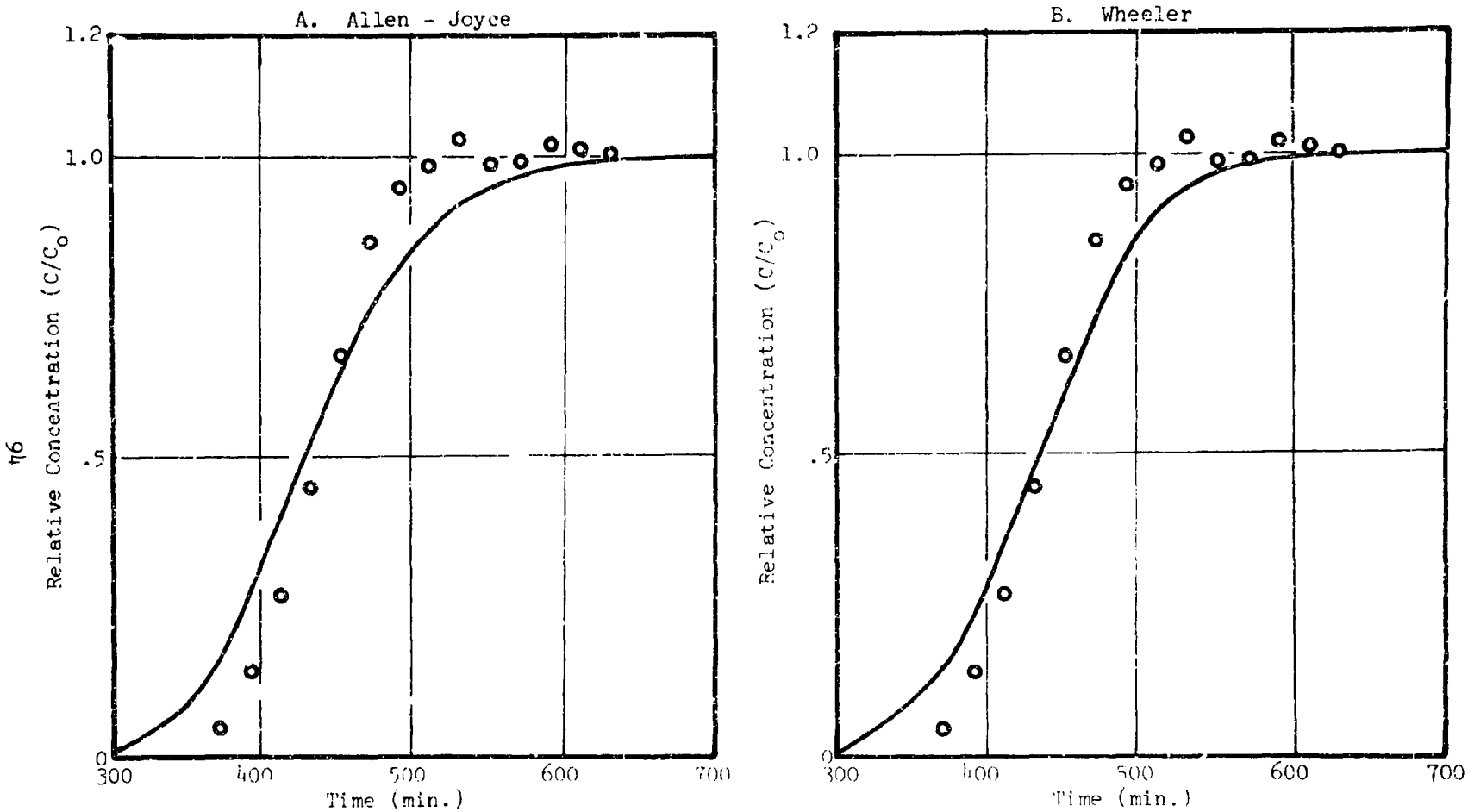

III $$\ln \frac{1 + A}{1 - A} - 2 \frac{1 - A}{A} = - \frac{K_v M C_o^*}{W_e \rho} t_b + \frac{K_v L}{V_L} \qquad [7]$$

where $$A = \left[\frac{C_o - C}{C_o}\right]^{1/2}$$

The logarithmic concentration function on the left side of each equation was regressed against the times, $t_b$, corresponding to effluent concentrations $C_b$, and least squares estimates of the slope and intercept terms where performed with an IBM 1130 Computer. From these, one can calculate values for the rate term, $K_v$, and the capacity, $W_e$.

Typical results of such an analysis, corresponding to Run 2, are shown in Figure 42 for the three cases. Table VIII shows the values of the rate constant and the bed capacity $W_e$* calculated by this method for the six experimental runs. In addition this table gives the correlation coefficients which indicate the degree of fit of the data to a straight line and also lists the directly observed bed capacities for comparison.

Case I, which consistently exhibits the highest correlation coefficient, best describes the present data. For this case breakthrough curves have been recalculated using a value of $K_v$ which is the average of the rate constants found for all runs except Number 4. Comparisons of the calculated breakthrough curves (solid lines) with the corresponding experimental results (points) are shown in Figures 36B - 41B.

F. Discussion of Flow Adsorption Results

In regard to comparisons between theoretical breakthrough curves as computed by the Allen-Joyce and the Wheeler methods, they are distinguished mainly by their similarity. Although the fit to the experimental data predicted by the two methods may vary somewhat for particular runs, the differences are due almost entirely to differences in their predictions of bed capacity. The effect of this is to produce shifts of the entire breakthrough curve on the time scale. The shapes of the curves calculated for a particular run by the two methods are practically identical. It is noteworthy that this observation persists as the influent concentration changes. Both methods predict a broadening of the breakthrough curve with decreasing concentration.

The fit of the computed breakthrough curves to experimental data was found to be generally poor. The reason for this is that the experimental breakthrough curves gradually become less sharp as the bed length increases. This can be seen by comparing

FIGURE 42
Correlation of Breakthrough Results with Wheeler's Equation - Run 2

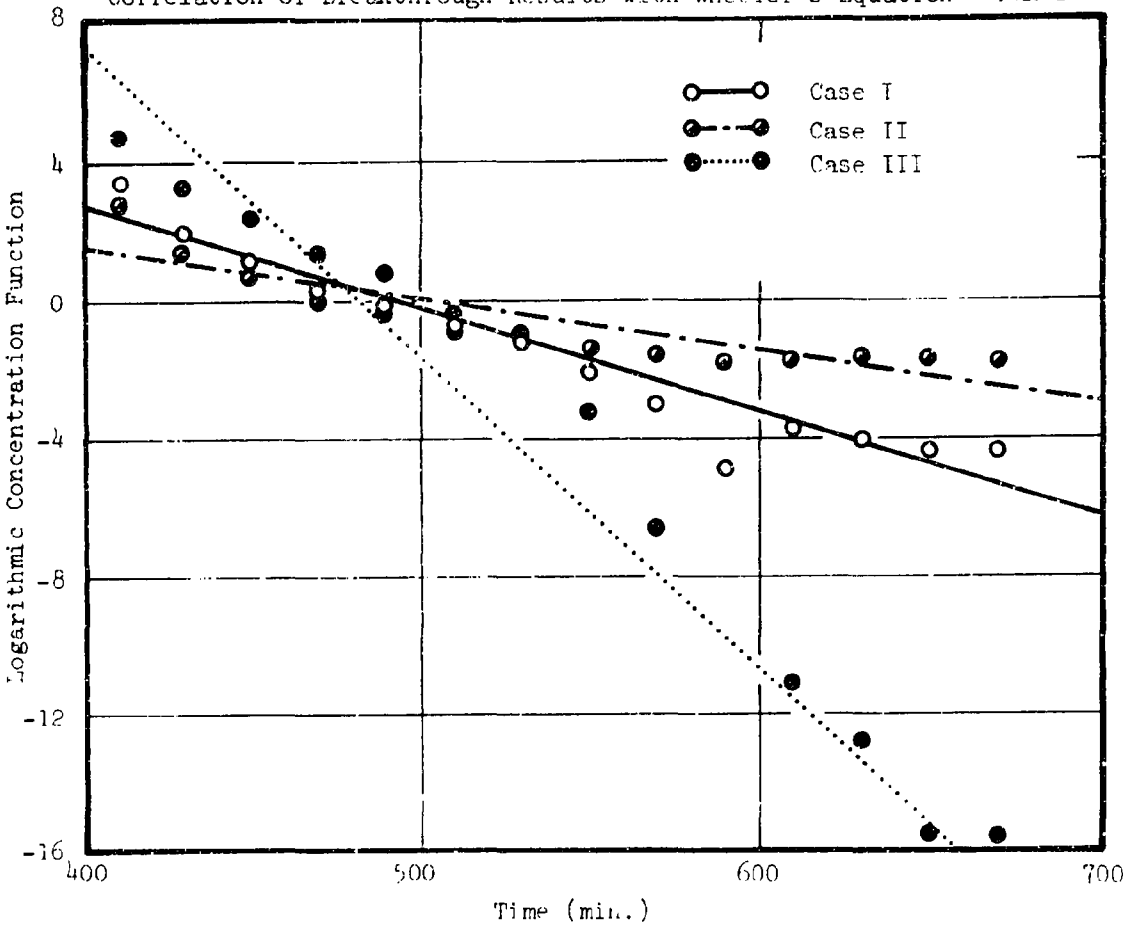

TABLE VIII

BREAKTHROUGH PARAMETERS FOR WHEELER ANALYSIS

| Run | Term | Case I | Case II | Case III | Observed Capacity |
|---|---|---|---|---|---|
| 1 | $K_v$ | 1222 | 733 | 3044 | |
| | $W_e$ | 0.850 | 0.870 | 0.826 | 0.790 |
| | CC | 0.965 | 0.927 | 0.820 | |
| 2 | $K_v$ | 890 | 452 | 2605 | |
| | $W_e$ | 0.837 | 0.853 | 0.824 | 0.788 |
| | CC | 0.965 | 0.902 | 0.912 | |
| 3 | $K_v$ | 834 | 446 | 2389 | |
| | $W_e$ | 1.30 | 1.33 | 1.27 | 1.29 |
| | CC | 0.968 | 0.962 | 0.878 | |
| 4 | $K_v$ | 465 | 243 | 1262 | |
| | $W_e$ | 1.64 | 1.66 | 1.60 | 1.62 |
| | CC | 0.906 | 0.879 | 0.785 | |
| 5 | $K_v$ | 803 | 465 | 1849 | |
| | $W_e$ | 0.788 | 0.810 | 0.765 | 0.795 |
| | CC | 0.932 | 0.912 | 0.814 | |
| 6 | $K_v$ | 1161 | 507 | 558 | |
| | $W_e$ | 0.573 | 0.584 | 0.577 | 0.567 |
| | CC | 0.965 | 0.875 | 0.801 | |

Runs 6, 2, 3, and 4 in the order of increasing bed length. It seems likely that the shapes of the experimental curves have been influenced by axial dispersion of the adsorbate which was not taken into account in the mathematical models. Such dispersion would have been strongly abetted by extremely high flow rates used in these experiments and it is recommended that future work be performed at lower linear velocities. It should be noted, however, that this will significantly increase the duration of experiments. At a concentration of about 105 µg/l. and 90 cm/sec. velocity, 12 hours were required for initial breakthrough from a 3 cm bed.

Although the amount of axial dispersion found in adsorbent beds is less than that in beds with an inert packing (9), an effect probably due to the usual nonlinearity of adsorption isotherms, its possible occurrence should be kept in mind. Significant dispersion would broaden concentration profiles within the bed, decrease break time, and decrease the adsorption rate constant as determined by mathematical models in which it is neglected.

## V. GENERAL SUMMARY

Equilibrium adsorption isotherms were determined experimentally at several temperatures using the agents GB, GA, and GF, the simulent DMMP and also carbon tetrachloride and benzene. The adsorbents used were Pittsburgh Activated Carbon Co. Type BPL and a "super activated" Barnebey-Cheney coconut shell carbon. Efforts to predict adsorption isotherms for the agents based upon the adsorptive behavior of the simulents and using the relationship $\ln W = \ln W_o - B/\beta^2 (T \log Po/P)^2$ after Dubinin et al., were not successful. This was because plots of the experimental data as $\ln W$ vs. $(T/\beta \log Po/P)^2$ were not linear as implied by the equation. Despite this reasonably good isotherm predictions were obtained by assuming that the resultant curves were characteristic of the particular adsorbent and by working directly from such plots. Values of the term $\beta$ which represents the strength of the adsorptive interaction of a particular adsorbate relative to that of a reference adsorbate were determined experimentally. This was done by adjusting the value until the best fits were obtained between the predicted isotherms and the experimental data for the Pittsburg carbon. The same values were found to produce reasonably good fits for the "super activated" carbon. Values of $\beta$ calculated from the ratios of molar parachors did not lead to acceptable isotherm predictions in the cases studied.

The present work indicates that the adsorption properties of a carbon can be characterized by a plot of $\ln W$ vs. $(T \log Po/P)^2$ using adsorption data for a reference adsorbate. The adsorptivity of another adsorbate relative to that of the reference material should be determined experimentally. Such relative adsorptivities are expected to be independent of the adsorbate for most carbons.

The physical and adsorptive properties of an activated carbon impregnated with siloxane resins were investigated. Such impregnation caused a large loss in surface area and adsorptive capacity but did not selectively increase the hydrophobic properties of the carbon. Deposition of the resin appeared to have taken place principally in the larger pores and resulted in the blockage of a portion of the micropores.

Flow adsorption experiments were performed using the Pittsburgh Type BPL carbon and the simulent DMMP. Predictions of the breakthrough properties of this system were attempted for a range of adsorbate/air concentrations around 100 µg/l and at linear velocities of flow of about 90 cm/sec. These predictions were based upon the theoretical methods of Wheeler and of Allen and Joyce and neither was found to yield accurate description of the experimental breakthrough curves. It is thought that the results may have been adversely influenced by the very high experimental flow rates.

## NOMENCLATURE

| | |
|---|---|
| A | $\left[\frac{C_o - C}{C_o}\right]^{1/2}$ in Equations [6] and [7] |
| a | Amount adsorbed, (moles) |
| B | Characteristic constant in Equation [1] |
| C | Concentration, (µg/l.) |
| $C_{in}$ | Adsorbate concentration influent to a bed element, (µg/l.) |
| $C_{eff}$ | Adsorbate concentration effluent from a bed element, (µg/l.) |
| $C_o$ | Concentration influent to an adsorbent bed, (µg/l.) |
| $C_b$ | Concentration effluent from an adsorbent bed at time $t_b$, (µg/l.) |
| $C_o$* | Influent concentration, (moles/$cm^3$) |
| CC | Correlation coefficient |
| K | Rate constant in Equation [3], (defined by $dy/dt = -K \ln y$) |
| $K_v$ | Rate constant in Equations [5], [6], [7]. ($Sec^{-1}$) |
| L | Bed length, (cm) |
| M | Molecular weight |
| P | Equilibrium adsorbate pressure |
| $P_o$ | Adsorbate vapor pressure |
| Q | Capacity of adsorbent as defined by adsorption isotherm equation, (gm/gm) |
| T | Temperature, (°K) |
| $T_r$ | Residence time of air carrier in adsorbent bed per gm carbon, (sec./gm C) |
| $t_b$ | Time from start of flow run. Time at which effluent concentrations is $C_b$ |
| V | Superficial volume of column per gm carbon, ($cm^3$/gm) |
| $V_L$ | Superficial linear velocity of air carrier, (cm/sec.) |

| | |
|---|---|
| $v$ | Molar volume, (cm /mole) |
| $W$ | Volume adsorbed at equilibrium (gm/gm Carbon) in Equation [1] |
| $W_s$ | Gm of carbon per bed segment |
| $W_e$ | Equilibrium amount adsorbed per gm carbon at concentration $C_o$, (gm/gm C) |
| $W_e^*$ | Equilibrium amount adsorbed on entire bed at $C_o$, (gm) |
| $W_o$ | Characteristic constant in Equation [1] |
| $y$ | Fractional saturation of bed segment at the local adsorbent concentration |
| $\beta$ | Affinity coefficient |
| $\rho$ | Bulk density of bed, ($gm/cm^3$) |

## LITERATURE CITED


1. Bering, B. P., Dubinin, M. M., Serpinsky, V. V., Journal of Colloid and Interface Science 21:378 (1966).

2. Makowski, J. et al., Collective Protection Against CB Agents, CB 1008, p. 46, Garrett Corporation, AiResearch Manufacturing Division, Los Angeles, California, February 1966.

3. Roberts, B. F., Journal of Colloid and Interface Science 23:266 (1967).

4. Janov, J., Thesis, The Pennsylvania State University (1968).

5. Makowski, J. et al., Collective Protection Against CB Agents, CB 1009, Vol. 1, Garrett Corporation, AiResearch Manufacturing Division, Los Angeles, California, June 1966.

6. Schwartz, C. E., Smith, J. M., Industrial and Engineering Chemistry 45:1209 (1953).

7. Allen, J. B., Joyce, R. S., Column Calculations for Intra Partical Diffusion Controlled Adsorption. Presented at 59th Annual AIChE Meeting, Detroit, Michigan (December 4-8, 1966).

8. Makowski, J., et al., Collective Protection Against CB Agents, CB 1010, Task 12 Section, Garrett Corporation, AiResearch Manufacturing Division, Los Angeles, California (1966).

9. Chao, R., Hoelscher, H. E., AIChE Journal 12:271 (1966).

UNCLASSIFIED

Security Classification

**DOCUMENT CONTROL DATA - R & D**

*(Security classification of title, body of abstract and indexing annotation must be entered when the overall report is classified)*

1. ORIGINATING ACTIVITY *(Corporate author)*
WEST VIRGINIA PULP AND PAPER COMPANY
North Charleston, South Carolina

2a. REPORT SECURITY CLASSIFICATION
UNCLASSIFIED

2b. GROUP
NA

3. REPORT TITLE
SORPTION PROPERTIES OF ACTIVATED CARBON

4. DESCRIPTIVE NOTES *(Type of report and inclusive dates)*
Comprehensive Progress Report - June 1966-April 1968

5. AUTHOR(S) *(First name, middle initial, last name)*
Tolles, E. D.

6. REPORT DATE
August 1968

7a. TOTAL NO. OF PAGES
108

7b. NO. OF REFS
9

8a. CONTRACT OR GRANT NO.
DA-18-035-AMC-1053(A)

b. PROJECT NO.
1C622401A095

c.

d.

9a. ORIGINATOR'S REPORT NUMBER(S)
PR-6/COMP

9b. OTHER REPORT NO(S) *(Any other numbers that may be assigned this report)*

10. DISTRIBUTION STATEMENT This document is subject to special export controls and each transmittal to foreign governments or foreign nationals may be made only with prior approval of the CO, Edgewood Arsenal, ATTN: SMUEA-TSTI-T, Edgewood Arsenal, Maryland 21010.

11. SUPPLEMENTARY NOTES
Chemical physical protection investigations
Biological physical protection investigations

12. SPONSORING MILITARY ACTIVITY
Edgewood Arsenal Research Laboratories
Edgewood Arsenal, Maryland 21010
(L. Jonas, Proj. O., Ext 25253)

13. ABSTRACT

Equilibrium adsorption isotherms were determined experimentally at several temperatures for CB, GA, and GF on ~~Pittsburgh~~ BPL activated carbon and a super activated coconut carbon. Prediction of these isotherms using experimental DMMP, $CCl_4$ and benzene adsorption data and the Polanyi-Dubinin equation was not too successful because the data were not linear as required by the equation. Reasonably good isotherm predictions were, however, obtained using the experimental characteristic curves for DMMP and $CCl_4$ to define the adsorptive properties of the adsorbents. Affinity coefficients were determined experimentally since those calculated from parachors were not accurate. The physical and adsorptive properties of an activated carbon impregnated with siloxane resins were investigated. Such impregnation caused a large loss in surface area and adsorptive capacity, but did not selectively increase the hydrophobic properties of the carbon. Deposition of the resin apparently took place principally in the larger pores and resulted in blockage of a portion of micropores. Flow adsorption experiments were made on ~~Pittsburgh~~ BPL carbon with DMMP vapor at a concentration of 100 ~~μg~~/l and at a velocity of 90 cm/sec. Breakthrough concentration curves, predicted by the theoretical methods of Wheeler and of Allen and Joyce, did not accurately correlate with the experimental points possibly because of the high flow rate used.

DD FORM 1 NOV 1473 REPLACES DD FORM 1473, 1 JAN 64, WHICH IS OBSOLETE FOR ARMY USE.

UNCLASSIFIED

Security Classification

| 14 KEY WORDS | LINK A | | LINK B | | LINK C | |
|---|---|---|---|---|---|---|
| | ROLE | WT | ROLE | WT | ROLE | WT |
| Sorption properties | | | | | | |
| Activated carbon | | | | | | |
| Chemical agents | | | | | | |
| Chemical agent simulents | | | | | | |
| Equilibrium adsorption measurements | | | | | | |
| Adsorptive properties | | | | | | |
| Adsorbents | | | | | | |
| Physical properties | | | | | | |
| Impregnated carbons | | | | | | |
| Dynamic adsorption studies | | | | | | |
| Flow adsorption experiments | | | | | | |
| Breakthrough data | | | | | | |
| Porosity measurements | | | | | | |
| Water adsorption | | | | | | |
| GB | | | | | | |
| PCC | | | | | | |
| DMMP | | | | | | |
| BC | | | | | | |
| GA | | | | | | |
| GF | | | | | | |